Sudan University of Science and Technology

College of Graduate Studies

CHARACTERIZATION OF SPHENOID SINUS IN SUDANESE POPULATION USING COMPUTED TOMOGRAPHY

توصيف الجيب الوتدي لدي السودانيين بإستخدام الأشعة المقطعية

A Thesis Submitted for the Requirements of the fulfillment of the Award of Ph.D. Degree in Diagnostic Radiological Technology

Presented By:

Samih Awad Ali Kajoak

(M.Sc. in Diagnostic Radiological Technology, University of Sudan, 2006)

Supervisor:

Prof. Dr. Caroline Edward Eyad Khela

Co – Supervisor:

Dr. Mohammed Najem Aldeen Awad Eljak

June 2015

الآيـــة

بِسْمِ اللَّهِ الرَّحْمَنِ الرَّحِيمِ

اقْرَأْ بِاسْمِ رَبِّكَ الَّذِي خَلَقَ (1) خَلَقَ الإِنسَانَ مِنْ عَلَقٍ (2) اقْرَأْ وَرَبُّكَ الأَكْرَمُ

(3) الَّذِي عَلَّمَ بِالْقَلَمِ (4) عَلَّمَ الإِنسَانَ مَا لَمْ يَعْلَمْ (5)

صَدَق اللّه الْعَظِيْم

سورة العلق : الآيات (1–5)

Dedication

This work is lovingly dedicated:

- *To my Wife and my daughters "Lamees, Linda & Alaa" for their patience, understanding and encouragement*

- *To my parents, brothers and sisters for their help and support*

- *To my friends for their valuable advice*

- To the all dearest people in my life

Acknowledgement

- *I would like to thank ALLAH who has blessed and guieded me to accomplish this thesis.*

- *I wish to express my sincerest gratitude to my supervisor* ***Prof. Dr. Caroline Edward,*** *the Associate Professor at Sudan university of Science and Technology for her contact supervision, inexhaustible patience, constant encouragement, and for giving me a valuable times, guidance, criticism and corrections to this thesis from beginning up to end ..*

- *I would also like to express sincere appreciation to my co-supervisor to* ***Dr. Mohammed Najem Aldeen,*** *MD, Radiologist, who helps me in diagnosis all images in this study with his full patience and cooperation.*
- *Moreover, I would like to thanks* ***Mr. Mohammed Abdulwahab*** *for skillful technical assistance in CT scan*

machine and all staff in (Royal care Hospital) especially CT department for their help and support.

- *I thank* ***Mr. Abobaker Bashir*** *who helps me in statistical analysis of this thesis.*

- *Also I want to express my deepest thanks to* ***Mr. Abdalla Ahmed Eldaw*** *for his support and valuable advices.*

ABSTRACT

Sphenoid sinus is surrounded by critical structures and this can make sphenoid sinus surgeries very dangerous. The aims of this research were to study the anatomical relationships between the sphenoid sinus and their important adjacent neurovascular structures using the multiplanar reconstruction technique and to measure some important surgical distances of sphenoid sinus including, roof, bottom, posterior wall, anterior wall, in terms of their relevancy to the Sudanese patients.

Coronal and sagittal CT scans of 201 patients attending Radiology Department of Royal Care Hospital in Sudan, between June 2012 and July 2014 were reviewed regarding the anatomical variations of the sphenoid sinus. The study assessed pneumatization of pterygoid process (PP), anterior clinoid process (ACP), and greater wing of sphenoid (GWS); the study also examined protrusion and dehiscence of internal carotid artery (ICA), optic nerve (ON), maxillary nerve (MN), and vidian nerve (VN) into the sphenoid sinus cavity. Moreover Characterization of the sphenoid sinus and seven horizontal and vertical measurements were evaluated.

Pneumatization of (ACP), (GWS) and (PP) were seen in 13.9%, 34.8% and 40.3% patients respectively. Protrusion of the (ICA), (ON), (MN) and (VN) were noticed in 25.4%, 3%, 27.9% and 42.3% patients respectively; dehiscence of these structures was encountered in 12.4%, 15.9%, 45.3% and 55.2% patients respectively. Statistically, there was a significant association between (ACP) pneumatization and (ICA) protrusion and (ON) dehiscence (p = 0.003), also a significant association between (GWS) pneumatization and (MxN) protrusion and (MxN) dehiscence (p = 0.003) was noted.

Significant association between (PP) and (VN) protrusion and (VN) dehiscence (p = 0.004) was also noted.

The mean length of vertical lines from the center of sphenoid ostium to the roof and bottom were 9.9 ± 3.3 mm, 10.7 ± 3.4 mm respectively. When the sphenoid ostium was located superior to the lowest point of the sella, the line from the center of the sphenoid sinus ostium to the posterior wall of the sinus was 16.4 ± 4.7 mm and when was located inferior, the line was 18.4 ± 4.7 mm on average. The mean length of line 4 from the lowest point of the sella to the anterior wall of sphenoid sinus was 16.4 ± 3.7 mm. The line from anterior wall to posterior wall of sphenoid sinus lining skull base was 10.6±3.4mm mm. The maximum depth was 24.5 ± 6.7 mm and the maximum width was 17.3 ± 5.7mm. The differences in the sphenoid sinus measurements take place between males and females.

The knowledge on the dimentions, anatomic variations and morphology of the sphenoid sinus and its related structures is important in order to avoid the surgical complications when entering the pituitary gland and sella turcica. The study provides essential anatomical information of the sphenoid sinus for Sudanese subjects and its impact in the clinical surgical practice.

ملخص البحث

الجيب الوتدي محاط بأوعية دموية وعصبية حساسة، مما يجعل العمليات الجراحية للجيب الوتدي خطيرة جدا. أهداف هذا البحث هو دراسة العلاقات التشريحية بين الجيب الوتدي والبنى الوعائية الدموية والعصبية الهامة والمجاورة له وذلك بإستخدام تقنية إعادة بناء الخطوط المتعددة، كما تم قياس بعض المسافات الهامة للجيب الوتدي بما في ذلك السقف، القاع، الجدار الخلفي، الجدار الأمامي ، ومعرفة أهميتة هذه المسافات للجيب الوتدي على المرضى السودانيين.

تم مراجعة صور الاشعة المقطعية ذات المقاطع التاجية والرأسية لعدد 201 مريض، وذلك لدراسة الاختلافات التشريحية للجيب الوتدي. وقمنا بتقييم وجود التجاويف الهوائية للجيب الوتدي في كل من: الناتئ الجناحي والناتئ السريري والجناح الكبير للعظم الوتدي، كما تمت دراسة بروز وملامسة الشريان السباتي الباطن، والعصب البصري، وعصب الفك العلوي وعصب فيديوس لجدار الجيب الوتدي. وعلاوة علي ذلك تم توصيف وقياس سبعة مسافات للجيب الوتدي.

تم رؤية التجاويف الهوائية للجيب الوتدي في كل من: الناتئ السريري والجناح الكبير والناتئ الجناحي للعظم الوتدي بنسبة 13.9 % و 34.8 % و 40.3 علي التوالي. وتم ملاحظة بروز الشريان السباتي الباطن والعصب البصري وعصب الفك السفلي وعصب فيديوس علي جدار الجيب الوتدي بنسبة 25.4%، 3%، 27.9% و42.3% علي التوالي. ووجد أن هذه الاعضاء تلامس جدار الجيب الوتدي بنسبة 12.4%، 15.9%، 45.3% و55.2% علي التوالي. إحصائيا لوحظ وجود علاقة قوية بين ظهور التجويف الهوائي للجيب الوتدي في الناتئ السريري للعظم الوتدي وبروز الشريان السباتي الباطن وملامسة العصب البصري لجدار الجيب الوتدي (القيمة الإحتمالية = 0.003). وايضا تم ملاحظة بروز وملامسة عصب الفك العلوي عند ظهور التجويف الهوائي للجيب الوتدي في جناحه الكبير القيمة الإحتمالية = 0.003) ، وايضا تم ملاحظة بروز وملامسة عصب فيديوس للجيب الوتدي عند ظهور التجويف الهوائي للجيب في الناتئ الجناحي للعظم الوتدي القيمة الإحتمالية = 0.004).

كان متوسط المسافة بين فتحة الجيب الوتدي الي سطحه والي قاعه هي 3.3± 9.9 ملم و 3.7± 10.7 ملم علي التوالي. وعندما تكون فتحة الجيب الوتدي أعلي من الحافة السفلية للسرج التركي

تكون المسافة 4.7± 16.4 ملم ، وعندما تكون الفتحة أسفل من الحافة يكون متوسط المسافة 4.7± 18.4 ملم. وأما بالنسبة لمتوسط المسافة من أسفل نقطة للسرج التركي الي الجدار الأمامي للجيب هي 3.7 ± 16.4ملم. ومتوسط المسافة ما بين الجدار الامامي والخلفي للجيب بمحازاة قاعدة الجمجمة هي 3.4 ± 10.6ملم. ومتوسط المسافة لأقصي عمق وأقصي عرض للجيب الوتدي هي 6.7 ± 24.5 و5.7 ± 17.3 ملم علي التوالي. تم ملاحظة إختلافات في قياسات الجيب الوتدي بين الذكور والإناث.

معرفة الأبعاد والإختلافات التشريحية بالإضافة الي شكل الجيب الوتدي وعلاقته بالأوعية الدموية والعصبية التي من حوله مهم جدا لتجنب المضاعافات التي يمكن أن تحدث عند العمليات الجراحية للغدة النخامية والسرج التركي. هذه الدراسة أضافت معلومات أساسية ومهمة للجيب الوتدي في السكان السودانيين وسيؤثر إيجاباً علي العمليات الجراجية للجيب الوتدي.

List of Contents

الآيــة ……..……...…….……..… I

Dedication ……..…….……..… II

Acknowledgement…….…….……..…..…III

Abstract (English) …….……...……...…V

Abstract (Arabic)……..…….…..VII

Lis of Contents…….……..…….... IX

List of Table…….……. XIII

List of Figure…….....….XIV

List of Abbrivation…….……..……... XV

1.0 Chapter one ……..…..……..…….. 1

1.1 Introduction ……...…..…...…….……..……1

1.2 Problem of the Study …….…….……..5

1.3 Objective of the Study…….……..…..……5

1.3.1General Objectives…….…….……5

1.3.2 Specific Objective……...….…….……5

2.0 Chapter Two: Litreture Reviews ……..……..…….6

2.1 An Overview of the History of Paranasal Sinus …….……6

2.2 Embryology of sphenoid Sinus ……..……..……9

2.3 Phsiology of sphenoid Sinus …….……11

2.4 Anatomy of sphenoid Sinus ……..……..……13

2.4.1 Sphenoid sinus ……...……...……13

2.4.2 Vascular supply …….……..……15

2.4.3 Innervation ……..……15

2.4.4 Sphenoid Bone ……15
2.4.4.1 Normal Anatomy……16
2.4.4.2 Sphenoid Body ……16
2.4.4.3 Greater Wing ……17
2.4.44 Lesser Wing …….. 17
2.4.4.5 Pterygoid Process …… 18
2.4.4.6 Foraminal Anatomy …… . 18
2.4.5 Pneumatization of the sphenoid sinus …….. 22
2.4.6 Internal Sphenoid sinus Anatomy ……29
2.4.7 Sphenoethmoidal cells (Onodi cells) …… 37
2.4.8 The sphenoid sinus ostia and the intersphenoid septum …… 40
2.5 Pathology of Sphenoid Sinuses …… 43
2.6 Absence of sphenoidal sinuses …… 48
2.7 Surgical Approaches to the Sphenoid Sinus …….. 51
2.7.1 Indications …….. 52
2.7.2 Surgical Approaches …… 53
2.7.2.1 External Transorbital-Transethmoid Approach …… 54
2.7.2.2 Transantral-Transethmoid Approach …… 54
2.7.2.3 Transpalatal Approach …….. 55
2.7.2.4 Transnasal Approaches …… 56
2.7.2.4.1 Transnasal - Transseptal Approach …… 56
2.7.2.4.2 Transnasal - Nontransseptal Approaches …….. 57
2.7.2.5 Transnasal - Transethmoid Approach …… 57
2.7.2.6 Direct Transnasal-Nontransethmoid Sphenoidotomy …….. 58
2.7.2.7 Functional Endoscopic Sinus Surgery …… 58
2.7.2.7.1 Pathophysiology of Sinusitis …….. 63

2.7.2.7.2 Initial Evaluation and Treatment ……. 64
2.7.2.7.3 Candidates for Sinus Surgery ……66
2.7.2.7.4 Nonendoscopic, 'Conventional' Sinus Surgery vs. FESS ……. 67
2.7.2.7.5 Surgical Technique ……..…… 68
2.7.2.7.6 Postoperative Care …… 69
2.7.2.7.7 Outcome ……...…….……69
2.7.2.7.8 Complications ……...…… 70
2.7.2.7.9 Limitations of FESS ……...…….. 71
2.7.2.7.9.1 Acute Severe Ethmoid and Frontal Sinusitis …….…… 71
2.7.2.7.9.2 Nasal and Sinus Malignancies ……..…….. 71
2.8 Computer Tomography and PNS …..…… 72
2.8.1 Basic Concepts ……...…… 73
2.9 Previous Studies ……..…….. 76
3.0 Chapter Three: Materials and Methods …….……...84
3.1 Materials ……..…….. 84
3.2 Data Collection & Analysis ……..……..…...… 85
3.2.1 Data collection ……..……..…….85
3.2.2 Statistical analysis ……...……..……..88
4.0 Chapter Four: Result ……...……..…..89
4.1 Table & Graphs ……..……..……..92
5.0 Chapter Five ……..……..…….. 112
5.1 Discussion ……...…….112
5.1.1 Anterior clinoid process ……...…… 112
5.1.2 Greater wing of sphenoid ……...…….. 113
5.1.3 Pneumatization of the pterygoid process …….……. 114
5.1.4 Internal carotid artery ……...…… 115
5.1.5 Optic nerve ……117

5.1.6 Maxillary nerve ……119
5.1.7 Vidian nerve ……..120
5.1.8 PosteriorEthmoid Cell ……..…… 120
5.1.9 Classification of the Sphenois Sinus …… 121
5.1.10 Measurement of the Sphenoid Sinus …….…….. 122
5.2 Conclusion ……...…… 127
5.3 Recommendation ……...…….. 129
References ……..……...……..……. 130
Appendix ……...……..…….…… 150

List of Tables

Table 2.1: Comparison of studies of CT-demonstrated Onodi Cells…...…38
Table 4.1: Distribution of the study sample according to (Gender)……..…92
Table 4.2: Distribution of the study sample according to (Age group)……93
Table 4.3: Distribution of the study sample according to (Pneumatization, Protrusion and Dehiscence)…… ……...…….....94
Table 4.4: Association Relationship between (Pneumatization of ACP, GWS and PP) and (Protrusion & Dehiscence of ICA, ON, MxN and VN respectively) ……..…95
Table 4.5: Relationship between (Pneumatization) and (Gender)…….....97
Table 4.6: Relationship between (Pneumatization) and (Age)……..98
Table 4.7: Relationship between (Protrusion) and (Gender)……..…...…...99
Table 4.8: Relationship between (Protrusion) and (Age)…… …...…100
Table 4.9: Relationship between (Dehiscence) and (Gender)…… …101
Table 4.10: Relationship between (Dehiscence) and (Age)…….. …….102
Table 4.11: Descriptive statistics of line……103
Table 4.12: Over all mean for lines……104
Table 4.13: Descriptive statistics of age ……...…104
Table 4.14: Cross tabulation between line & gender……..……105
Table 4.15: Cross tabulation between line, Onodi cell & gender…...…….106
Table 4.16: Cross tabulation between superior & Inferior with gender..…108
Table 4.17: Cross tabulation between Onodi cell & lines……..….109
Table 4.17: Cross tabulation between Onodi cell & gender……..……..110
Table 4.18: Cross tabulation between Sellar, presellar and conchal with gender…...111

List of Figures

Figure 2.1: Vesalius' images of the skull and the sphenoid bone……...7
Figure 2.2: Embryology of paranasal sinuses……..……..…… 10
Figure 2.3: Anatomy of disarticulated sphenoid bone specimen……...…..19
Figure 2.4: Radiological anatomy of sphenoid bone……...…….21
Figure 2.5: major classifications of the sphenoid sinus……....23
Figure 2.6: The SS was classified into five extra pneumatic extension types……..28
Figure 2.7: Critical structures around the SS……..…..……34
Figure 2.8: Axial and coronal CT images of the SS in four different patients 35
Figure 2.9: vital structures around the sphenoid sinus ……...……..36
Figure 2.10: Onodi cell extending into sphenoid bone ……..……..38
Figure 2.11: sphenoethmoidal cell……..…… 39
Figure 2.12: Absence of the sphenoidal sinus……..……50
Figure 2.13: A patient undergoing nasal endoscopy……..……..59
Figure 2.14: Endoscopic appearance of the left nostril in a normal nose 60
Figure 2.15: Endoscopic view of the normal middle turbinate……..…..61
Figure 2.16: Nasal polyps in the left nostril, blocking the osteomeatal complex ..…. 61
Figure 2.17: Coronal computed tomographic scan showing normal OMC ……..….62
Figure 2.18: Coronal computed tomographic scan showing ethmoidal polyps…..….62
Figure 2.19: *(Top)* Lateral nasal wall (right side) showing turbinates and frontal SS ..65
Figure 2.20: Anatomy of the sinuses…….……66
Figure 4.1: Distribution of the study sample according to (Gender)…….…92
Figure 4.2: Distribution of the study sample according to (Age group)…...93
Figure 4.3: Distribution of the study sample according to (S.S Classification) ...96
Figure 4.4: Cross tabulation between Onodi cell & gender……...…….110

List of Abbrivations

ACA	Anterior Cerebral Artery
ACP	Anterior Clinoid Process
ACH	adrenocorticotropic hormone
BC	Before Chirst
CA	Carotid Artery
CSF	Cerpro Spinal Fliud
CN	Cranial Nerve
CT	Computed Tomography
ETS	Extended trans Sphenoidal
FESS	Functional Endoscopic Sinus Surgery
FISS	Fissure
FSH	Follicle Stimulating Hormone
FOR	foramen
FSDP	Frontal Sinus Drainage Pathway
FR	Foremen Routuntum
GR	Greater
GWS	Greater Wing of Sphenoid bone
ICA	Internal Carotid Artery
Less	Lesser
MCA	Middle Cerebral Artery
MRI	Magnatic Resonance Imaging
MxN	Maxillary Nerve
N	Nerve
OMC	OsteoMeatal Complex

ON	Optic Nerve
OnC	Onodi Cell
Proc	Process
PP	Pterygoid Process
SS	Sphenoid Sinus
Sup	superior
TSH	Thyroid Stimulating Hormone
VN	Vidian Nerve
VR line	Vidian–rotundum line

CHAPTER ONE

1.1 Introduction:

The sphenoid sinus is deeply seated in the skull and is the most inaccessible to surgeons (Cappabianca et al., 2002). In the past, known as the "neglected sinus", has attracted growing attention over the past 10 years due to the development of diagnostic techniques, such as Computer tomography and magnetic resonance imaging (Castelnuovo et al., 2009).

The sinus cavity may be contained entirely within the body of the sphenoid bone, or may extend into the rostrum, pterygoid processes, greater wing, or even into the basiocciput. The degree of pneumatization of the sphenoid sinus may vary considerably. The sphenoid sinus has been described as being sellar, presellar or conchal. The sellar type of sphenoid sinus is well pneumatized with bulging of the sellar floor into the sinus.The presellar type of sinus is situated in the anterior sphenoid bone and does not penetrate beyond the perpendicular plate of the tuberculum sellae. The conchal type of sphenoid sinus does not reach into the body of the sphenoid bone, and its anterior wall is separated from the sella turcica by approximately 10 mm of cancellous bone (Sareen et al., 2005).

The sphenoid sinus has the largest number of important, vulnerable, some vital, structures in close proximity. They include the optic nerve and chiasm, the cavernous sinus, the internal carotid artery, the pituitary gland, the dura, the third, fourth and sixth cranial nerves, the second division of the fifth nerve, the sphenopalatine ganglion, the vidian nerve, and the terminal

branches of the internal maxillary artery (Gady, 2007). More than 50% of the bone covering these structures may be less than 0.5 mm thick and in many cases there may be a bony dehiscence in the sinus (Tan and Ong, 2007). To make things harder, there are some diseases, for example, ascending nasopharyngeal lesions, descending intracranial lesions, mucocele, cholesterol granuloma and neoplasms that may destroy the walls of the sphenoid sinus, which in turn could distort the delicate anatomy of the sinus and its surrounding structures (Chapman et al., 2011).

Complications such as arterial haemorrhage, visual loss, and extra-ocular palsies occurring in the course of endoscopic sinus surgeries or transsphenoidal pituitary procedures can be attributed to the proximity of carotid artery and cranial nerves to the sphenoid sinus. A sound knowledge of sphenoid anatomy is thus essential to avoid such complications (Tan and Ong, 2007).

Computed tomography (CT) is currently the modality of choice in the evaluation of the paranasal sinuses and adjacent structures. Its ability to optimally display bone, soft tissue, and air provides an accurate depiction of both the anatomy and the extent of disease in and around the paranasal sinuses (Zinreich et al., 1987; Zinreich, 1990; Zinreich et al., 1993). In contrast to standard radiographs, CT clearly shows the fine bony anatomy of the ostiomeatal channels (James et al., 2003*)*. With the use of double spiral scanners or multidetector technology, the slice thickness can be reduced to 0.5 mm or less. For the pediatric, elderly, and debilitated patients who may not be able to remain still for prolonged periods of time, this technique offers the best opportunity to acquire a motion-free, high-quality study. The patient may be positioned prone with the head hyperextended or supine with the head in neutral position on the scanning table. Given the ability of spiral

CT to generate very thin images, the quality of reconstructed coronal and/or sagittal images is virtually indistinguishable from that of images obtained in the primary scan plane (James et al., 2003). Besides, being aware of the exact knowledge of anatomic morphology and probable anomalies are of particular importance to the surgeon.

For many years, surgical access to the sphenoid sinus was problematic. The most popular technique was the sublabial transseptal approach; other routes were the transethmoidal and transpalatal approaches (Cakmak et al., 2000; Doglietto et al., 2005; Elwany et al., 1999). The external fronto-orbital approach to this region was aggressive and sometimes disfiguring, hence the ever-growing interest in endoscopic intranasal techniques, which offer a practical alternative to the classic approaches.

Functional endoscopic sinus surgery (FESS) has been put into practice for almost a quarter of a century. Like traditional sinus surgery, it is associated with serious risks. In order to avoid potential complications of FESS, it is essential to know well defined anatomy and anatomic variations. The advent of functional endoscopic sinus surgery (FESS) and modern imaging techniques have allowed this sinus to be approached more often not only to treat diseases within it, but also as a route to the pituitary gland. In view of the excellent minimally invasive surgical access and advancements in endoscopic techniques, the sphenoid sinus in turn can be used as a path to approach tumors involving the anterior skull base, parasellar region, clivus, petroclival region and the cavernous sinus (Greenfield et al., 2010). Hence, CT scan and endoscopy complement each other [68] and make for a full evaluation of the patient and the disease state (Stammberger and Hawke, 1993) .

There have been several studies focus on the anatomy of the sphenoid sinus and anatomic variation of neurovascular structures adjacent sphenoid sinus by using CT, (Mustafa et al., 2005; Davoodi et al., 2009; Hai-bo et al., 2011; Kazkayasi et al., 2005) These examined the anatomy of the sphenoid sinus and its intimate relationship with surrounding structures. Other authors have studied and made surgical measurement to sphenoid sinus and some proposed scales of sizes (Hai-bo et al., 2011; Jae Min Shin et al., 2012) and reported that the anatomical figures are the key know-how for the surgeon in sinus surgery. Sphenoid sinus surgery is rather difficult because of the situation with the variation in its structure, and designed several lines to assess sphenoid sinus by using multiplanar CT scan, although all these published studies on the anatomy of the paranasal sinuses, there are still dimensions of the sphenoid sinus and the surrounding structures that need to be investigated.

1.2 Problem of the Study:

- Sphenoid sinus is surrounded by several important structures such as internal carotid artery, optical nerve, maxillary nerve, vidian nerve and pituitary gland, which can make sphenoid sinus surgeries very difficult, as the endoscopes and operating microscope are all used in the sinus surgery. However, accurate identification of these structures and well known of surgical measurement of (SS) is the best way to avoid failure of the surgery and severe complications such as bleeding.
- There is no specific characterization of the size and measurements of the normal sinus or related changes due to age gender, side as standard in Sudanese population which make the sinus surgery accommodated with different complications.

1.3 Objectives:

1.3.1 General objectives:

- To study the anatomical relationships between the sphenoid sinus and their important adjacent neurovascular structures using the multiplanar reconstruction technique.

1.3.2 Specific objectives

- To assess the sphenoid sinuses normal dimensions.
- To measure some important distances of sphenoid sinus including, roof, bottom, posterior wall, anterior wall, in terms of their relevancy to the Sudanese population.
- To correlate and determine the sphenoid sinuses variations related with age, side and gender in Sudanese population.
- To generate an index for Sudanese and compare it to standard index.

CHAPTER TWO

LITERATURE REVIEW

2.1 An Overview of the History of Paranasal Sinus

Paranasal sinuses were first identified inside the bones of the skull by ancient Egyptians. Medical writings dating back from 3700 to 1500 BC provide evidence that Egyptians were familiar with the structure of the maxillary bones (Formby, 1960), which means that they might also have been aware of the maxillary sinuses.

After Egyptians, ancient Greek physicians, like Hippocrates, Galen, and Celsus, may have also recognized the paranasal sinuses as part of the structure of the skull. However, they didn't describe them in detail in their works.

A few years later in history, the brilliant mind of Leonardo da Vinci, the "homo universalis," set new foundations for science, especially medicine. He created anatomical drawings of the human body including the skull and the paranasal sinuses, which, however, were discovered many years later by the scientific community (Tsoucalas et al., 2013). This development was followed in 1521 by Berengario da Carpi's initial descriptions of the sphenoid and frontal sinuses (Márquez et al., 2014). The absence of the sphenoid sinus in young children and its subsequent development with maturity was noted by Fallopius, a contemporary of Vesalius.

The great anatomist of the Renaissance, Andreas Vesalius (1514–1564), gave an inadequate description of the paranasal sinuses in his work 'De Humani Corporis Fabrica' written in 1543. Nonetheless, there is a drawing of the sphenoid bone in which the sphenoid sinuses are depicted to be

separated by the sphenoid septum (Fig. 2.1). In terms of the function of the paranasal sinuses, Vesalius stated that these empty cavities reduced the weight of the bone and contributed to the formation of the voice (Garrison, 1993; Garrison, 2003).

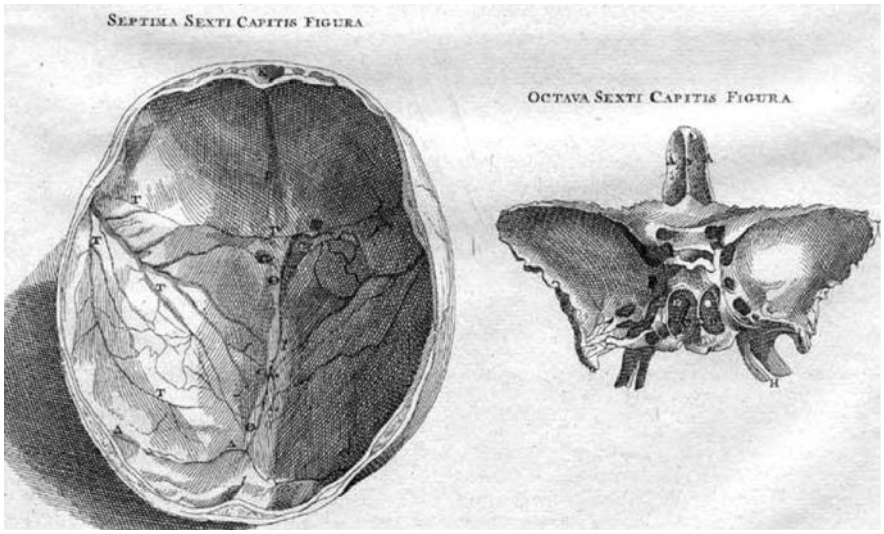

Figure 2.1: Vesalius' images of the skull and the sphenoid bone.
The images constitute anatomical drawings from Vesalius' work 'De Humani Corporis Fabrica.' Most of the illustrations in this book were created by Jan Stephan van Calcar, an Italian artist, one of Titian's students. The left half of the picture shows a transverse cross-section of the skull, depicting the calvaria whereas the right half shows the sphenoid bone. The right-hand image shows the frontal sinus as well as the two sphenoid sinuses, which are separated by the sphenoid septum. Reprinted from Andreas Vesalius, De Humani Corporis Fabrica (Feldmann, 1998).

Nathaniel Highmore is the anatomist whose name is perhaps most associated with the history of the paranasal sinuses, especially the maxillary sinus. This is why for many years, the maxillary sinus was known as "Highmore's antrum." Even today, the maxillary sinus is referred to as "Highmore's antrum" in medical schools, although Highmore was not actually the first anatomist to discover it (Alexandra & George, 2013). It is remarkable that even Highmore was confused about the function of the maxillary sinus and even more about the origin of the mucus that he had sometimes observed in

it. The first to identify that the mucus was not produced by the brain, but was a product of the paranasal structures themselves, was Schneider, in 1660 (Nogueira et al., 2007; Feldmann, 1998).

Another anatomist who contributed to the understanding of the anatomy of the paranasal sinuses was Emil Zuckerkandl from Austria who described the nose and the paranasal sinuses in great detail in 1870 (Nogueira et al., 2007). Furthermore, at the beginning of the twentieth century, Harris Peyton Mosher of Harvard University dissected many cadavers so that he could study the anatomy of the paranasal sinuses (Leopold, 1996). He is also well known for his accurate anatomical description of the ethmoid sinuses. Noting their close relation to the skull base and the orbit, he claimed that intranasal ethmoidectomy, as a surgical procedure, was “the easiest way to kill a patient” (Kaluskar, 2008; Mosher, 1903).

Today's knowledge of the anatomy to a great deal go back to the basic work of Lateral nasal wall anatomy from an endoscopic perspective was described by Walter Messerklinger in Graz, Austria which led to the publication of "Endoscopy of the Nose" in the English language in 1978. Lang and Ritter published detailed anatomical studies including a range of measurements of thickness and distances within the paranasal sinuses from cadaveric studies (Siow, 2005).

2.2 Embryology of sphenoid Sinus

The sphenoid bone consists of the body, the lesser and greater wings and the pterygoid plates, all of them with different and complex ossification centers. The body of the sphenoid develops from the presphenoid and postsphenoid centers, with a contribution from the medial crus of the orbitosphenoid (Madeline and Elster, 1995; Kodama, 1976). The lesser wings develop from the orbitosphenoid and the greater wings from the larger alisphenoid. The pterygoid plates follow a complex development being formed by both intramembranous ossification (the lateral pterygoid plate) and endochondral ossification (the medial pterygoid plate from the lateral cartilage of the embryonic skull) (Curtin et al. 1996; Stool and Post, 1996). Adjacent to the vomer, two paired ossification centers appear called bones of Bertin. They enclose the unossified rostrum of the basisphenoid. This will be the first site of sphenoid pneumatization (Curtin et al., 1996; Bosma, 1976). The relation of vascular and nervous structures such as the optic nerve, maxillary nerve, Vidian nerve and the internal carotid artery to the ossification centers of the sphenoid body explains their close relations to the sphenoid sinus.

The sphenoid sinus develops differently from the other paranasal sinuses. The sphenoid sinus originates during third fetal month as an evagination of the nasal capsule of the embryologic nose. At birth, it arises as a recess between the sphenoid concha and the presphenoid body. Then it starts to develop inferiorly and posteriorly. In the second or third year of life, part of the sphenoid concha fusses with the presphenoid thus forming the sphenoid sinus cavity. The presphenoid recess becomes the sphenoethmoidal recess. After this stage, pneumatization occurs in the presphenoid and the basisphenoid of the sphenoid bone. The origin of the sphenoid sinus on the posterior nasal wall can be clearly identified from the location of its ostium

(Levine and Clemente, 2005). The body of the sphenoid sinus is usually pneumatized by the age of 7 years. The sinus grows throughout childhood, reaching its peak size of 14 X 14 X 12 mm to 20 X 23 X 17 mm at about the age of 20 years. This corresponds to a reported average adult sinus volume of 7.4 cm (range 0 to 14) (Jonathan et al., 2003).

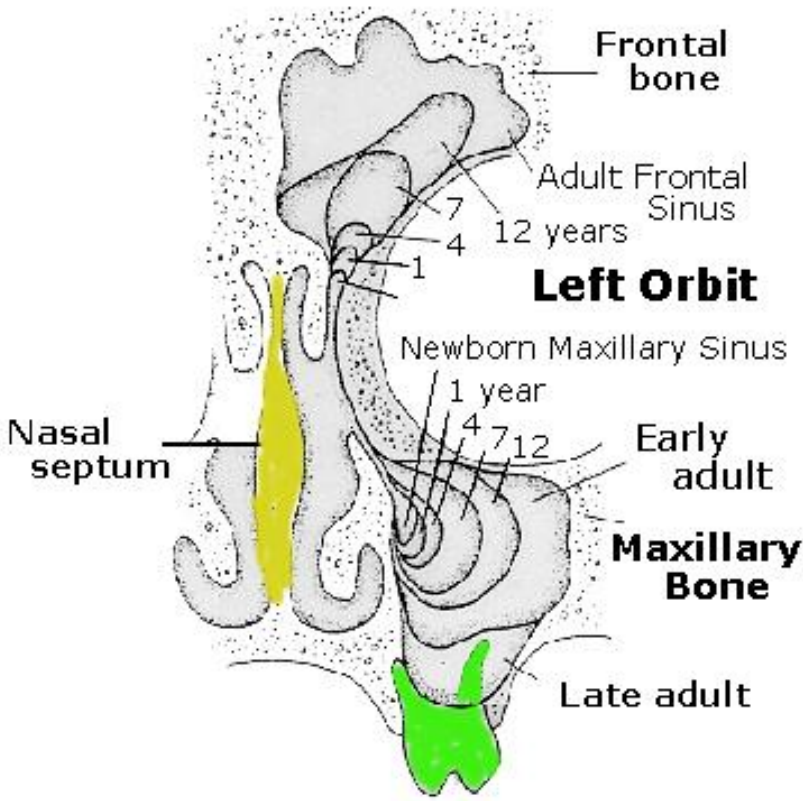

Figure 2.2: Embryology of paranasal sinuses (Balasubramanian, 2012)

2.3 Phsiology of sphenoid Sinus

The function of the paranasal sinuses is not yet completely understood. It has been suggested that the sinuses assist with the warming and humidification of inspired air, and contribute to mucous production. It has also been noted that the paranasal sinuses are important for contributing to increased vocal resonance, and are instrumental for buffering increased pressure in the upper aerodigestive tract. On a more theoretical level, Pneumatization of the bones of the face and skull base may have evolved as a way of decreasing the weight of these bones. Physiologically, there appears to be nothing that separates the sphenoid sinus from the rest of the paranasal sinuses.

The sinuses are lined by respiratory (ie, pseudostratified columnar) epithelia. The paranasal sinuses produce only a small amount of the mucous present in the nasal cavity. The "mucous blanket" is made up of 2 layers: an inner layer and an outer layer. The inner "sol" layer is composed of thin mucous, while the outer "gel" layer mucous is more viscous and tenacious. The mucous is composed of 96% water and 3% to 4% glycoproteins, and is produced by a combination of mucous and serous glands. It contains immunologically active substances and is responsible for trapping foreign particles as small as 2 pm and facilitating immunologic processing.

The clearance of the mucous blanket, from the anterior nasal cavity to the nasopharynx and within the paranasal sinuses, occurs approximately every 10 to 15 minutes in healthy individuals. The movement of mucous occurs as a result of ciliary activity. Cilia are long, thin organelles, 0.3 Frn in diameter and 0.7 Frn in length. When functioning optimally, the ciliary beat frequency is 10 to 15 per second, with an average flow rate of about 0.84 cm per minute. Cilia function best under warm humid conditions, with function significantly impaired when the humidity is less than 50%, or the

temperature is less than 18°C. Ciliary motility is also hampered by apposition of mucosal surfaces, which results in the stasis of the mucous blanket.

In general, normal sinus drainage is dependent on ostial patency, adequate mucous production, and viable ciliary function. The flow of the mucous blanket in the sphenoid sinus is directed towards the natural ostium. The mucous then drains into the sphenoethmoid recess where it is directed towards the nasopharynx (Jonathan et al., 2003).

2.4 Anatomy of sphenoid Sinus

Paranasal sinuses are air filled sacs found in the skull bone. These sacs infact surround the nasal cavity.

There are 4 paired sinuses:

1. Maxillary sinuses.
2. Frontal sinuses.
3. Ethmoidal sinuses.
4. Sphenoidal sinuses.

Each of these sinuses is named according to the skull bones.

2.4.1 Sphenoid sinus

The word sphenoid is derived from the Greek word, sphen, which means wedge-shaped (Bannister et al., 1995**)**. In 1949, Van Alyea described the sphenoid sinus as "…the most neglected of all nasal sinuses." He also agreed with Proetz, who compared the sphenoid sinus to a man whose name begins with Z, because "They are always at the bottom of the list…."

During the last 25 years, we have seen a renewed interest in the sphenoid sinus and its diseases. With the introduction of advanced and sophisticated surgical optics and instrumentation, followed by the introduction of novel surgical techniques (endoscopic and nonendoscopic), most rhinologic surgeons are now more comfortable with approaching the sphenoid sinus surgically (Har-El G, 2003). The sphenoid sinus is now in a process of reclaiming its position in the "center of the head."

The sphenoid sinus is a paired structure that is located predominantly in the sphenoid bone. The two sinus cavities are separated by a complete bony septum, approximately 0.6 mm thick, located in the midsagittal plane. Some

asymmetry in size and shape is nearly always present, but marked septal deviations are relatively rare (Kevin et al., 2000).

The sphenoid sinus reflects its anatomic relations in its walls. Adjacent structures, present before the development of the sinus, produce irregularities in the walls of the sinus as the cavity grows to contact and pass beyond them. Often the extension is such as to form recesses on either side of an elevation, and in the well pneumatized cavities the walls commonly present a continuous sequence of depressions and elevations. In such cases only a thin bony plate separates the sinus from the adjacent structures, and the intimate relationship thus established contributes much to the clinical importance of the sphenoid sinus.

The structures usually involved in this relationship are the blood vessels and nerves which course alongside the sinus on their way to or from the cranial cavity. Also closely related to a sphenoid sinus are its fellow sinus, contiguous posterior ethmoid cells and the sella turcica, which protrudes downward into the sinus (VAN ALYEA, 1941).

Although the attachment of the posterior aspect of the nasal septum to the sphenoid rostrum is almost always in the midline, the intrasphenoidal septum, which originates in the posterior aspect of the sphenoid rostrum, usually changes direction in both the horizontal and the vertical planes. Thus, it creates different sizes and shapes of sinus compartments which are almost always asymmetric. Because of asymetry the intersinus septum could be deviated to one side. This intersinus septum could attach posteriorly to the bony carotid canal.

The sphenoid sinus ostia are located just lateral to the sphenoid rostrum within the anterior wall of the sphenoid sinus. The exact location of the sphenoid ostium may vary, but it is usually found within the middle third of

the distance between the skull base and the sphenoid sinus floor/ roof of nasopharynx (Gady Har-El, 2007).

2.4.2 Vascular supply

The posterior ethmoid artery supplies the roof of the sphenoid sinus. The rest of the sinus is supplied by the sphenopalatine artery. Venous drainage is via the maxillary veins to the jugular and pterygoid plexus systems.

2.4.3 Innervation

The sphenoid sinus is supplied by branches from both V1 and V2. The nasociliary nerve (from V1) runs into the posterior ethmoid nerve and supplies the roof. The branches of the sphenopalatine nerve (V2) supply the floor (Francis et al., 2002).

2.4.4 Sphenoid Bone

The sphenoid sinus is arguably the most variable cuboidal-shaped sinus of all the paranasal sinuses, there being an average of six surfaces in the adult: the anterior, posterior, superior, inferior, medial, and lateral walls. However, in addition to its functional relationship with the nasal cavity, the sinus is strategically located in one of the more complex regions in all of human anatomy by virtue of its location within the sphenoid bone. The endocranial surface of this bone serves as the seat for endocrine activity, as a conduit for cranial nerves responsible for vision, ocular movements, nasal mucosal gland stimulation, and nasal sympathetic innervation and as a major vascular supply for the nasal cavity (Dixon, 1973).

The sphenoid bone is located in the central skull base between the frontal and ethmoid bones anteriorly, the temporal bones laterally and the occipital

bone posteriorly. The optic canal, superior orbital fissures, foramena rotundum and foramena ovale are found in this complex bone. They form important transition zones between intracranial and extracranial structures.

2.4.4.1 Normal Anatomy

The sphenoid bone consists of four parts: body, greater wing, lesser wing and pterygoid process. Viewed anteriorly, the greater wings of the sphenoid resemble wings of a bird while the pterygoid processes resemble the extended limbs (Fig. 2.3).

2.4.4.2 Sphenoid Body

The sphenoid body is cuboidal and contains the sphenoid sinus. The superior surface, termed the planum sphenoidale, is fiat and it articulates anteriorly with the cribriform plate (Fig. 2.3). The limbus sphenoidale demarcates the posterior limit of the planum sphenoidale while the tuberculum sellae forms the anterior margin of the pituitary fossa.

The sella turcica is a large depression in the sphenoid body and contains the pituitary gland. The dorsum sellae forms the posterior boundary of the sella and extends laterally as the posterior clinoid process. The clivus extends from the dorsum sellae to the foramen magnum. It is derived from the fusion of the sphenoid bone (basisphenoid) and the occipital bone (basiocciput). The anterior margin of the clivus blends into the sphenoid sinus while the petroclival fissure forms the lateral border. The anterior face of the sphenoid bone has a midline crest called the sphenoidal crest. This crest articulates with the nasal septum. The ostia of the sphenoid sinus can be seen on either side of the sphenoidal crest. The cavernous sinus and related structures form the lateral face of the sphenoid bone. The carotid artery frequently grooves

the sphenoid sinus. The inferior face of the clivus forms the roof of the nasopharynx.

2.4.4.3 Greater Wing

The paired greater sphenoid wings contribute to the formation of the middle cranial fossa and the orbit (Fig. 2.3). The foramen rotundum is located anteromedially while the foramina ovale and spinosum are seen posterolaterally. The posteromedial surface forms the anterior margin of the foramen lacerum. The orbital surface forms the posterolateral wall of the orbit. The medial margin of the greater sphenoid wing forms the inferior margin of the superior orbital fissure.

2.4.4.4 Lesser Wing

The paired lesser wings extend laterally from the planum sphenoidale. Medially they are attached to the body of the sphenoid by two roots. These two roots define the optic canal. The lower root, the optic strut, separates the optic canal superiorly from the superior orbital fissure inferolaterally. The lesser wing forms the superior margin of the superior orbital fissure. The posteromedial extension of the lesser wing gives rise to the anterior clinoid process.

2.4.4.5 Pterygoid Process

The pterygoid processes extend inferiorly from the junction between the body and greater sphenoid wing. Each pterygoid process consists of two plates, the medial and the lateral, which fuse anteriorly and superiorly. The pterygoid process is separated from the maxillary sinus anteriorly by the pterygopalatine fossa (CHONG et al., 1998).

2.4.4.6 Foraminal Anatomy

The foramen ovale is located in the posterolateral aspect of the greater wing (Figs 2.3 and 2.4). It connects the middle cranial fossa and the masticator space and transmits the mandibular nerve. The size of the foramen varies from side to side and from patient to patient. As a general rule, the foramina should not differ by more than 4 mm.

The foramen spinosum is also located in the posterolateral aspect of the greater wing. It lies immediately posterolateral to the foramen ovale and transmits the middle meningeal artery. The diameter also varies from side to side but should not exceed 2 mm. If the diameter exceeds 5 ram, the patient should be evaluated for middle meningeal artery abnormality (Sondheimer, 1971).

The foramen rotundum is located at the base of the greater wing, just inferior to the superior orbital fissure (Figs 2.3 and 2.4). It connects the middle cranial fossa with the pterygopalatine fossa and transmits the maxillary nerve.

At the junction of the pterygoid process and the sphenoid body is the Vidian canal, which connects the foramen lacerum posteriorly and the pterygopalatine fossa anteriorly. It lies inferior and medial to the foramen rotundum and their distance apart is determined by the degree of pneumatization of the sphenoid sinus.The Vidian canal transmits the Vidian artery, a branch of the maxillary artery and the Vidian nerve (the greater superficial petrosal nerve together with the deep petrosal nerve forms the Vidian nerve).

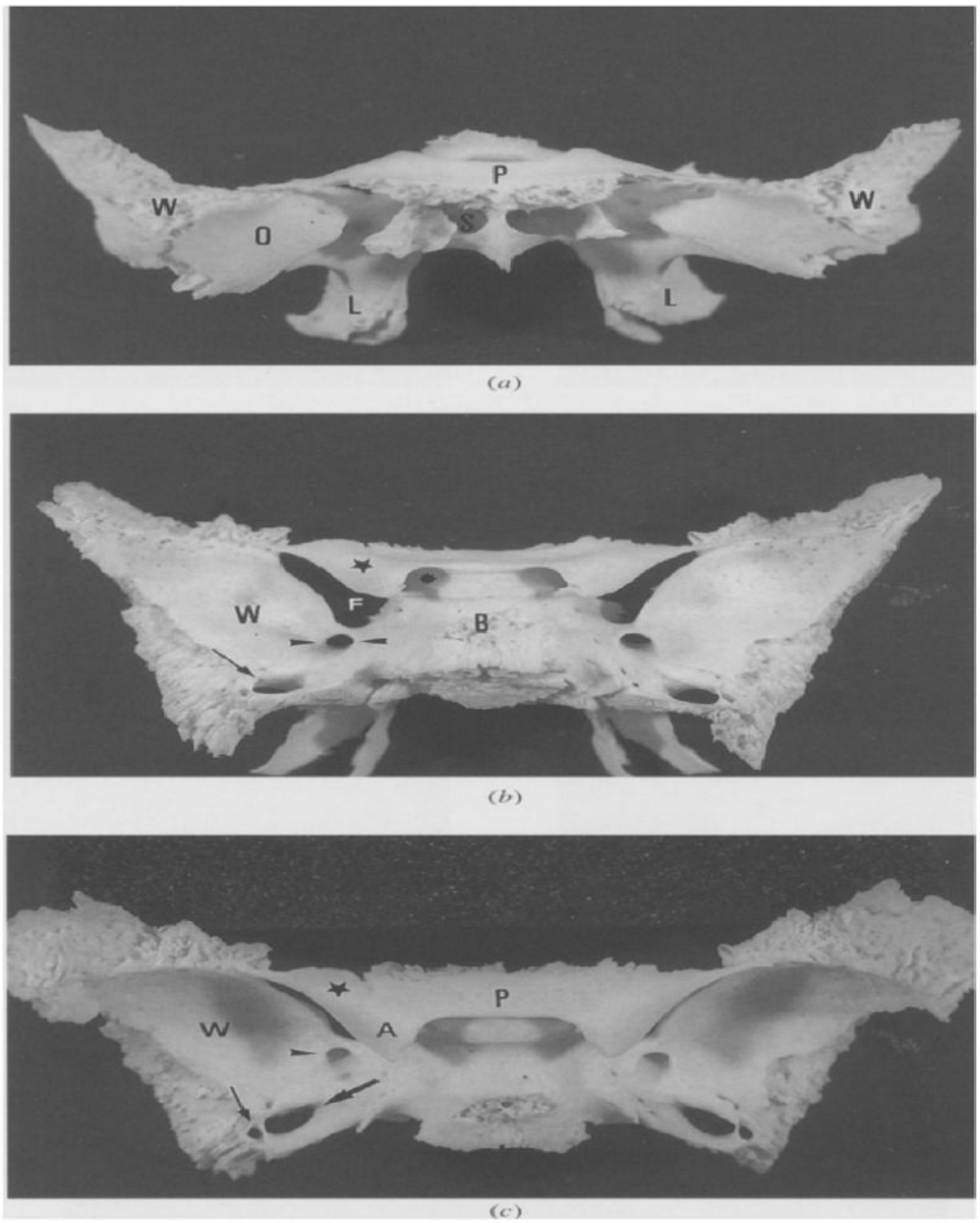

Figure 2.3: Anatomy of disarticulated sphenoid bone specimen.

(a) Anterior view shows the greater wings of the sphenoid bone resembling the wings (W) of a bird with the pterygoid process (L) forming the extended limbs. Note the posterior wall of the right orbit (O), sphenoid sinus (S) and planum sphenoidale (P). (b) Posterior view shows the left lesser wing (star), greater wing (W) and body (B) of the sphenoid bone. Note the optic foramen (asterisk), superior orbital fissure (F), foramen rotundum (arrowheads) and foramen ovale (arrow). (c) Superior view shows planum sphenoidale (P), left lesser wing (star), greater wing (W), anterior clinoid process (A), foramen rotundum (arrowhead), foramen ovale (thick arrow) and foramen spinosum (thin arrow) (Chong et al., 1998).

The optic canal is the only canal passing through the lesser wing (Figs 2.3 and 2.4). The lesser wing is attached to the sphenoid body by two roots. These roots therefore define the roof, lateral wall and floor of the canal. The sphenoid body forms the medial wall. The inferior root or optic strut separates the optic canal from the superior orbital fissure. The optic canal transmits the optic nerve and the ophthalmic artery. The superior orbital fissure is formed by the lesser wing superiorly, the greater wing inferiorly and the sphenoid body medially.

The superior orbital fissure transmits the cranial nerves III, IV, VI and the ophthalmic division of V. It also transmits the ophthalmic vein. The middle third of the fissure also contains the annulus of Zinn, the common tendinous origin of the extraocular muscles (Chong et al., 1998).

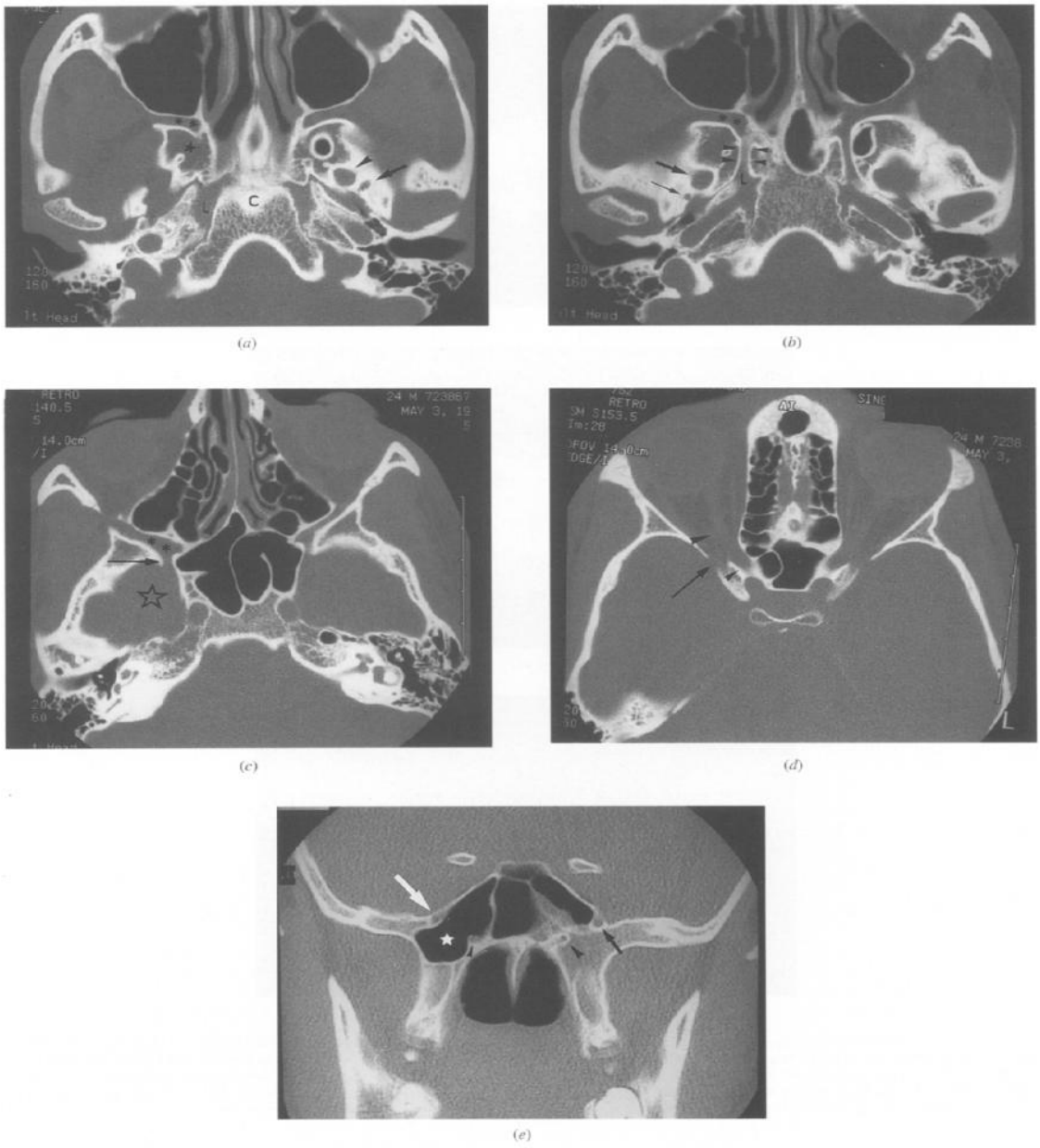

Figure 2.4: Radiological anatomy of sphenoid bone.

(a) Axial CT at the level of the skull base shows the left foramen ovale (arrowhead) and foramen spinosum (arrow). Note the right pterygopalatine fossa (asterisks), pterygoid process (star), foramen lacerum (L) and clivus (C). (b) Axial CT 3 mm superior to (a) shows the right Vidian canal (arrowheads) connecting the pterygopalatine fossa (asterisks) with the superior portion of the foramen lacerum (L). Note the right foramen ovale (thick arrow) and foramen spinosum (thin arrow). (c) Axial CT 6 mm superior to (b) shows the right foramen rotundum (arrow) connecting the middle cranial fossa (star) with the upper portion of the pterygopalatine fossa (asterisks). (d) Axial CT 12 mm superior to (c) shows the superior portion of the right superior orbital fissure (arrow), the optic nerve (large arrowhead), and the optic canal (small arrowhead). (e) Coronal CT shows the left foramen rotundum (black arrow) and Vidian canal (large arrowhead). The right foramen rotundum (white arrow) and Vidian canal (small arrowhead) are widely separated by pneumatised root of the pterygoid process (star) (Chong et al., 1998).

2.4.5 Pneumatization of the sphenoid sinus

The body of the sphenoid bone develops from two paired ossification centers: the presphenoidal anteriorly and the postsphenoidal posteriorly. A laterally located ossification center forms the greater and lesser wings and pterygoid process. Pneumatization of the sphenoid sinus progresses from anterior to posterior, forming the main sinus cavity that occupies the body of the sphenoid bone, and may extend into the dorsum sellae and clivus. Aeration of the more peripheral ossification centers results in pneumatization of the greater and lesser wings, anterior clinoids, and pterygoid processes (Yonetsu et al., 2000).

There are various ways to classify the types of sphenoid sinus. Cope (1917) used the planes of fusion between ossification centers as the boundary line and classified the sinus into presphenoidal, postsphenoidal, and intermediate types according to variations in its posterior limits.

The widely adopted classification of the sphenoid sinus proposed by Hammer and Radberg classified the sinus into three general types that occur at different frequencies and reflect the degree of pneumatization of the sphenoid bone: sellar, presellar, and conchal (Fig 2.5**).** The sellar type of sphenoid sinus occurs in approximately (86%) of individuals, and represents a well pneumatized sphenoid body with full indentation of the sella into the sinus (sinus pneumatization extends beyond a vertical line drawn through the tuberculum sellae). The presellar type (11%) has a moderate amount of sphenoid Pneumatization with no sellar indentation (the sinus cavity remains anterior to a vertical line drawn through the tuberculum sellae), while in the conchal type (3%), there is minimal pneumatization of the sphenoid bone. The various patterns of pneumatization are illustrated in (Fig. 2.5a–c), respectively. This classification was widely adopted because transsphenoidal

surgery focused mainly on the sellar region during that era (Hammer and Radberg, 1961).

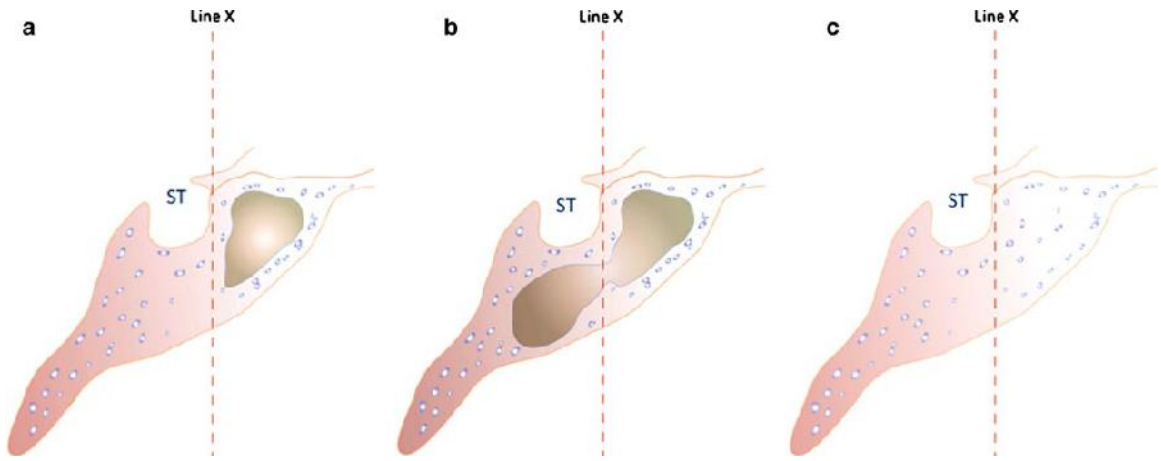

Figure 2.5: **a** Presellar type of pneumatization, **b** sellar type of pneumatization, **c** conchal pneumatization (ST sella turcica) line X vertical line drawn through tuberculum sellae, presellar type: pneumatization remains anterior to line X, sellar type: pneumatization extends beyond line X, conchal type: filled with bone. Figures a–c illustrating the types of pneumatization pattern (Anusha et al., 2013)

There are some modifications to this classification system. For example, Lang adds a fourth classification that he refers to as postsellar (Lang, 1989). This designation indicates the extension of Pneumatization posterior to the hypophysial indentation. In a small number of people, there is no pneumatization of the sphenoid bone. There is, of course, additional variability in younger people who have not undergone complete Pneumatization of the sphenoid bone. Elwany et al. (1983) divided the sphenoid sinus into presellar and postsellar types using a vertical line running through the tuberculum sella boundary. Cho et al. (2010) subdivide the sellar type into the complete and incomplete sellar types, and Li et al.

(2010) divide the SS into six types: no development, conchal, presellar, half sellar, full sellar, and postsellar. Although these modifications provide more details regarding the morphological features of the SS, all of the above classification systems are based on the traditional transsphenoidal approach while focusing on the sellar floor area.

During recent decades, with a better understanding of the anatomy of the sellar and parasellar regions as well as the tremendous development of endoscopy, the traditional transsphenoidal approach has expanded beyond the area of the sellar floor. An increasing number of neurosurgeons in different centers worldwide are reporting their experiences in treating suprasellar, parasellar, petrous apex, and clival lesions or even neoplasms located in the middle cranial floor using the ETS approach (Wang et al., 2004; Kitano & Taneda, 2007; Kassam et al., 2008a; Kitano et al., 2008; Zhao et al., 2010). Moreover, Kitano & Taneda (2009) report the use of the ETS trans-lamina terminalis approach to surgically treat two cases of purely intraventricular CPs, which indicates that the ETS approach can be used to surgically treat lesions inside the third ventricle. In this situation, the previous morphological description of the SS is insufficient.

Wang et al. (2010), adopted new classification for the sellar pattern of pneumatization into six types depending upon extent of sphenoid sinus Pneumatization into the surrounding bony structures; which provides a new understanding of the natural corridor required to reach the target surgical region during the ETS approach.

1- Sphenoid body type where the pneumatization is confine to the body of the sphenoid bone and does not extend beyond the VR line directed along

the medial edge of the anterior end of the vidian canal and the extracranial end of the foramen rotundum.

2- Lateral type where the sinus extends lateral to a line connecting the medial edge of the anterior opening of vidian canal, which is located in the line of fusion between the pterygoid process and the body of the sphenoid bone transmitting the vidian nerve and vessels, and the extra cranial end of foramen rotundum (VR line). Three lateral subtypes were found: greater wing, pterygoid, and full lateral types. These rates are reported 12%, 42%, 77% by Wang et al. and 21.2%, 37.2%, and 41.6% by Lu et al., respectively (Wang et al., 2010; Lu et al., 2011).

Pneumatization of the greater wing is seen in 10.7 - 34% of the population. The superior wall is facing to the middle cranial fossa and contains arachnoid pits. Pneumatization of the pterygoid process is seen in 29 - 67%. The lateral recess enables access to the anteromedial part of the cavernous sinus, middle fossa and Meckel's cave by extended transsphenoidal approach (Wang et al., 2010).

3- Posterior (Clival) type where the posterior wall of sphenoid sinus extended beyond the vertical coronal plane of the posterior wall of pituitary fossa. There are 4 types of clival extensions:

- ***Subdorsum***, The sinus extends posterior to a line directed along the posterior wall of the sella but not into the dorsum sellae or into the clivus below the level of the vidian canal.
- ***Dorsum***, The sinus extends above the line directed along the floor of the sella (line 2) and into the dorsum sellae.

- ***Occipital***, The expansion of the sinus behind the posterior wall of the sella (line 1) extends inferiorly below the level of the horizontal plane directed along the upper edge of the paired vidian canals (line 3).
- ***Combined dorsum-occipital types***. The sinus extends superiorly into the dorsum and downward below the horizontal plane directed along the upper edge of the vidian canals.

Their rates are reported 23.5%, 63.2%, 1.5%, and 11.8% by Wang et al. and 12.4%, 71.9%, 14.6%, and 1.1% by Lu et al., respectively [2,8]. The carotid arteries may protrude lateral wall of the clival recess. This space enables access to clival and petrous apex lesions, furthermore anterior lip of the foremen magnum, the odontoid process and anterior surface of the brain stem by extended transsphenoidal approach.

4- Superior type referred as lesser wing type (optico carotid or tuberculum recesses) where the pneumatization extended into the lesser wing and possibly into the anterior clinoid process. Pneumatization of the anterior clinoid process makes opticocarotid recess between the optic canal and carotid prominence (Wang et al., 2010). This anatomical relationship is crucial for optic nerve disturbance due to surgical complication or fungus sinusitis. Pneumatization of the anterior clinoid process is seen in 4-43%. The anterior clinoid process is also aerated by sphenoethmoidal cells (Hiyama et al., 2015).

5- Anterior type; The sinus has an anterolateral protrusion that extends anterior to a transverse line crossing the sphenoid sinus side of the sphenoid crest to form an anterior recess facing the maxillary sinus. The sphenomaxillary plate separates the sphenoid and maxillary sinuses in this

anterior type of recess. This type of sinus extends anteriorly above the sphenopalatine artery and foramen. Identification of the sphenomaxillary plate is important for preventing from misrecognizing the SS as a posterior ethmoid cell.

6- Combined type, more than one type of extension appears in the same sinus.

Most relevant to the surgeon is sphenoid pneumatization that extends to those segments of bone that cover vital structures. Depending on the pneumatization process, the bone covering the sella, carotid arteries, optic nerves, branches of the trigeminal nerve, and the vidian nerve can either be very thin or even absent, causing these structures vulnerable to injury during surgery. The right and left sphenoid sinuses are divided by a central indentation. The brain and optic chiasm are retracted sagittal intersinus septum. It is located in the mid- line, producing symmetric paired sinuses in only 27% of specimens, and it is fully vertical 25% of the time (Hammer & Radberg, 1961). In the majority of sinuses, the intersinus septum is situated in the midline anteriorly and then deviates to either side as it extends posteriorly (43%). Furthermore, there may be multiple septa and, in some cases, none at all.

The size of the sinus is highly variable. Schaeffer reported general dimensions of 14 x 14 x 12 mm (Schaeffer, 1920). In elderly patients, Lang showed an average width of 13.5 mm superiorly, 16.9 mm in the middle, and 18.7 mm inferiorly (Lang, 1989). The length was 19.4 mm superiorly, 4.8 mm in the center, and 18.5 mm inferiorly.

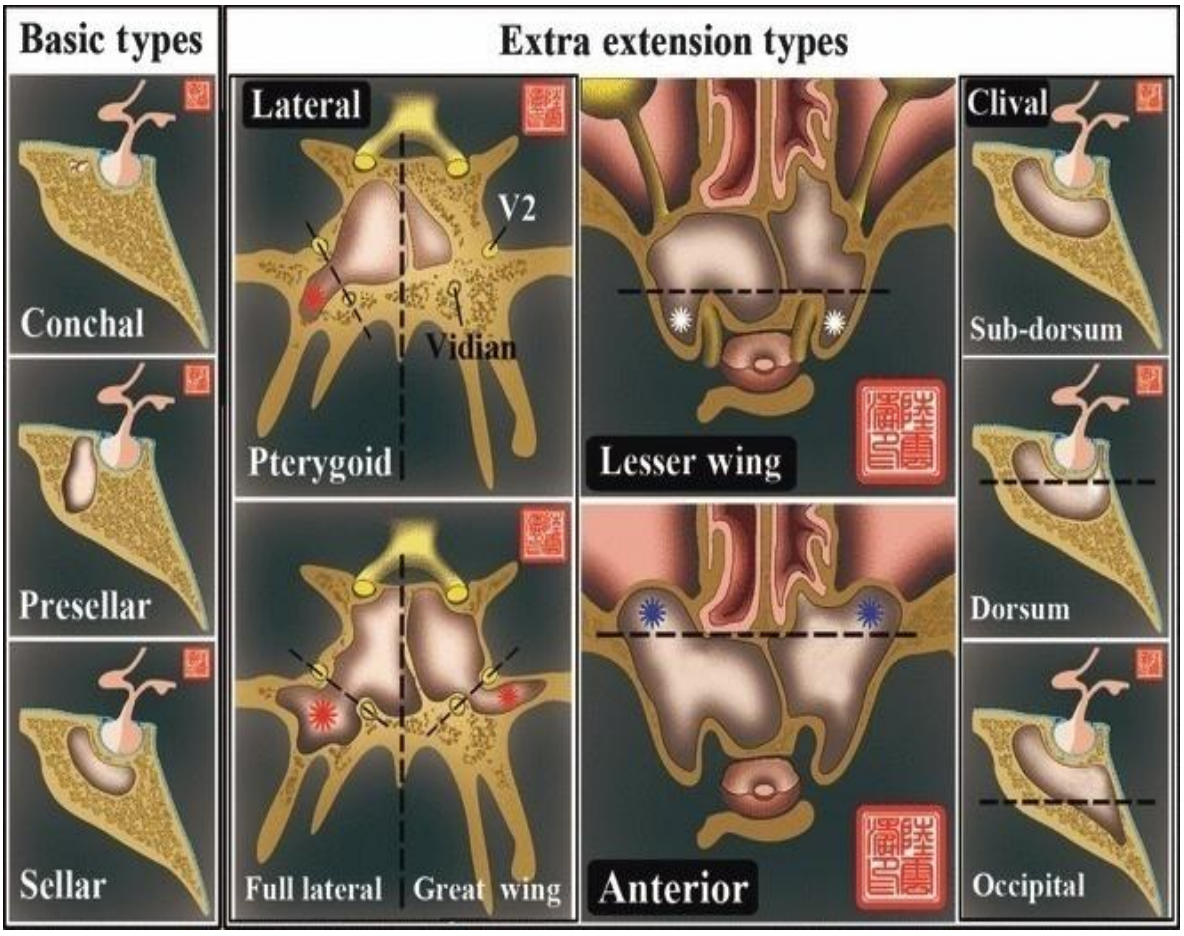

Figure 2.6: The sphenoid sinus was classified into three basic types: conchal, presellar, and sellar; and five extra pneumatic extension types: lateral, clival, lesser wing, anterior, and combined with reference to Rhoton's classification (Wang et al., 2010).

2.4.6 Internal Sphenoid sinus Anatomy

An understanding of the internal anatomy of the sphenoid sinus is particularly important because of the centrality of the sinus relative to vital neural and vascular structures. Centrally, in the roof of the sphenoid sinus lays the sella turcica, which contains the pituitary gland (hypophysis). The average distance between the sphenoid ostium and the sella is 17.1 mm according to (Fujii et al., 1979) and 14.6 mm according to (Lang, 1989). The roof of the sphenoid sinus anterior to the sella, which separates the sinus from the dura of the anterior cranial fossa, is referred to as the planum sphenoidale.

The degree of sella exposure in the sphenoid is dependent on the degree of pneumatization, as described previously. The thickness of the bone overlying the hypophysis varies. In a sellar sphenoid sinus, anteriorly, the area most crucial for surgical access to the pituitary gland, the average bone thickness is 0.4 mm (range 0.1 to 0.7) (Fujii et al., 1979). The bone on the undersurface of the sella tends to be slightly thinner.

Intracranially, just anterosuperior to the sella turcica lays the tuberculum sella and the chiasmatic sulcus, which corresponds to the junction of the planum sphenoidale and the sella turcica. Within the sinus, this produces the tuberculum recess. Although the chiasmatic sulcus does not create a visible impression within the sinus, the prominence created by the optic nerves, as they extend anteriorly in the optic canal, can be seen on the lateral wall of the sphenoid sinus.

In clinical context, the optic nerve can be divided into four segments in order, namely the intraocular segment, intraorbital segment, intracanalicular segment and finally the intracranial segment. The shortest segment measuring about 1 mm in length is the intraocular segment, whereas the

intraorbital segment is the longest segment, measuring 3 cm in length. The intracanalicular segment, which is enclosed by dura, runs along the optic canal.

The intracranial segment, which is the most variable segment of all, based on the position of the optic chiasm, lies medial to the ICA.This segment courses on the superolateral wall of the the sphenoid sinus. The nerve travels medially till the nasal fibers decussate at the optic chiasm, which in turn lies on the tuberculum sellae.

In its course, the optic nerve is the least nourished in its optic canal. It is at this area that it is the most susceptible to injury via direct inflammation of the sinus disease (Bayram et al., 2001). If the sphenoid sinus is accessed by opening the anterior and posterior ethmoids, it is advocated to stay as medially and inferiorly as possible to avoid optic nerve penetration and injury (Stammberger, 1991).

The bone covering the optic nerves is thin and can frequently be dehiscent. Reports of dehiscence have been as high as 23% in radiographic studies (Sirikci et al., 2000), while some cadaveric studies have shown a very low incidence of optic nerve dehiscence. Lang reports that within the sinus, the presence of supraoptic and infraoptic recesses 33% and 38% of the time, respectively (Lang, 1989). The distance between the optic nerves as they enter the optic canals is 14 mm (range 9 to 24) (Renn & Rhoton, 1975). The opticocarotid recess is the small space on the lateral wall of the sphenoid sinus, between the optic canal, superiorly, and the carotid prominence, inferiorly.

The ICA may be categorized into four segments as per the recommendation of Terminologia Anatomica (1998), which is an official anatomical

nomenclature body. The four segments are cervical, petrous, cavernous and cerebral. It essentially segregates the components of the artery as it courses from the point of bifurcation to its terminal branches. The cervical segment begins at the point of bifurcation up to the point of entering the carotid canal, as described earlier.

Once the artery enters the carotid canal, it curves laterally into the foramen lacerum and from this foramen; it curves upwards to enter the posterior part of the cavernous sinus. This segment is termed the petrous segment. Within the cavernous sinus, which makes up the cavernous segment, the artery runs forward and deeply grooves the body of the sphenoid and base of its greater wing. It then curves upwards, pierces the roof of the cavernous sinus medial to the anterior clinoid process and curves immediately backwards to lie on the roof of the cavernous sinus.

Upon exiting the cavernous sinus, the artery makes up the cerebral segment. It subsequently curves upwards lateral to the optic chiasm, and finally reach the anterior perforated substance where it gives off its terminal branches. Each of the right and left internal carotid arteries ultimately divides into the anterior and middle cerebral arteries to supply the cerebral cortex (Sinnathamby, 2006). Besides the main branches, it also gives off the striate arteries, posterior communicating artery and the anterior choroidal artery.

Another classification, the Bouthillier classification of ICA segments describes a seven-segment classification, i.e., the cervical segment, petrous segment, lacerum segment, cavernous segment, clinoid segment, ophthalmic (supraclinoid) segment and the communicating (terminal) segment (Bouthillier et al., 1996). This classification is commonly used by radiologists and neurosurgeons as its segmental course is well appreciated on angiography. Regardless of the classification used to describe the course

of the ICA, a minor injury to any part can result in dire consequences as it is the branch of a main artery from the heart.

Just lateral to the sella extending into the lateral wall is the carotid prominence. This prominence corresponds to the cavernous and anterior clinoid segments of the internal carotid artery (ICA). The degree of bony covering and the length of the carotid that comes into relief in the sinus are highly variable. Fujii et al reports the presence of lateral (cavernous) ICA prominence in the vast majority of cases (Fujii et al., 1979), while Lang noted the lateral ICA prominence in a minority (Lang, 1989). Most articles have identified the anterior (clinoid) ICA creating a carotid prominence in approximately 50% of specimens. The bone overlying the carotid artery is often thinner than that overlying the sella and can, like the bone of the optic canal, be dehiscent. The reported incidence of ICA dehiscence is similar to the optic nerve, ranging from 0% in some cadaveric specimens to 23% in radiographic studies (Lang, 1989; Sirikci et al., 2000). Although the prominence of the ICA is generally in the lateral wall of the sphenoid, it can be in a more medial position. Together with the relatively thin bony covering, this underscores the importance of caution during transsphenoidal surgery of the hypophysis. Mean distance between the internal carotid arteries tends to be shortest at the tuberculum sella, with an average distance of 13.9 mm (range of 10 to 17) (Fujii et al., 1979). The ICA in this particular location is relatively immobile, making it more susceptible to injury than in other locations.

The dura of the cavernous sinus is in contact with a large part of the lateral wall of the sphenoid sinus. Lang reported the mean distance between the medial walls of the cavernous sinuses to be 14.9 mm (range 10.1 to 18.2)

(Lang, 1989). The carotid artery is generally medial to the nerves within the cavernous sinus. However, the maxillary division of the trigeminal nerve, which runs along the lateral and inferior aspect of the cavernous sinus, produces a visible ridge in 29% to 40% of specimens. The prominence produced by the second division of cranial nerve (V2) is known as the trigeminal prominence.

In the floor of a well pneumatized sphenoid sinus inferior and medial to the trigeminal prominence, the vidian nerve in its canal will occasionally come into relief. The vidian canal measures an average of 16.2 mm (range 11.5 to 23). Lang reported that the nerve ran below the floor of the sinus in 38% of specimens, at the floor in 34%, within the sinus in 18%, and was dehiscent 10% of the time (Lang, 1989). The posterior wall of the sphenoid sinus separates the sinus from the brain stem and basilar artery. The bone here tends to be thicker than the other walls. There is generally little need for surgical dissection in this area.

Anteriorly, an incomplete bony wall separates the sinus mucosa from the nasal mucosa and from the posterior ethmoid sinuses. If the sphenoid sinus is larger, it may extend over the pterygopalatine fossa with its contents, and it may be located directly posterior to the maxillary sinus.

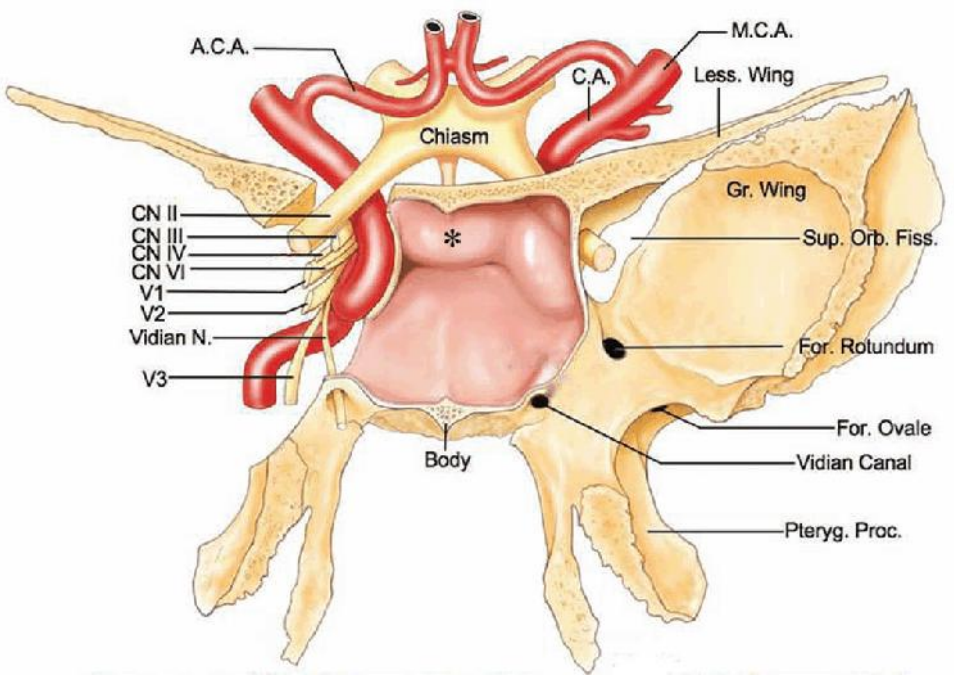

Figure 2.7: Critical structures around the SS. The pituitary body (*), the optic nerve and chiasm, the internal carotid artery, the cranial nerve III, IV, V1, V2 and VI, and the vidial nerve and its canal are demonstrated. The cavernous sinus, the dura matter, the sphenopalatine ganglion and the sphenopalatine artery are also important structures. A.C.A., anterior cerebral artery; C.A., carotid artery; CN, cranial nerve; Fiss., fissure; For., foramen; Gr., greater; Less., lesser; M.C.A., middle cerebral artery; N., nerve; Orb., orbital; Proc., process; Pteryg., pterygoid; Sup., superior. (Wang et al., 2010)

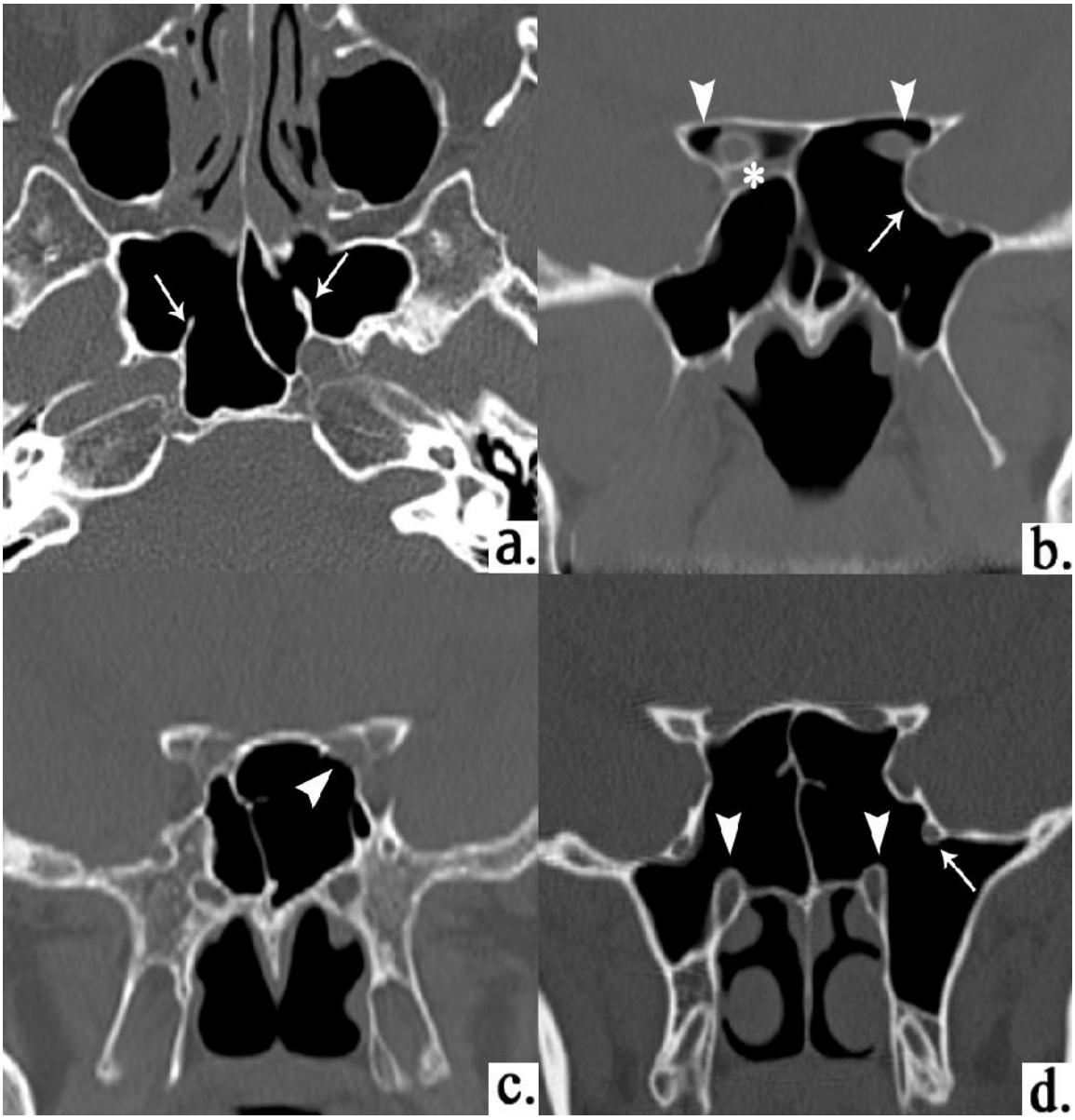

Figure 2.8: Axial (a) and coronal (b-d) CT images of the SS in four different patients. (a)Bilateral accessory septae (arrows) attach to the bilateral ICAs. (b) Bilateral optic nerve protrusion and a left ICA protuberance (arrow) are demonstrated within the SS. Bilateral pneumatization of the anterior clinoid process is also depicted (arrowheads). There is a small opacity under the right optic nerve (*). (c) Left optic canal dehiscence is demonstrated (arrowhead). (d)Left maxillary protuberance (arrow) and bilateral vidian nerve protuberances (arrowheads) are seen on coronal CT image (Hiyama et al., 2015).

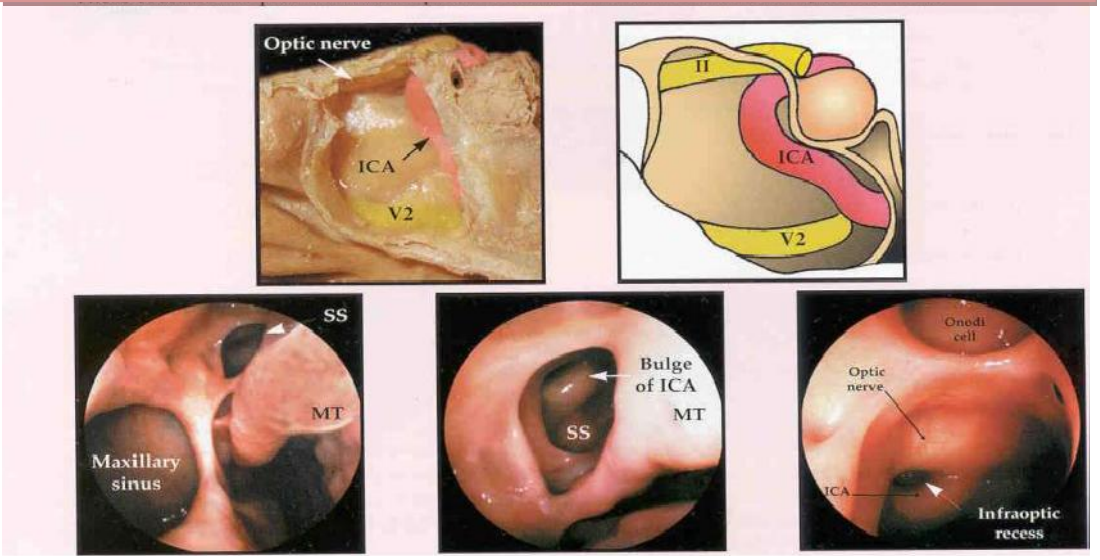

Figure 2.9: vital structures around the sphenoid sinus, bluge of the ICA into sphenoid Sinus (Stammberger, 1991)

2.4.7 Sphenoethmoidal cells (Onodi cells)

Onodi cells were first described in 1903 by Dr. Adolfo Onodi as the posterior-most ethmoid cell that extends superolateral to the sphenoid sinus. Sphenoethmoidal cells are not derived from the SS but from the posterior ethmoid sinus. Sphenoethmoidal cells are the most posterior ethmoid cell that pneumatizes superiorly and laterally into the sphenoid sinus and closely associated with the optic nerve and internal carotid artery. This close proximity of the Onodi cells to the optic nerve and ICA is a risk factor for surgical complications. Identification of the Onodi cell is therefore imperative to minimize perioperative morbidity.

The anterior wall of the SS shares a common wall with the posterior wall of the ethmoid sinus, so there is the reciprocal relation between the sphenoethmoidal cells and the SS. Lesions of the sphenoethmoidal cells such as inflammation or mucocele cause visual disturbances. The presence of onodi cells could be investigated via the endoscopic method, gross anatomical dissection or using Computed Tomography (CT) scans. The study of anatomical variation by CT-scans has become a reliable and non-invasive method in the diagnosis of anatomical variations of paranasal sinuses and the treatment of its complications. It also serves as a road map in surgical planning to prevent the aforementioned surgical complications.

During endoscopic sinus surgery, sphenoethmoidal cells may be misrecognized as the SS and induce insufficient surgery. Recognition of onodi cells can prevent iatrogenic blindness or bleeding, and also to diagnose difficult cases of complications related to onodi cells. Sphenoethmoidal cells also have risk for injury of the optic nerve or ICA, so it is important to identify these cells before surgery.

Table 2.1: Comparison of studies of CT-demonstrated Onodi Cells

Study on CT scans	Prevalence of Onodi Cells in Percentage
Basˇ icˊ (Croatia)	10.4
Jones (UK)	8
Perez-Pinas (Spain)	11
Driben (US)	7
Arslan (Turkey)	8
Weinberger (US)	12
Aibara (Japan)	7
Polynesian (NZ)	11
NZ European (NZ)	24

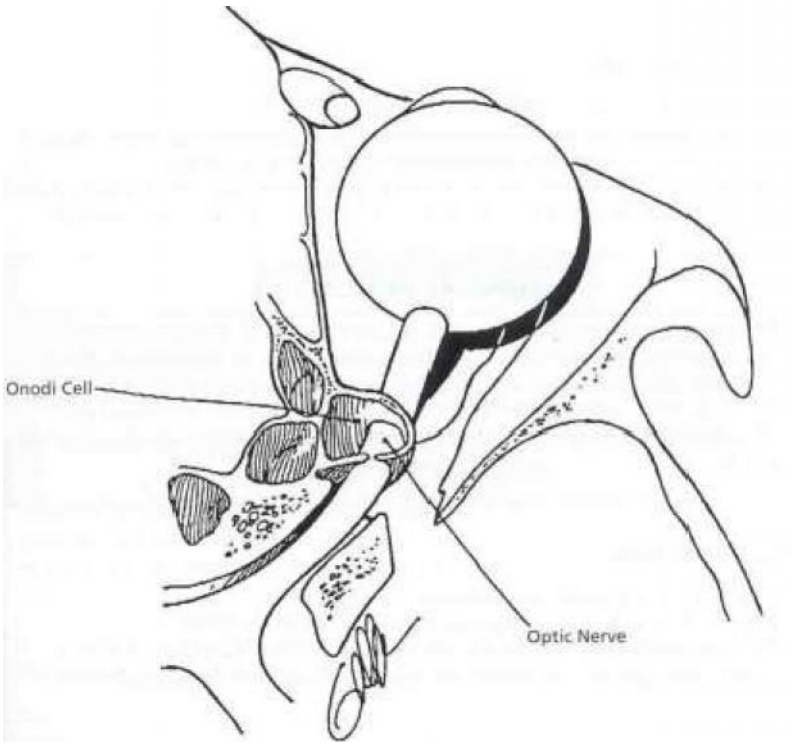

Figure 2.10: Onodi cell (Posterior ethmoid cell) extending into sphenoid bone situated adjecnt to the optic nerve (Stammberger, 1991).

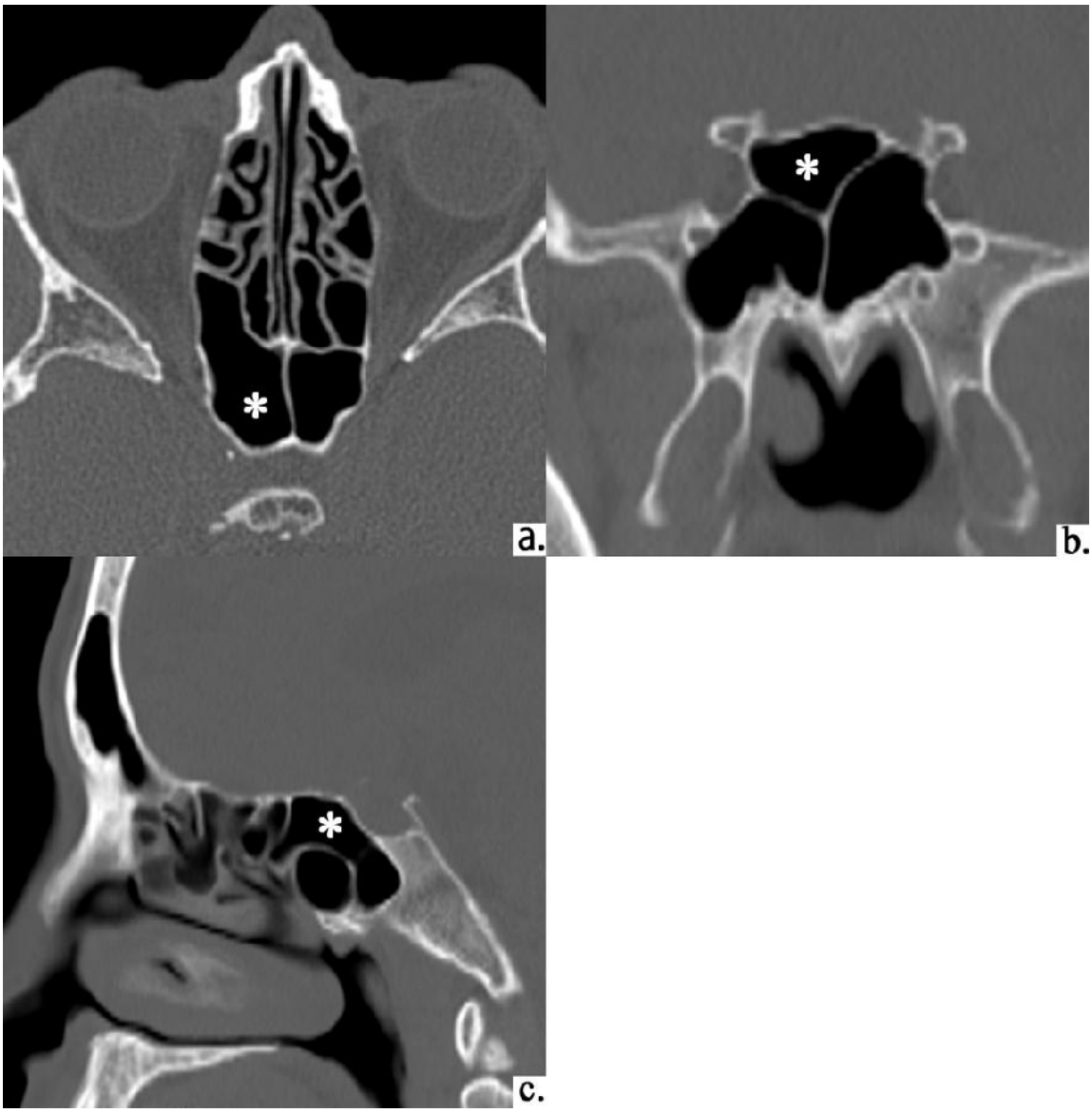

Figure 2.11: Axial (a), coronal (b) and sagittal (C) CT images show the right sphenoethmoidal cell (* in a-c) extending above the right side SS posteriorly (Hiyama et al., 2015).

2.4.8 The sphenoid sinus ostia and the intersphenoid septum

The sphenoid sinus ostia are located on the anterior wall of the sinus and opens into the spheno-ethmoidal recess. It may be round or oval in shape. Madiha et al. (2007) reported 58 % of the 50 ostias in their 25 cadaveric dissections to be oval in shape, and the remainder round, while Lang (1985) found that 70% of the ostia were round-shaped, whereas 28% were ovoid-shaped, with the greater diameter usually oriented in the vertical plane. 68 % of the ostia were more than 4 mm in size, whereas the balances were less than 4 mm in size (Madiha et al., 2007).

The sphenoid sinus ostium can be located and visualized on the medial aspect of the superior turbinate, and this has been considered to be one of the most constant and reliable landmark for endoscopic sinus surgery. Having said that, the vertical, horizontal and oblique distances of the sphenoid ostium from various points serve as good guides to access the ostium during sinus surgery. The vertical distance from the roof of the posterior choanae is a well-described landmark to access the ostia of the sinus. In a study published by Hidir et al. (2011), the vertical height of the sphenoid ostium from the roof of the choanae ranged between 5.7 and 21.5 mm with an average of 10.9 mm, and Abuzayed et al. (2009) reported the vertical height from the posterior choanae to the ostia to be 15 mm in their study on Turkish patients.

The ostia were found to be located at an average of 2.2 cm from the anterior end of the superior turbinate (Sareen et al., 2005). The superior turbinate has been noted to be a reliable and consistent horizontal landmark for localizing the ostia of the sphenoid sinus, be it the anterior end or the posterior end (Bolger et al., 1991; Sareen et al., 2005). The ostia can be localized within 1

cm of the posterior inferior edge of the superior turbinate, and between 1.5 and 3 cm above the superolateral angle of the posterior choana (Gupta et al., 2013).

Most studies report the sphenoid ostia to be located on the middle portion of the anterior wall of the sinus (Hidir et al., 2011; Kim, 2001). The anterior nasal spine and the limen nasi have been used as landmarks to measure the distance of the ostia. The anterior nasal spine has been mentioned as a reference point by Davis et al. (1996) and Turgut et al., 1996). Gupta et al. reported the distance of the ostia as 55 mm from the limen nasi. It is interesting to note that all these different landmarks described by different authors vary not only between the studies, but also between the respective populations.

The intersphenoid septae may occur as a single septum or be present in multiples, for Elwany et al. (1983) found 73 % of their sinuses had multiple septae. 80 % of the intersphenoid septae in Sareen et al.'s work was also multiple in natures. This implies that the septum may not exactly be a reliable guide for approaching the midline in endoscopic sinus surgery.

Although the intersphenoid septae separates the right from the left sphenoid sinus, the septum is often deviated to the right or left side, and only occasionally be found in the midline. It has been found that only one in four septums are located in the midline (Elwany et al., 2005; E lwany et al., 1983). 16.6 % of the septae were in the midline and 56.3 % were found to be deviated to the left and the remainder inclined towards the right side in the 48 Asian cadaveric heads examined by Tan et al. (2007). In 25 Turkish sinuses examined by Madiha et al. (2007), five septaes were deviated to the left, 15 to the right and the remainder five was located in the midline.

The intersphenoid septum may occasionally be deflected to one side attaching to the bony wall covering the optic nerve and/or the ICA, and can be injured when the septum is avulsed during sinus surgery (Chong et al., 2007) Hence, it is important to determine the location of the septum and if it is attached to the wall overlying the carotid artery or optic nerve prior to embarking on surgery.

2.5 Pathology of Sphenoid Sinuses

As stated, sphenoid sinus disease is difficult to diagnose due to a lack of specific symptoms. Sphenoid pathology commonly results as an extension of disease from the posterior ethmoid sinuses. Occasionally, pathology may arise within the sphenoid sinus and may remain isolated within. Pathology from the surrounding region such as the skull base, orbit and petrous apex may expand into the sphenoid sinus. As other paranasal sinuses remain uninvolved such lesions are categorised as part of isolated sphenoid lesions. Isolated sphenoid lesions are uncommon but have been reported with increasing frequency in the past decade (Sethi, 1999; Kieffand Busaba, 2002; Soon et al., 2010; Lee et al., 2009). Due to their non-specific signs and symptoms, these lesions are difficult to diagnose at first presentation (Sethi, 1999). Headache is the most common symptom and may be present in both inflammatory and expansile lesions of the sphenoid sinus. The incidence of headache ranges from 33% to 81% and is typically retroorbital. Space-occupying lesions such as tumors and mucoceles are more likely to present with visual changes than with inflammatory disease. Visual symptoms include diplopia, blurring, isolated oculomotor palsies, and transient loss of vision. Involvement of the cavernous sinus may also result in palsies of the third, fourth, and sixth cranial nerves as well as paresthesias from the fifth cranial nerve. The sixth cranial nerve is the most frequently affected cranial nerve in sphenoid sinus tumors.

The most common disease of the sphenoid sinus is sinusitis. Symptoms include dull-aching headache, nasal discharge, and occasionally visual symptoms. Physical findings are that of mucosal oedema and hypertrophy with opacification of the sinus noted on CT scans. MRI scans would be

indicated if there is any suspicion of extra sinus involvement. Early diagnosis and aggressive treatment are the most important factors in reducing morbidity. The acute phase is managed with antibiotics and decongestants. If possible, the sinus can be cannulated and irrigated. The most common surgical management would be endoscopic sphenoidotomy.

A mucocele is the most common space-occupying lesion in the sphenoid sinus. Mucocoeles of the sphenoid sinus are lined with respiratory epithelium. As there is no drainage pathway in these closed sacs, the mucocoele expands as the secretions collects. As a result it exerts pressure on the surrounding structures, resulting in visual loss from compression of the optic nerve, third (Sethi, 1997), fourth and sixth nerve palsies and even increased intracranial pressure. A rare clinical entity, mucocoeles seem to be more common in patients with a history of radiation to the head and neck. Patients with mucoceles may present with headaches, visual disturbances, anosmia, or even endocrine abnormalities. Soon et al reported up to 30% of patients with isolated sphenoid mucocoeles had a history of previous radiation (Soon et al., 2010). Physical examination is often normal and diagnostic modalities of choice are either CT scan or MRI. CT scans show evidence of expansion and bony resorption whilst an MRI is able to differentiate between the mucocoele and surrounding inflammation based on the varying protein content of the secretions. Radiographs are usually diagnostic. Treatment is sinusotomy with either drainage or removal of the mucocele.

Fungal infections of the sphenoid sinus are the least common of the inflammatory lesions (Lawson and Reino, 1997). They include non invasive

fungal sinusitis, allergic fungal sinusitis and invasive fungal sinusitis. Non-invasive fungal infections with the formation of “fungal balls” are uncommon. In addition to generally vague symptoms, nasoendoscopic findings are often normal (Lee et al., 2009). The presence of ‘fungal balls” is treated by the removal of all fungal debris via a wide sphenoidotomy. Allergic fungal sinusitis occurs in immunocompetent individuals where there is a strong inflammatory response to the fungal infection. This commonly results in a thick mucin that can be expansile and cause bony decalcification. There is also marked mucosal thickening and bone resorption due to the secretion of enzymes. Treatment is a combination of surgical resection and medical treatment with corticosteroids. The role of topical or systemic antifungals remains to be proven. Chronic invasive fungal sinusitis is a slowly progressive disease where patients often present with long standing symptoms of nasal obstruction or a gradually enlarging mass. The fungal elements incite a granulomatous response and histology shows non caseating granulomas with giant cells and evidence of tissue invasion by fungal elements. Treatment of this condition is conservative with long term intraconazole therapy. Acute invasive fungal sinusitis is a rapidly progressive disease with a high mortality rate. It is commonly seen in immunecompromised patients. The offending organism is often Rhizophus or aspergillus. Vascular invasion leads to widespread necrosis of the surrounding tissue. Management is aimed at restoring the immune function of the patient as well as wide debridement of the infected tissue. Systemic therapy consists of intravenous antifungal agents.

Polyps can occur as isolated sphenoid lesions but are more commonly associated with polyps of the posterior ethmoid air cells. The patient usually

has long-standing rhinosinusitis, postnasal discharge, and headache. Radiologic evaluation will show sinus opacification and mucosal thickening.

Inverting papillomas usually result from extension of antral and ethmoidal tumors but primary tumors of the sphenoid have been reported. Treatment should be aggressive as they tend to recur and can undergo malignant transformation. Excision with a wide margin of normal tissue is recommended. High recurrence rates in the sphenoid sinus are typical since margins are difficult to obtain due to the adjacent vital structures.

Malignant lesions rarely occur but include squamous cell carcinomas, adenocarcinomas, lymphoepitheliomas, melanomas, and various sarcomas. Complete excision is usually impossible but sphenoidotomy for biopsy and decompression is usually required in the initial stages of treatment.

Benign tumors of the pituitary constitute the majority of sellar lesions requiring transsphenoidal surgery. These tumors are often described as being encapsulated and are often demarcated from the normal pituitary on radiologic exam. Classically, the tumors were described as basophilic, acidophilic, or chromophobic depending on how they stained during pathologic study. With newer immunostaining techniques, the specific cell origin can be determined in approximately 75% of cases. They now can be classified as containing prolactin, growth hormone, adrenocorticotropic hormone (ACTH), follicle stimulating hormone (FSH), or thyroid stimulating hormone (TSH). Prolactinomas represent 40% to 50% of all adenomas. Somatotropic adenomas causing acromegaly account for 15% to 25% of adenomas. Corticotropin secreting tumors, causing Cushing’s

disease or Nelson's syndrome, represent 5% of tumors. The rarest type of pituitary adenomas includes thyrotropin or gonadotropin secreting tumors and account for less than one percent of tumors. In addition, 10% to 15% of tumors are found to secrete multiple hormones.

Craniopharyngiomas are one of the most common intracranial tumors of childhood but can be seen in older patients. They may be cystic or solid and many show calcifications on radiography. These are slow growing tumors that cause symptoms by compressing adjacent structures including the pituitary, optic chiasm, and other basal brain structures. Total extirpation is the goal as subtotally resected tumors tend to recur. Other sellar lesions include the occasional dermoid and epidermoid cysts, germ cell tumors, chordomas, and both benign and malignant osseous lesions. Also, nearly ten percent of meningiomas occur in the region of the sella (Kevin et al., 2000).

2.6 Absence of sphenoidal sinuses

To treat the disease effectively and avoid complications, otorhinolaryngologist must possess a detailed understanding of paranasal sinus anatomy and its variations (Anik et al., 2005). Furthermore, the surgeon must pay attention to the other anatomical risk factors even after the opening has been identified. These factors, include the skull base, which comes into contact with the superior wall of the sphenoidal sinuses (SS), the cavernous sinus touching its lateral border, and the branches of the sphenopalatine artery running along the inferior to the ostium (Aydinlioglu and Erdem, 2004; Wong, 2004). Despite all these difficulties, not much anatomical research has been dedicated to the location of the opening in the sphenoidal sinuses.

As we mention before in this study, there are three general types of pneumatization of the sphenoid sinus have been described. The first type is the conchal or fetal type, in which only a rudimental sinus is present and is confined to the rostral portion to keep pneumatization at minimal. The second type is called as the presellar type or hypoplastic sinus where the pneumatization extends to the anterior wall of the pituitary fossa. The third type is the sellar, postsphenoid or occipital type. In this type, the pneumatization extends beyond the tuberculum sella (Hammer and Radberg, 1961).

The sphenoid sinus cavities are variable in size, and are often asymmetrical (Peres-Pinas et al., 2000; Tasar et al., 2003). In the fourth fetal month, the sphenoid sinus emerge as evaginations from the posterior nasal capsule into the sphenoid bone and at birth; they become visible as minute (0.5 x 2 x 2 mm) cavities (Anik et al., 2005). By the age of 7, they extend posteriorly to the level of the sella turcica, and by the age of 12, sphenoid pneumatization

reaches its adult size and the sinuses measure on average 14 x 14 x 12 mm(Anderhuber et al., 1992; Peres-Pinas et al., 2000; Tasar et al., 2003).

The lack of any sinus pneumatization by the age of 10 should suggest the possibility of sphenoid pathology (Digre et al., 1989; Lang, 1988). Hajek (1926) described "deficient resorption from corpus sphenoidale" as the pathogenesis of absence of the SS. The absence of paranasal sinuses is an uncommon clinical sign and it refers primarily to the frontal sinuses (12%) and secondarily to the maxillary sinuses (5–6%) (Anderhuber et al., 1992; Digre et al., 1989). The incidence of absence of the sphenoid sinus is reported as 1–1.5% in previous studies (Anik et al., 2005; Antoniades et al., 1996; Degirmenci et al., 2005; Digre et al., 1989; Keskin et al., 2002). The absence of the sphenoid sinus usually occurs with syndromes, such as craniosynostosis, osteodysplasia and Down's syndrome and has also been reported as Hand–Schuller–Christian Disease (Anderhuber et al., 1992; Antoniades et al., 1996). Pneumatization can extend into the greater wing, pterygoid process, and rostrum and the basilar part of the occipital bone (Hajek, 1926; Lang, 1988).

The pathogenesis of absence of the sphenoid sinus has been regarded as the cause of deficient resorption from the body of the sphenoid bone (Hajek, 1926). (Keskin et al., 2002) pointed out that sphenoidal absence can also be categorized as the fourth type of pneumatization.

Making differentiation between the types of the sphenoid sinus is important clinically in planning pituitary surgery. Transnasal surgery would be difficult and dangerous in conchal or absence of the SS. In such cases, employing other operative techniques might be useful (Keskin et al., 2002). Surgeons should also consider the possibility of sphenoidal absence or a rudimentally SS before transsphenoidal hypophysectomy. As a supplement

to the traditional classiffication, absence of the SS can be described as the fourth type of pneumatization.

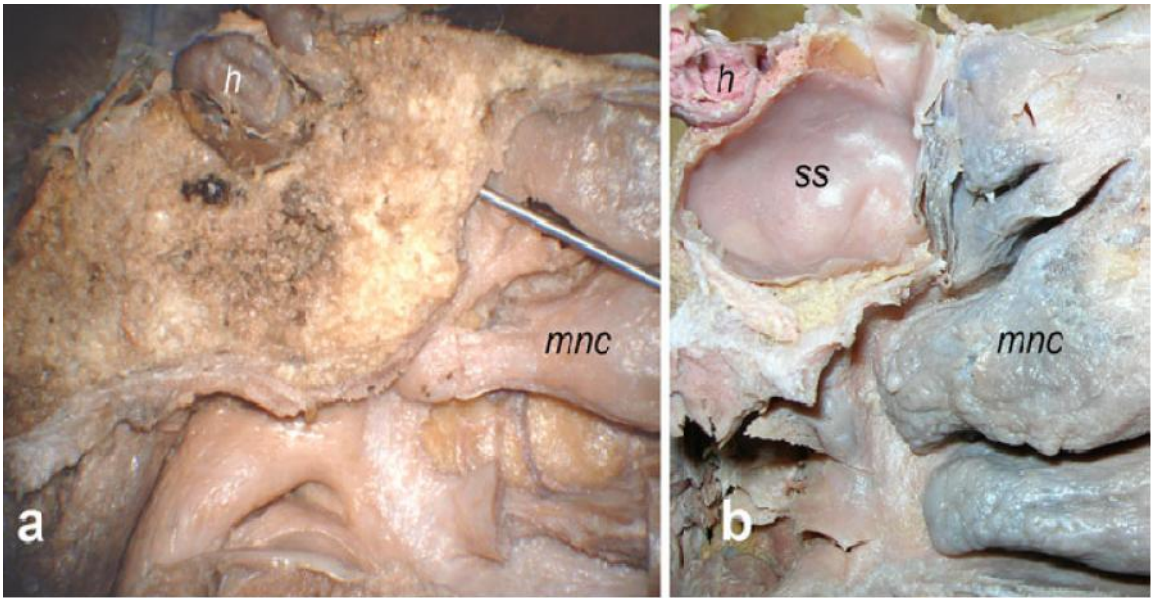

Figure 2.12: a. Absence of the sphenoidal sinus. Probe in the opening of posterior ethmoidal cell, b. presence of the sphenoidal sinus. *h* hypophysis, *ss* sphenoidal sinus, *mnc* middle nasal turbinate (Mustafa et al., 2010).

2.7 Surgical Approaches to the Sphenoid Sinus

The sphenoid sinus is situated in the center of the skull base (Anon, 1996; Levine & May 1993; Rice, 1995; and Sethi, 1995). It is the most posteriorly located of the paranasal sinuses. The sphenoid sinus has the largest number of important, vulnerable, some vital, structures in close proximity. They include the optic nerve and chiasm, the cavernous sinus, the internal carotid artery, the pituitary gland, the dura, the third, fourth and sixth cranial nerves, the second division of the fifth nerve, the sphenopalatine ganglion, the vidian nerve, and the terminal branches of the internal maxillary artery. Although the attachment of the posterior aspect of the nasal septum to the sphenoid rostrum is almost always in the midline, the intrasphenoidal septum, which originates in the posterior aspect of the sphenoid rostrum, usually changes direction in both the horizontal and the vertical planes. Thus, it creates different sizes and shapes of sinus compartments which are almost always asymmetric.

Surgical approaches to the sphenoid sinus began in the early 20th century as recognition of sellar tumors became known with advances in neurology, pathology, and radiology. Krause credits himself with the first transfrontal approach to the pituitary in 1905 and described much difficulty with gaining access to the sella due to the incompressibility of the frontal lobes. Schloffer performed the first transnasal route in 1907. Via a lateral rhinotomy incision, he removed the septum, turbinates, and ethmoids to access the sella, with only the sun as lighting. The next several years led to many advances in the transnasal approach with contributions by von Eiselberg, Stumme, Kanaval, Halstead, and Kocher. In 1910, Cushing performed essentially the present-day sublabial transseptal operation with success. In the 1920's there was a shift back to extracranial routes to the pituitary when antibiotics were

introduced. In the 1960's, Hardy reintroduced Cushing's approach which is now the most common route to the sella (Kevin et al., 2000).

Currently, there are many available surgical approaches to the sphenoid sinus, endoscopic and nonendoscopic. The decision as to which approach to use depends on factors such as the nature of the lesion, the exact location of the lesion, the extent of the lesion, coexisting pathologic processes, the goal of the surgery (e.g., complete tumor removal vs. biopsy), and the experience and comfort of the surgeon with the different approaches. For example, a polypoid process that involves also the ethmoid sinuses will probably dictate transethmoid sphenoidotomy; isolated acute sphenoid sinusitis which requires a large opening for drainage may dictate direct transnasal sphenoidotomy; a midline noninfectious process which does not require permanent drainage may benefit from the relatively "clean" transseptal route.

2.7.1 Indications

For more than a century, the most common indication for sphenoid sinus surgery has been an infectious process. This may include acute, chronic, and fungal or polypoid process as well as complications of sphenoid infection such as sphenoid pyocele. With advancements in surgical optics and instrumentation as well as the introduction of intraoperative computerized navigation systems, sphenoidotomy is increasingly being used as an approach to other structures which are in close proximity. The current indications for sphenoidotomy and sphenoidectomy can be summarized as follows:

- Sphenoid sinusitis (acute, chronic, fungal)
- Sphenoid mucocele/pyocele
- Sphenoid polyposis

- Repair of CSF leak
- Repair of encephalocele (with or without CSF leak)
- Biopsy of tumor (sphenoid, adjacent structure, brain)
- Management of medial temporal bone lesion (e.g., petrous apex cholesterol cyst)
- Approach to the clivus
- Pituitary surgery
- Endoscopic brain surgery
- Approach to the optic nerve/chiasm

2.7.2 Surgical Approaches

The extracranial approaches to the sphenoid sinus can be summarized as follows;

1. Transorbital transethmoid-external
2. Transantral transethmoid
3. Transseptal
   (a) Sublabial
   (b) Transnasal
   - With alotomy
   - With external rhinoplasty approach
4. Transnasal-nontransseptal

(a) Transethmoid

(b) Direct transnasal

5. Transpalatal

2.7.2.1 External Transorbital-Transethmoid Approach

For centuries this has been the most popular surgical approach to the sphenoid sinus. Currently, it is still being performed by some surgeons for the treatment of acute infection. This approach requires ethmoidectomy in order to access the sphenoid sinus. The approach provides excellent control of the orbit, which is important for both the treatment of intraorbital extension of the infection and the avoidance of orbital complications. The procedure has an advantage when the inflammatory process includes the ethmoid complex. However, the constant manipulation of the orbital contents as well as the need for external facial skin incision makes this approach less attractive. Also, we believe that this approach is not useful for isolated sphenoid sinus disease because it requires ethmoidectomy, whether ethmoid sinus disease is present or not. With the increasing popularity of transnasal endoscopic techniques, this approach is seldom used today.

2.7.2.2 Transantral-Transethmoid Approach

The transantral approach to the sphenoid sinus was very popular when the Caldwell-Luc procedure was the standard approach for chronic maxillary, ethmoid and sphenoid sinus disease. The procedure is begun with a sublabial maxillary sinusotomy, followed by posterior ethmoidectomy through the superomedial aspect of the maxillary antrum. The anterior sphenoid wall is now exposed and may be entered. The lamina papyracea is kept under direct vision throughout the procedure; therefore, the orbit is well protected. Also, with this procedure, the surgeon bypasses the infundibulum; therefore, possible damage to the frontal sinus outflow tract is avoided. Because we rarely use the Caldwell-Luc procedure these days to treat maxillary or

ethmoid sinus disease, this route is seldom used for sphenoidotomy. However, this approach has gained recently some renewed interest. This procedure used to treat lesions in extreme lateral extensions of the sphenoid sinus (i.e., pterygoid recess) and lesions of the pterygopalatine fossa (Har-El G, 2005)

2.7.2.3 Transpalatal Approach

This approach may be suitable for certain tumors that extend beyond the sinus into the nasopharynx and into the pterygopalatine space. It is not suitable for the treatment of infections. Also, tumors isolated to the sphenoid sinus and sella turcica are better approached with the transnasal route. The transpalatal approach is also used to treat small and medium sized juvenile angiofibroma tumors with or without extension to the sphenoid sinus (Goldsmith, 1999). The procedure is begun with a palatal incision line and elevation of palatal flap. Different incision lines are used: (**1**) midline incision with or without splitting the uvula; (**2**) lateral incision through the soft palate with preservation of one greater palatine vascular pedicle; and (**3**) a U-shaped palatal incision along the gingival margin. The surgeons favor the U-shaped incision because it minimizes the likelihood of an oronasal fistula and/or palate shortening. The incision is made parallel to the gingival margin, leaving several millimeters of gingival mucosa for closure. The incision extends posteriorly beyond the third molar. A mucoperiosteal palatal flap is elevated off the bony hard palate. Both greater palatine vascular pedicles are identified and preserved. This will ensure flap viability. Next, the soft palate musculature is separated from the posterior edge of the hard palate, allowing initial visualization of the nasopharynx and the floor of

the sphenoid sinus. With use of a drill or Kerrison rongeur, portions of the posterior hard palate and vomer are removed until adequate exposure of the anteroinferior aspect of the sphenoid sinus is achieved. At the end of the procedure, the palatal flap is replaced and closed with interrupted absorbable sutures. Again, this procedure is not appropriate for isolated sphenoid disease or for sphenoethmoid disease.

2.7.2.4 Transnasal Approaches

There are many transnasal approaches to the sphenoid sinus and adjacent structures. We usually divide them into two main groups: transnasal-transseptal and transnasal-nontransseptal approaches.

2.7.2.4.1 Transnasal - Transseptal Approach

The transseptal route provides an excellent approach to the sphenoid sinus. It is a safe, avascular and easy to learn procedure. During the last decade of the nineteenth century and the first decade of the twentieth century, this approach was introduced for management of pituitary lesions. Soon after, this procedure fell into disfavor because of the limited surgical exposure obtained in the absence of surgical microscopes.

Hardy, in the 1950s, introduced microsurgical techniques and reestablished the transseptal-transsphenoidal route as the standard approach to the sella turcica (Hardy, 1969).

Since the size of the nostril is usually the limiting factor in providing wide exposure, and in cases where wide exposure is essential (e.g., transsphenoid pituitary surgery), most transnasal-transseptal approaches incorporate an additional incision line. The most commonly used incision is the sublabial

one through which the septum is approached. Other options include an alotomy incision or a transcolumellar (external rhinoplasty) incision. In 1985, Kennedy introduced the endoscopic transsphenoidal approach for pituitary lesions. Many surgeons use sinus endoscopes to perform the transnasal-transseptal approach to the sphenoid sinus. The surgical steps are the same as those for the conventional, nonendoscopic transseptal approach. The main disadvantage of the transseptal approach is the fact that it is not suitable for management of infection. It does not provide a permanent wide drainage pathway into the nasal cavity.

2.7.2.4.2 Transnasal - Nontransseptal Approaches

This group of surgical approaches to the sphenoid sinus includes the transnasal-transethmoid and the direct transnasal route. With the introduction of endoscopic sinus techniques and instrumentation, transnasal-nontransseptal sphenoidotomy has become increasingly popular. In fact, it is the most common approach to the sphenoid sinus used by rhinologic surgeons. However, it should be noted that these techniques are not new and have been used, without endoscopes, since the late nineteenth century.

2.7.2.5 Transnasal - Transethmoid Approach

The endoscopic version of this approach is the most common one used today for access to the sphenoid sinus. This approach is certainly appropriate in cases where the ethmoid and the sphenoid sinuses require simultaneous exploration. A common example is ethmoid and sphenoid sinusitis with/without polyposis. However, if the goal of the surgical procedure is to address isolated sphenoid sinus disease, or to use the sphenoid sinus as an

access to adjacent structures, violation of the ethmoid complex can be avoided by using the direct transnasal approach. Transnasal ethmoidectomy, although a very common procedure, is not without potential complications and sequelae. Possible immediate serious complications are well known and, fortunately, uncommon. However, delayed sequelae are not rare and may result in significant morbidity. They include synechiae formation, nasal airway obstruction, ethmoid sinusitis, frontal outflow tract obstruction and possible frontal sinusitis, maxillary outflow obstruction and possible maxillary sinusitis, and persistent ethmoid cavity dryness and crusting.

2.7.2.6 Direct Transnasal-Nontransethmoid Sphenoidotomy (The Superior Turbinectomy Approach)

This approach does not involve transseptal surgery and does not include ethmoidectomy; therefore, it avoids any complications related to those procedures. This approach is the fastest, least invasive and overall the best approach for management of isolated sphenoid sinus disease and for approaching lesions adjacent to the sphenoid sinus (Har-El, 2002; Har-El G & Todor, 2003).

2.7.2.7 Functional Endoscopic Sinus Surgery

Functional endoscopic sinus surgery (FESS) is a minimally invasive technique in which sinus air cells and sinus ostia are opened under direct visualization. The goal of this procedure is to restore sinus ventilation and normal function (Stammberger, 1991 and Kennedy 1985).

The ability to treat paranasal sinus disease has been revolutionized by fiberoptic endoscopes and computed tomographic (CT) scanning. Fiberoptic endoscopes have made it possible to examine the nose thoroughly from the anterior nares to the postnasal space. The endoscopic procedure requires local anesthetic and may be performed in the office (Figures 2.13 & 2.14). The specific features that must be identified and assessed during the examination are the middle turbinate and the middle meatus (osteomeatal complex), anatomic obstruction, mucopus and nasal polyps (Figures 2.15 & 2.16).

CT scanning identifies the anatomic relationships of the key structures (orbital contents, optic nerve and carotid artery) to the diseased areas, a process that is vital for surgical planning. CT also defines the extent of disease in any individual sinus, as well as any underlying anatomic abnormalities that may predispose a patient to sinusitis (Figures 2.17 & 2.18).

Figure 2.13: A patient undergoing nasal endoscopy (Robert and Grant, 1998)

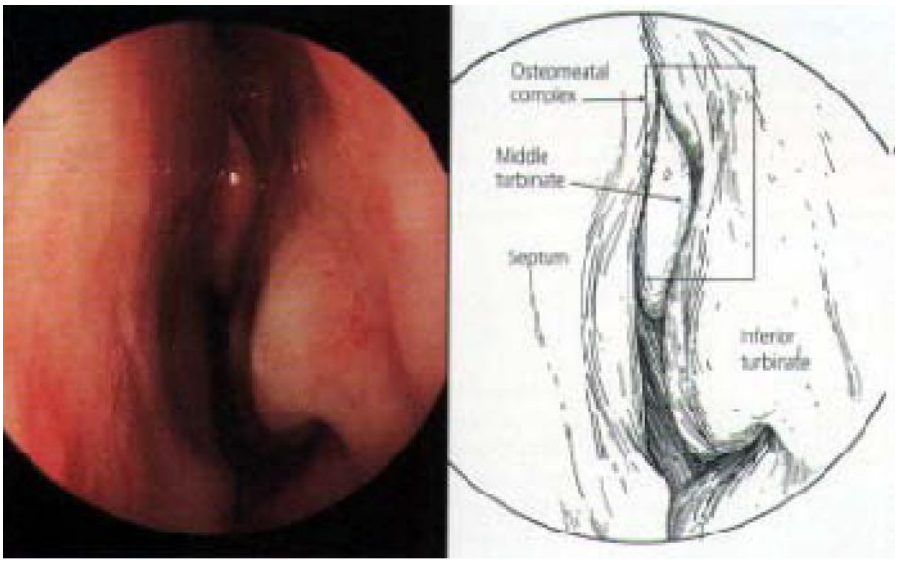

Figure 2.14: Endoscopic appearance of the left nostril in a normal nose. The septum is visible to the left, and the inferior turbinate and middle turbinates are also visible (Robert and Grant, 1998).

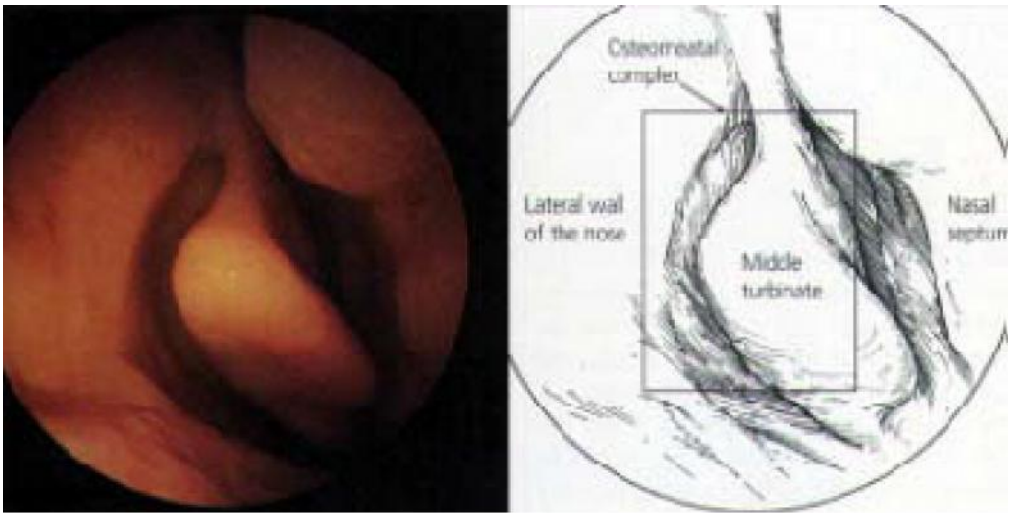

Figure 2.15: Endoscopic view of the normal middle turbinate, looking into the right nostril. The septum is to the right, with the lateral wall of the nose to the left (Robert and Grant, 1998).

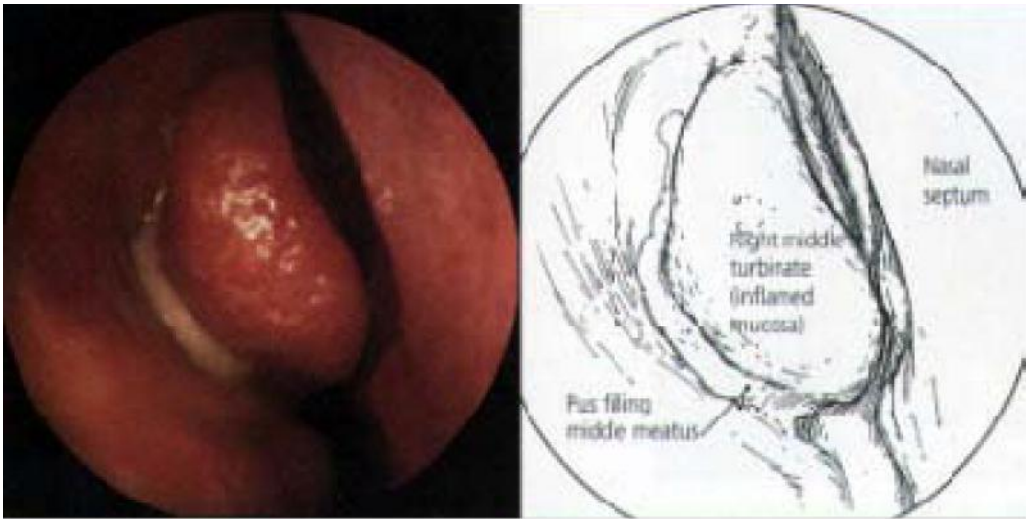

Figure 2.16: Nasal polyps in the left nostril, blocking the osteomeatal complex (Robert and Grant, 1998).

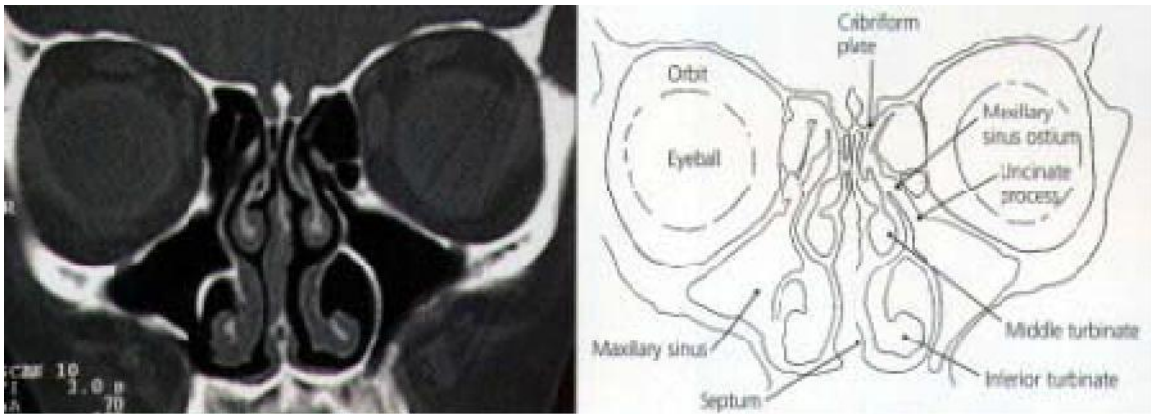

Figure 2.17: Coronal computed tomographic scan showing normal osteomeatal complex. Patent ostia are visible on both sides, and sinuses are well ventilated (Robert and Grant, 1998).

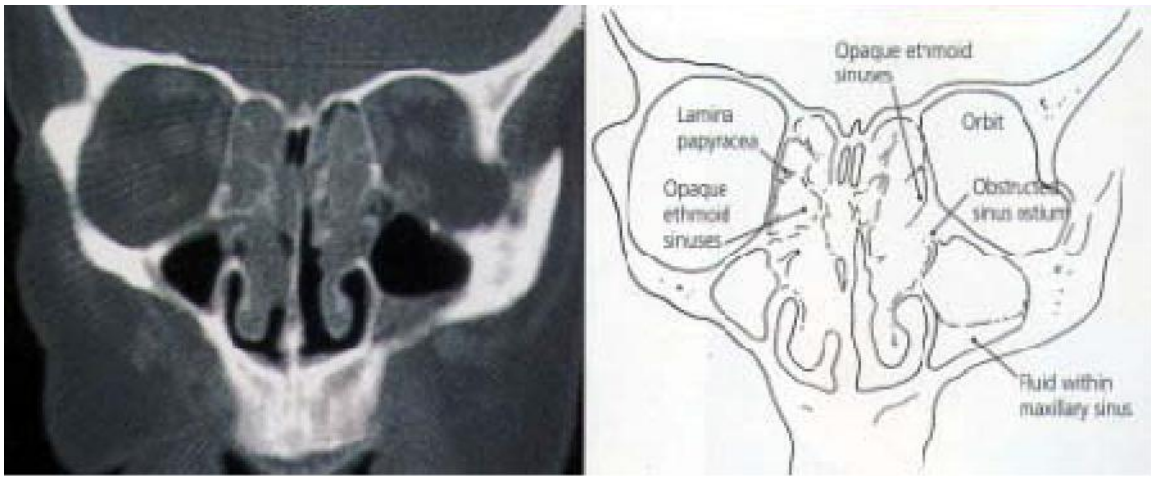

Figure 2.18: Coronal computed tomographic scan showing ethmoidal polyps. Ethmoid opacity is total as a result of nasal polyps, with a secondary fluid level in the left maxillary antrum (Robert and Grant, 1998).

The reasoning and concepts supporting the use of FESS have recently become widely accepted. (The term "functional" was introduced to distinguish this type of endoscopic surgery from nonendoscopic, "conventional" procedures. (Kennedy, 1985) The goal of FESS is to return the mucociliary drainage of the sinuses to normal function. The paranasal sinuses are maintained in a healthy state by ventilation through the individual ostia and by a mucociliary transport mechanism that keeps a continuous protective layer of mucus flowing out of the sinuses.

2.7.2.7.1 Pathophysiology of Sinusitis

All of the sinuses need ventilation to prevent infection. In the normal state, this ventilation is provided through openings (ostia) into the nose *(Figures 2.17 and 2.18).* The natural ostia open into the middle meatus under the middle turbinate, with the exception of the posterior ethmoid air cells and the sphenoid sinus, which have ostia situated more posteriorly. Cilial activity in the sinuses directs the flow of mucus toward these ostia. The middle turbinate and the middle meatus together represent the key area of the nose, known as the osteomeatal complex.

Most cases of sinusitis are caused by a problem in the nose (rhinogenic). Occasionally another problem, such as a primary dental infection, leads to sinusitis. During any episode of rhinosinusitis, the cilia function less efficiently, resulting in mucus stasis. The nasal sinus mucosa becomes engorged, often closing the ostia. A poorly ventilated sinus is the result, and the hypoxia and mucus stasis produce ideal conditions for bacterial infection.

2.7.2.7.2 Initial Evaluation and Treatment

As with many disease processes, the history of a patient with sinusitis is probably the most important part of the preoperative assessment. All patients with severe or persistent symptoms should be evaluated, and many can be helped with advice and medical treatment.

The fiberoptic endoscope enables the surgeon to examine the nose in great detail and is an essential tool for diagnosis. Patients with seasonal or perennial rhinitis should be given advice about avoidance of allergens and treatment with topical nasal steroid sprays and antihistamines. Acute infective sinusitis is treated with antibiotics and vasoconstrictor nasal sprays. If medical treatment has failed, the patient may be a suitable candidate for an endoscopic procedure.

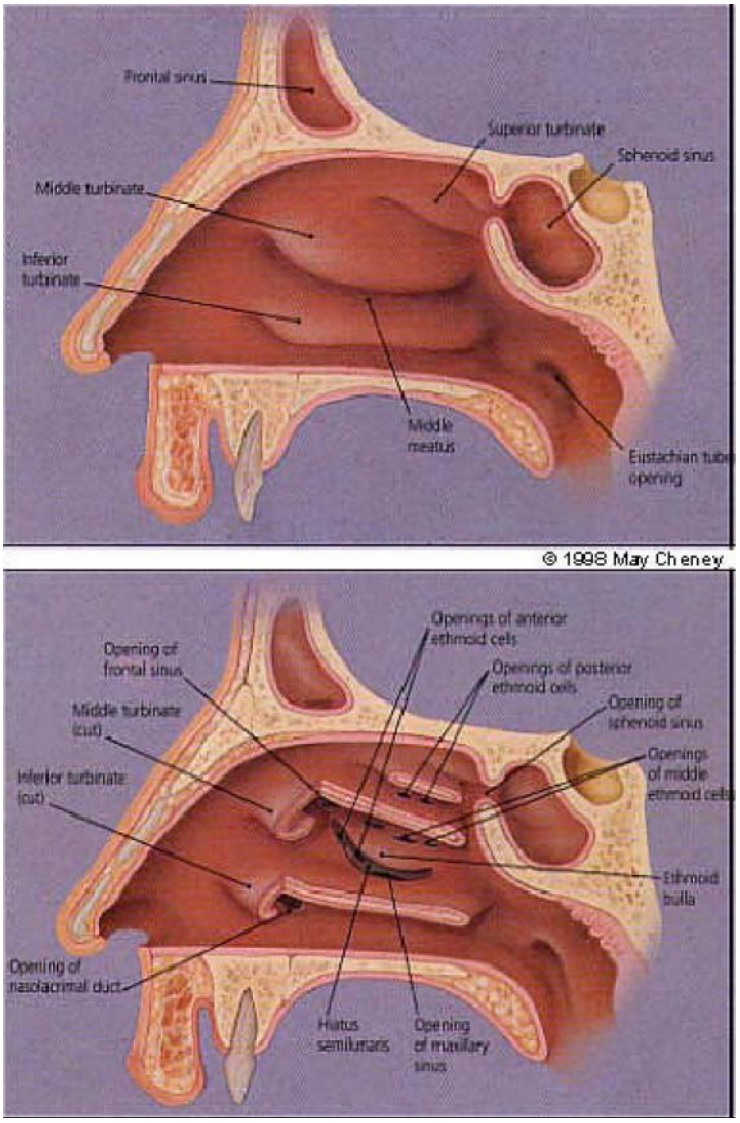

Figure 2.19: *(Top)* Lateral nasal wall (right side) showing turbinates and frontal sphenoid sinuses. *(Bottom)* Lateral nasal wall (right side), turbinates cut (Robert and Grant, 1998).

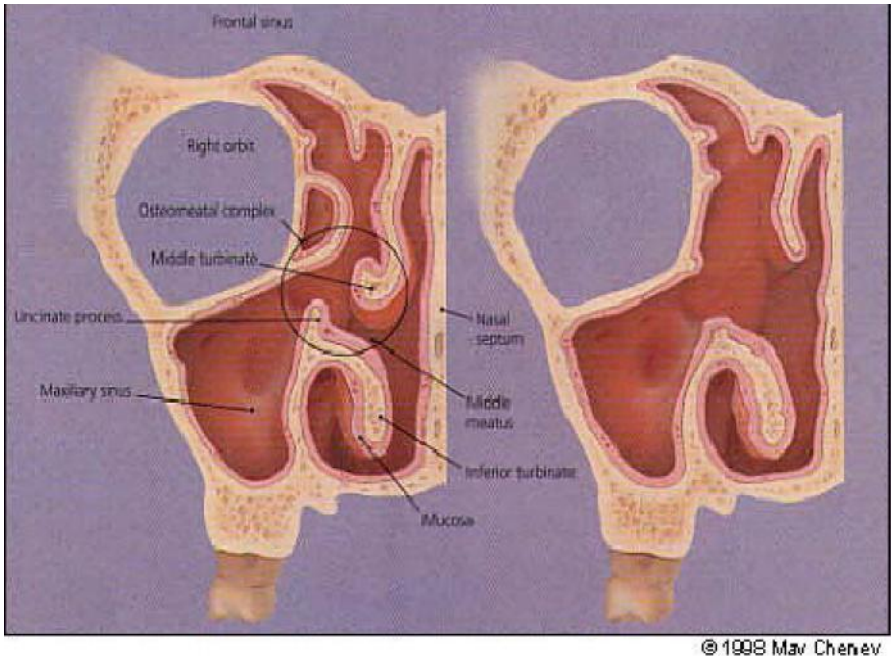

Figure 2.20: Anatomy of the sinuses. *(Left)* Narrowing in the circled region (middle meatus, middle turbinate, uncinate process) may precipitate sinusitis. *(Right)* After functional endoscopic sinus surgery, the osteomeatal area is open.Functional endoscopic sinus surgery is less invasive than traditionaltechniques and avoids scars and nerve damage to the teeth (Robert and Grant, 1998).

2.7.2.7.3 Candidates for Sinus Surgery

FESS (like any sinus surgery) is most successful in patients who have recurrent acute or chronic infective sinusitis. Patients in whom the predominant symptoms are facial pain and nasal blockage usually respond well. The sense of smell often improves after this type of surgery.

A CT scan before FESS is mandatory to identify the patient's ethmoid anatomy and its relationship to the skull base and orbit. CT scanning also allows the extent of the disease to be defined, as well as any underlying anatomic abnormalities that may predispose a patient to sinusitis.

Patient selection therefore involves a thorough history and physical examination, a trial with medical treatment and, finally, CT scanning. The result is a highly selected group of patients who can expect an improvement of up to 90 percent in their symptoms.

In patients with nasal polyposis that is not controlled with topical corticosteroids, FESS permits the accurate removal of polyps using suction cutters (Setliff, 1995). It is not known whether the disease-free interval is extended for patients having endoscopic ethmoidectomies for polyposis compared with conventional polyp surgery, but the postoperative discomfort is minimal.

2.7.2.7.4 Nonendoscopic, 'Conventional' Sinus Surgery vs. FESS

It was previously believed that once the mucosa had become chronically inflamed, it was irreversibly damaged and had to be removed. This was the rationale behind the Caldwell- Luc surgical technique, which involves removal of the diseased lining of the maxillary antrum. Similarly, the external surgical approaches to the ethmoid and frontal sinuses were designed to be "radical operations" in which the disease was completely cleared. These procedures left scars and caused significant bruising and discomfort. The Caldwell-Luc procedure also caused numb teeth. These "conventional procedures," as well as the sinus washout, concentrate on the secondarily infected sinus while ignoring the important pathology within the nose.

The rationale behind FESS is that localized pathology in the osteomeatal complex blocks the ostia and leads to inflammation in the dependent sinuses *(Figure 2.20).* The surgical interventions of the procedure are designed to

remove the osteomeatal blockage and restore normal sinus ventilation and mucociliary function *(Figure 2.20).*

FESS, like all minimally invasive surgery, is designed to combine an excellent outcome with minimal patient discomfort. As mentioned, the main advantage of FESS compared with traditional techniques is that it is less invasive, resulting in minimal postoperative discomfort. Scars and damage to the nerve supply of the teeth are also avoided. The use of the endoscope permits a better view of the surgical field, and this is probably responsible for the lower rate of complications.

The focal point of the surgery is the osteomeatal complex. The procedure may be performed with local anesthesia, with or without sedation. FESS is suitable for outpatient surgery.

2.7.2.7.5 Surgical Technique

After suitable vasoconstriction using cocaine or ephedrine, the middle turbinate is identified. This is the most important landmark for the procedure. On the lateral wall of the nose at the level of the anterior end of the middle turbinate lies the uncinate process. This is removed, exposing the ethmoid bulla and the opening called the hiatus semilunaris, into which the frontal and maxillary sinuses drain.

The anterior ethmoid air cells are then opened, allowing better ventilation but leaving the bone covered with mucosa. Following this, the maxillary ostium is inspected and, if obstructed, opened by means of a middle meatal antrostomy. This minimal surgery will often be sufficient to greatly improve the function of the osteomeatal complex and therefore provide better ventilation of the maxillary, ethmoid and frontal sinuses.

Occasionally the CT scan shows disease in the posterior ethmoids and the sphenoid sinus. It is then necessary to continue further into these sinuses. However, in most cases of sinusitis, the inflammation is confined to the osteomeatal complex and the anterior ethmoids.

2.7.2.7.6 Postoperative Care

Postoperatively, it is important to keep the nose as free from build-up of crusts as possible. The techniques used to achieve this vary from time-consuming nasal toilet performed two to three times a week by the surgeon to simple nasal douching carried out several times a day by the patient. Normal function usually returns within one to two months. In patients with gross inflammation or polyps, a short course of systemic steroids combined with antibiotics may hasten postoperative recovery. Topical steroids are used postoperatively in patients who have had polyps removed.

2.7.2.7.7 Outcome

The results after FESS are good; with most studies reporting an 80 to 90 percent rate of success (Stammberger and Posawetz, 1990; Lund and Scadding, 1994). Good results also have been obtained in patients who have had previous sinus surgery.The procedure is considered successful if the majority of the patient's symptoms are resolved. Nasal obstruction and facial pain are most likely to be relieved, although postnasal drip often remains a challenge. The technique has been compared with the Caldwell-Luc procedure and, although both methods were found to be effective, there was a strong patient preference for FESS (Penttila et al., 1994). The extent of

disease affects the outcome, with the best results obtained in patients with limited nasal pathology producing secondary sinusitis (Kennedy, 1992).

2.7.2.7.8 Complications

The most catastrophic complication of FESS is blindness resulting from damage to the optic nerve. However, the evidence indicates that the frequency of this complication is extremely low (Kennedy, 1994; Cumberworth et al., 1994).

Cerebrospinal fluid leak is the single most common major complication of FESS, occurring in about 0.2 percent of cases (Cumberworth et al., 1994). The leak is usually recognized at the time of surgery and can easily be repaired; it should be suspected if there is a clear nasal discharge postoperatively. Unless the discharge is contaminated with blood, the presence of glucose means that it is most likely to be cerebrospinal fluid. Absolute confirmation may be obtained by having a sample tested for the presence of $beta_2$ transferrin.

Other, less serious, but still rare complications include orbital hematoma and nasolacrimal duct stenosis. It should be emphasized that all of these complications also may occur with "conventional" sinus surgery and, therefore, patients are not undergoing a new treatment with complications that are more serious or more frequent than those in other surgeries. In the United Kingdom, the overall major complication rate of FESS was 0.44 percent, compared with 1.4 percent in patients having similar, nonendoscopic procedures (Cumberworth et al., 1994).

2.7.2.7.9 Limitations of FESS

2.7.2.7.9.1 Acute Severe Ethmoid and Frontal Sinusitis

Pus from an acute ethmoid sinusitis may break through the lamina papyracea and cause a painful proptosed eye with a risk of loss of vision. If the response to intravenous antibiotics is not very rapid, urgent orbital decompression is required. Bleeding is likely to occur because of the acute inflammation, making endoscopic surgery extremely difficult. An ethmoidectomy via an external incision may be the preferable option.

Severe frontal sinusitis may be associated with intracranial sepsis and under these circumstances; a direct trephine into the frontal sinus together with the appropriate neurosurgical intervention is the best option.

2.7.2.7.9.2 Nasal and Sinus Malignancies

Nasal and sinus malignancies are rare and often present late. If radical surgery is indicated, it is best performed via an external approach, such as midfacial degloving, lateral rhinotomy and various craniofacial procedures. However, the endoscope is useful for diagnosis and biopsy of tumors and for monitoring patients who have had radical cancer surgery.

2.8 Computer Tomography and PNS:

The introduction of head and neck CT imaging and the current wider use of this modality have undoubtedly helped the clinician. CT has become a useful diagnostic modality in the evaluation of the paranasal sinuses and an integral part of surgical planning. It is also used to create intraoperative road maps. Today, CT is the radiologic examination of choice in evaluating the paranasal sinuses of a patient with sinusitis (John, 2014).

The use of CT scanning combined with functional endoscopic sinus surgery (FESS) has empowered the modern sinus surgeon to treat patients more effectively, facilitating reduced morbidity and complications. Physicians who are interested in treating patients with sinus disease must be able to read and interpret sinus CT scans. Mastery of sinus anatomy and its variant features forms the basis from which radiologic interpretation begins. Familiarization with the radiologic landmarks and cross-sectional anatomy on patient CT scans, along with clinical correlation, can further enhance the reader's ability to understand sinus CT findings.

With experience, CT findings can be accurately correlated with the anatomic and clinical realities of the particular patient. As in all radiologic surveys, sinus CT scans must be read with a systematic approach. In addition to reviewing the scan to determine the presence of disease, CT scans of the sinuses can also be reviewed to evaluate potential areas of occlusion and variations of the patient's sinus anatomy in the setting of surgical planning.

2.8.1 Basic Concepts

CT scans typically obtained for visualizing the paranasal sinus should include coronal and axial (3-mm) cross sections. Soft tissue and bony windows facilitate evaluation of disease processes and the bony architecture. The use of intravenous contrast material just prior to scanning can help define soft tissue lesions and delineate vascularized structures, such as vascular tumors. Contrast-enhanced CT is particularly useful in evaluating neoplastic, chronic, and inflammatory processes (Yousem, 1993).However, for most patients with sinusitis, noncontrast CT of the paranasal sinuses generally suffices. For patients who may not tolerate the prone position required for coronal cuts, computer-generated reconstructed coronal views can be generated from thin axial sections. If sufficiently thin axial sections (1-2 mm) are available, sagittal reconstructions can also be helpful for teaching purposes and further delineating anatomic structures.

Proper positioning of the patient's head is important to obtain CT images. For axial views, the patient's hard palate is placed perpendicular to the CT scanner table. The images must be captured such that the external auditory canal is in line with the inferior orbital rim. The coronal images are taken so that the gantry is perpendicular to the patient's hard palate. Misalignment or rotation can lead to distortion of the true anatomy on the films.

Sinus CT is used in correlation with clinical examination procedures, including nasal endoscopy. Combined, the information gathered determines the extent of disease and forms the basis of the treatment plan. The timing of CT scanning can have a significant impact on the correlation of CT findings with actual disease state. The diagnostic yield of the scan for detecting

irreversible (surgically treatable) disease processes, such as chronic disease or structural problems, is increased once acute or reversible problems are treated. As such, CT scans should be obtained only after acute sinusitis episodes have been adequately treated. Changes from acute infections can last several weeks; waiting for at least 6 weeks before obtaining a scan is recommended to determine the patient's baseline disease status.

Patients with chronic inflammatory disease, such as strong allergies and/or sinonasal polyposis disease should receive maximized medical therapy for a few weeks before undergoing CT scanning. Depending on the patient's problems, this therapy may include antihistamines, nasal steroid sprays, antibiotics, or a brief course of oral steroids.

Some patients may be referred for evaluation after the discovery of radiologic disease on a screening CT scan. These screening sinus CT scans often only include thicker (5-10 mm) axial cross sections of the paranasal sinuses. They can help to establish disease diagnosis in a more cost-effective manner. One may argue against these so-called screening CT scans because of the superior diagnostic yield of properly obtained axial and coronal sections and the eventual need for coronal sections before surgery in some patients. Moreover, because the cost of CT scanning today is significantly reduced compared to that even a decade ago, complete CT is perhaps a more cost-effective test than screening CT, with a one-time order of a complete CT scan providing much more diagnostic and surgical usefulness.

With experience, CT findings can be accurately correlated with anatomic and clinical realities of the particular patient. As for all radiologic surveys,

sinus CT scans must be read with a systematic approach. After the primary survey of the CT scan is completed, including patient name, indications for the CT scan, type of scan, cross-sectional view being discussed, and major radiologic findings, particular attention is directed toward potential "bottle-neck" areas, where normal passages may be occluded by disease states or variant anatomy.

A systematic approach is helpful when interpreting CT scans. Reading the CT scan from anterior to posterior (on coronal views) or from top to bottom (on axial sections) can help organize one's approach in analyzing structures to be interpreted (John, 2014).

2.9 Previous Studies:

Sareen et al. L.N Hospital, New Delhi, India conducted a study of sphenoidal sinus anatomy in relation to endoscopic surgery using cadaveric skulls which showed that 75% of the sphenoidal sinuses revealed post sellar pneumatization, 80% of the sinuses had multiple septation and the antero posterior diameter of the sinuses ranged from 1.3 -3.4 cm, transverse diameter 1.2-5.0 cm, vertical diameter 1.4-3.6 cm and distance of sphenoidal ostium from the midline ranged from 1-4 mm, 5% of the superolateral wall of the sinuses showed dehiscence due to cavernous segment of the internal carotid artery (Sareen D et al., 2005)

Lagos State University College of Medicine, Nigeria conducted a study on the dimensions, septation and pneumatization of sphenoidal sinus on 60 patients using CT scan, showed that 83% of the patients showed sinuses with post sellar pneumatization with a main single inter sphenoid septum in 95% of the cases and the located usually right posteriorly in 38% and midline anteriorly in 65% of patients ,the anteroposterior diameter of the sinus ranged from 22.1-26.3 mm and transverse diameter was 17.1-20.3 mm. (Idowu et al, 2009).

In a study conducted by Hewaidi GH et al between May 2006 and May 2007, comprising of 300 paranasal computerized tomography (CT) scans of Libyan patients attending Al-Jalla Trauma Hospital, Libya was done. In all the patients, the existence of the following variants were investigated: pneumatization of pterygoid process (PP), anterior clinoid process (ACP), and greater wing of sphenoid (GWS i.e. floor of middle cranial fossa), protrusion of internal carotid artery (ICA), optic nerve (ON), maxillary

nerve (MN) and vidian nerve (VN), and dehiscence of the walls of internal carotid artery, optic nerve, maxillary nerve and vidian nerve. The anatomical variations of the sphenoid sinus in Libyan population were remarkably common. Prevalence of protrusion and dehiscence of the internal carotid artery and optic nerve were high. The internal carotid artery and optic nerve may not be well protected and thus could be damaged during endoscopic sphenoid surgery. Protrusion of the vidian canal into the sinus cavity was strongly associated with pneumatization of the pterygoid process on the same side. Coronal CT screening should be used in the pre-surgical evaluation of patients under consideration of endoscopic sphenoid sinus surgery to minimize perioperative neural and vascular injury (Hewaidi GH, Omami, 2008).

In 2004 a study on 64 cadaveric specimens was conducted by Citardi MJ et al. This study described computer generated anatomic symmetry plane as a framework for the quantitative description of sphenoid sinus anatomy. The aim of this study was to determine relationships and distances between a midline sphenoid reference points called the central sphenoid point and lateral sphenoid wall structures and assess the incidence of anterior clinoid process pneumatization and pterygoid recess pneumatization.

A total of 128 slides in 64 cadaveric specimens were available for review. The incidences of anterior clinoid process pneumatization and pterygoid pneumatization were 23.4 and 37.5%. Measurements from the maxillary spine to the optic canal midpoint, anterior clinoid process entrance point and pterygoid recess lateral wall on each side were performed. The approaches described in this study describe critical sphenoid anatomic relationships; such information will facilitate a wide variety of sphenoid procedures. This

approach provides both quantitative and qualitative understanding of sphenoid osteology and may be coupled with intraoperative surgical navigation to reduce the risks of sphenoid surgery (Citardi et al., 2004).

In a study conducted by Kantarci M et al on June 2004, a review of 512 (1024 sides) paranasal sinus tomographic scans was carried out to expose remarkable anatomic variations of this region. It mentioned that an Onodi (sphenoethmoid) cell is a posterior ethmoid cell which pneumatized far laterally and to some degree superiorly to the sphenoid sinus and is intimately associated with the optic nerve. The presence of an Onodi cell may possibly contribute to an increase in the risk of injury to the optic nerve and to the internal carotid artery. Identification of the Onodi cell before surgery may be extremely valuable in decreasing the risk of such complication. In the case of protrusion, an optic nerve injury can occur due either to a surgical trauma or as a complication of sinus disease. The risk of blindness is high if the surgeon damages the nerve within the sinus. Visual deficits may result from a sphenoid sinus infection or from a mucocele compressing the optic nerve in the canal (Kantarci et al., 2004).

In 2005 CT evaluation of sphenoid sinus was done by Kazkayasi et al. They studied anatomic structures, even subtle bony anatomic variations and mucosal abnormalities of region by CT scan. When the pneumatization extends below a plane between vidian canal (VC) and foramen rotundum (FR), it has been considered significant for pterygoid process (PP) pneumatization. It was regarded as ‘protrusion’ when more than 25% of the nerves were surrounded by the air. When the anterior clinoid process is pneumatized, the optic nerve protrudes against the superior lateral sinus

wall, forming an optic canal (OC) protrusion. Optic canal is very susceptible to injury through direct inflammatory invasion of the sinus diseases and additionally there is a risk of blindness if the surgeon damages the nerve within the sinus. The optic nerve is at risk during sinus surgery when the posterior ethmoid anatomical variation exists, i.e. sphenoethmoid or onodi cell (OnC). The internal carotid artery is critical owing its close proximity and bulging medially into the sphenoid sinus and this may create increased risk during surgery. The artery may occasionally protrude into the sphenoid sinus, especially when there is an over pneumatization in the sphenoid base. The thickness of bone separating the carotid artery from the sinus was found as 0.5-1 mm in 66-88% of the specimen. In some cases the thin bony wall over the vessel may be dehiscent and can lead to direct contact of the artery with sinus mucosa which may lead infection occurring within the cavernous sinuses (Kazkayasi et al., 2005).

Van Alyea performed a comprehensive study on cadaver heads and found that the carotid artery caused elevations on the lateral wall in 65% of sphenoid sinuses. The optic, vidian, and maxillary nerves were noted in 47%, 48%, and 42% of the sinuses, respectively (Van Alyea, 1941). He did not note any dehiscences in these sinuses but other authors have reported this (Van Alyea, 1941).

Neurovascular relationships of the sphenoid sinus is studied by Kiyotaka Fujii and Steven M by microscopic observations of 25 sphenoid sinuses in cadavers, with attention to the neural and vascular structures in the lateral wall of the sinus specially considering 1) the optic nerves, 2) the carotid arteries, and 3) the maxillary branches of the trigeminal nerve. They found

that over half of these structures had a bone thickness of less than 0.5 mm separating them from the sphenoid sinus, and in a few cases, they were separated by only sinus mucosa and dura. In 4% of the optic nerves, only the optic sheath and sinus mucosa separated the nerves from the sinus, and in 78%, less than a 0.5-mm thickness of bone separated them. The carotid arteries produced a prominent bulge into the sphenoid sinus in all but one side of one specimen. In 8% of the carotid arteries there were areas where no bone separated the artery and the sinus. The maxillary branches of trigeminal nerves bulged into the inferolateral part of the sphenoid sinus in all except one side of two specimens. One side of one specimen had no bone, and 70% had less than a 0.5-mm thickness of bone separating the nerve from the sinus (Fujii and Chambers, 1979).

The sphenoidal bones of 70 adults were removed at post-mortem and studied by Banna M and Olutola PS for degree of pneumatization, number of intersphenoidal septa and the relationship of the septa to the lowest portion of the sellar floor. They found, in 85.7%, pneumatization was of the sellar type, in 11.4% of the pre-sellar type and in 2.8% of the conchal type, as defined here. A single septum was noted in 61%, two septa in 14%, more than two septa in 12.8% and no septum was noted in 11.4%. The insertion of the septum represented the lowest point in the sellar floor in 50% of the bones. In these the septum was located in the center of the sellar floor (Banna and Olutola, 1983).

Ossama Hamid and Lobna El Fiky have evaluated retrospectively, the CT and MRI scans of 296 patients, who have operated for pituitary adenomas via a trans-sphenoid approach, regarding the different anatomical variations

of the sphenoid sinus: degree of pneumatization, sellar configuration, septation pattern, and the intercarotid distance. They found that there were 6 cases with conchal pneumatization, 62 patients with presellar, 162 patients with sellar, and 66 patients with postsellar pneumatization. There was sellar bulge in 232 patients, whereas this bulge was absent in 64 patients. There was no intersphenoid sinus septum in 32 patients, a single intersphenoid septum in 212 patients, and an accessory septum in 32 patients. They have concluded that a highly pneumatized sphenoid sinus may distort the anatomic configuration and cautioned about the importance of the midline when operating the sella to avoid the accidental injury to the carotid arteries and optic nerves (Ossama, 2008).

Liu S, Wang Z studied CT scans of 25 normal adults and stated that pneumatisation of sphenoid sinus can be divided into two types: Pneumatisation of the sphenoid body and the one of sphenoid process. The former was subdivided into three categories: concha (2%), pre sellar (20%), sellar (78%). The latter subdivided into four categories: lesser wing (38%), greater wing (40%), pterygoid process (34%) and dorsum sellar (6%). The thinnest part (< 1 mm) of the lateral sphenoid wall was found to be located at the inner wall of the optic nerve canal (96%), at the bony wall in the plane of sphenoethmoid recess (86%), the bony wall in the plane of the internal carotid artery (66%). They stated, over pneumatised sphenoid sinus could make the foramen rotumdum (64%) and pterygoid canal (44%) to protrude into the sphenoid cavity (Liu et al. 2002).

Szolar et al observed single intersphenoid septum in 77% of the subjects. According to Anthony J. Scuderi, the pterygoid processes are pneumatized

in 25-40% of adults and aeration of the anterior clinoid process (13%) and medial pterygoid process (44%) is more common than the dorsum sella and posterior clinoid process (Szolar et al.).

The sphenoid sinus and its surrounding structures were examined in 18 cadaver heads, and in correlation with 100 computed tomography images of the sinus by Wang Jian and Bidari Sharatchandra. They found that the sellar type of the sphenoid sinus pnematization extended beyond the anterior wall and it was divided into 6 types - sphenoid body, lateral, clival, lesser wing, anterior, and combined (Wang et al. 2010).

Surgical measurement to sphenoid sinus for the Chinese is studied by Hai-bo Wu et al based on CT using sagittal reconstruction images of 89 of normal adult participants (54 males and 35 females). The length of mean vertical line from the center of sphenoid ostium to the roof of sphenoid sinus of Non Onodi cell type is 10.6 ± 1.5 mm, and of Onodi cell type is 3.3 ± 1.5 mm. The length of vertical line from the center of sphenoid ostium to the lowest level of the bottom of sphenoid sinus is 12 mm ± 3.7 mm. The length of mean horizontal line from the sphenoid ostium to the posterior wall of sphenoid sinus is 18 ± 1.5 mm or 28 ± 2.5 mm. The mean horizontal line from the lowest point of the sella to the anterior wall of sphenoid sinus is 17.5 ± 1.3 mm in length. The mean horizontal distance from anterior wall to posterior wall of sphenoid sinus of Non Onodi cell type lining skull base is 10.1 ± 1.0 mm, and of Onodi cell type, is 5.2 ± 4.3 mm. The longest horizontal distance from the anterior wall to the posterior wall of sphenoid sinus is 22.0 ± 7.7 mm.

In 2013 surgical measurement of the sphenoid sinus on sagittal reformatted CT in the Turkish population wsa conucted by Hatice Kaplanoglu et al. They found that Line 1 is shorter, so the risk of skull base perforation is greater. Lines 4 and 6 are longer on the left side; thus, choosing the left ostium in sinus dilation is safer. Because of sex differences regarding Lines 2, 3,4 and 6, sex should be considered in sphenoid sinus procedures.

Taking all the above literature into consideration, it is evident that wide variations exist in the anatomy of sphenoidal air sinus and its relation to major neurovasucular structures. This study focuses on such antomical variations and relations in the Sudanese population.

CHAPTER THREE

MATERIALS AND METHODS

3.1 Materials

This prospective study comprised 201 normal Sudanese patients, 54.2% (109) were males and 45.8% (92) were females, their ages ranged between 18-90 years old attending to the Radiology Department of Royal Care Hospital in Sudan, between June 2012 and July 2014. All the patients underwent a complete medical history and head and neck physical examination. Patients having pathological changes were excluded, such as: Patients subject to neurological deficit and stroke, epilepsy, and vertigo, sinusitis, any congenital abnormalities in sphenoid sinuses and patients younger than 16 years were also excluded because, according to Gray, the extension of the nasal cavity into the body of the sphenoid bone to form the sphenoid sinus is present before birth but does not reach its full extension until adolescence (Gray H, 1989).

All patients were examined on a multi-slice CT scanner (Toshiba Aquilion 64 CT scanner) according to the following parameters: slice thickness 0.625 mm, 120 kV, 230 - 280 mA, Collimator width 3 - 5 cm, Scan type-Helical full 1.0 sec, FOV: 25.0, Bone window (center 200 HU, width 1500 HU). Taking the hard palate as reference axis, in the coronal study the plane of section was perpendicular to this structure. Axial sections were performed in a plane parallel to the hard palate from the upper dental arch to the roof of the frontal sinuses. Data acquired on the axial plane, coronal and sagittal plane were created by secondary reconstruction method in the workstation.

The thickness of reconstructed image slice was of −1 mm. The coronal computed tomography study has become the most requested and the precise imaging technique for demonstrating the par nasal sinuses (Arsalan et al., 1997). The advantage of the coronal sections over the axial ones is that they show the progressively deeper structures as they are encountered by the surgeon during functional endoscopic sinus surgeries (Zinreich, 1998). In order to get more surgical anatomical information, we must measure the line in sagittal plane via the operation path. The patients were prepared for the procedure by giving them full information about the procedure; restraint from food and fluids

3.2 Data Collection & Analysis

3.2.1 Data collection

In all the patients, the existence of the following variants was investigated: pneumatization of pterygoid process (PP), anterior clinoid process (ACP), and greater wing of sphenoid (GWS, i.e. floor of middle cranial fossa). Pneumatization is defined as the formation of air cavities in tissue, According to the study criteria. Pterygoid process (PP) pneumatization is recognized if it extends beyond a horizontal plane crossing the vidian canal. Likewise, the study define greater wing of sphenoid (GWS) pneumatization when it extends beyond a vertical plane crossing the maxillary canal.

As well as the study also investigated the type of sphenoid sinus (Sellar – pre-sellar – Conchal) according to the classification of Hammer and Radberg. It describes sphenoid sinus Pneumatization as conchal, presellar and sellar types, based on Pneumatization around the sella turcica. In the conchal type, pneumatization is absent, the sphenoid sinus is filled by

cancellous bone, and there is no association with the sella turcica. In the presellar type, the sinus cavity remains anterior to a vertical line drawn through the tuberculum sellae. Whereas in the sellar type, sinus Pneumatization extends beyond a vertical line drawn through the tuberculum sellae, and this type is related to the floor and anterior wall of the sella turcica.

The study moreover investigated protrusion of internal carotid artery (ICA), optic nerve (ON), maxillary nerve (MN), and vidian nerve (VN), and dehiscence of the walls of ICA, ON, MN, and VN.

Dehiscence is defined as the absence of the visible bone density which separates the sinus from the course of the concerned structures. The protrusions of the internal carotid artery and the optic nerve were determined by the finding of any degree of protrusion of the structures into the sinus cavity. The presence of air density around the vidian nerve and the maxillary nerve in at least one coronal section was accepted as protrusions of the vidian nerve and the maxillary nerve.

The existence of an Onodi cell in the sphenoid sinus had been evaluated and all these Data will be collected using the following variables: age, Gender and head circumference.

Measurements relating to sphenoid sinus with its surrounding structures were as the follows :(all measurements from the sphenoid ostium were from the midpoint of sphenoid ostium and were taken in mm):

- ***Line 1***: The distance to the roof of sphenoid sinus. The vertical line was measured from the center of sphenoid ostium to the roof sphenoid sinus.

- ***Line 2***: The distance to the bottom of sphenoid sinus. The vertical line was measured from the center of sphenoid ostium to the lowest level of sphenoid sinus bottom.
- ***Line 3***: The distance to the posterior wall of (SS). The horizontal line from the center of sphenoid ostium to the posterior wall of sphenoid sinus was measured, and analyzed separately because the sphenoid ostium is locate superior or inferior to the lowest level point of sella.
- ***Line 4***: The distance from the bottom of sella to the anterior wall of sphenoid sinus. The horizontal line was measured from the lowest point of the sella to the anterior wall of sphenoid sinus.
- ***Line 5***: The skull base length from the anterior wall of sphenoid sinus to the sella.
- ***Line 6***: The longest horizontal distance of sphenoid sinus.The longest horizontal distance was measured from the anterior wall to the posterior wall of sphenoid sinus (maximal depth).
- ***Line 7***: The longest horizontal distance of sphenoid sinus. The maximum width at the middle of the sphenoid sinus was measured from the lateral wall to the medial wall of sphenoid sinus.
- All Measurements were performed on sagittal images except Line 7, measurements were performed on coronal images.

The patients included in the study were evaluated by the same radiologist (M.N). The measurements were obtained with left and right side comparisons, and sex distribution was also analyzed.

3.2.2 Statistical analysis

SPSS software version 16.0 was used and for the statistical analysis, ANOVA test, Independent samples T-test, mean and Standard deviation were used.

CHAPTER FOUR

RESULT

A total of 201 normal patients (54.2% (109) males, 45.8% (92) females) were evaluated in this study. The ages were range between 18-90 years old with mean of (44.8 ± 16.8) year. The sample was individuals with no history of sinus pathology .The target population for this research included patients attended for head CT scanning in the radiology department of Royal Care Hospital in Sudan.

In all the patients, the existence of the following variants was investigated: pneumatization of pterygoid process (PP), anterior clinoid process (ACP), and greater wing of sphenoid (GWS, i.e. floor of middle cranial fossa).
As well as the study also investigated the type of sphenoid sinus (Sellar – pre-sellar – Conchal) according to the classification of Hammer and Radberg. The study moreover investigated protrusion of internal carotid artery (ICA), optic nerve (ON), maxillary nerve (MN), and vidian nerve (VN), and dehiscence of the walls of ICA, ON, MN, and VN.

The existence of an Onodi cell in the sphenoid sinus had been evaluated and all these Data will be collected using the following variables: age, Gender and head circumference.

Measurements relating to sphenoid sinus with its surrounding structures were as the follows :(all measurements from the sphenoid ostium were from the midpoint of sphenoid ostium and were taken in mm):

- ***Line 1***: The distance to the roof of sphenoid sinus. The vertical line was measured from the center of sphenoid ostium to the roof sphenoid sinus.
- ***Line 2***: The distance to the bottom of sphenoid sinus. The vertical line was measured from the center of sphenoid ostium to the lowest level of sphenoid sinus bottom.
- ***Line 3***: The distance to the posterior wall of (SS). The horizontal line from the center of sphenoid ostium to the posterior wall of sphenoid sinus was measured, and analyzed separately because the sphenoid ostium is locate superior or inferior to the lowest level point of sella.
- ***Line 4***: The distance from the bottom of sella to the anterior wall of sphenoid sinus. The horizontal line was measured from the lowest point of the sella to the anterior wall of sphenoid sinus.
- ***Line 5***: The skull base length from the anterior wall of sphenoid sinus to the sella.
- ***Line 6***: The longest horizontal distance of sphenoid sinus.The longest horizontal distance was measured from the anterior wall to the posterior wall of sphenoid sinus (maximal depth).
- ***Line 7***: The longest horizontal distance of sphenoid sinus. The maximum width at the middle of the sphenoid sinus was measured from the lateral wall to the medial wall of sphenoid sinus.
- All Measurements were performed on sagittal images except Line 7, measurements were performed on coronal images.

The results were presented in tables and figures. The distribution of the study sample according to sphenoid sinus morphology (pneumatization, protrusion and dehiscence) for Sudanese subjects was presented. Correlation

between Sphenoid Sinus morphology, gender and age was studied. Association between (pneumatization of ACP, GWS and PP) and (protrusion and dehiscence of ICA, ON, MxN and VN) were assessed using Chi-square test. The patients included in the study were evaluated by the same radiologist (M.N). The measurements were obtained with left and right side comparisons, and sex distribution was also analyzed.

4.1 Tables and Graphs:

Table 4.1: Distribution of the study sample according to (Gender)

Gender	Frequency	Percent
Female	92	45.8%
Male	109	54.2%
Total	201	100.0%

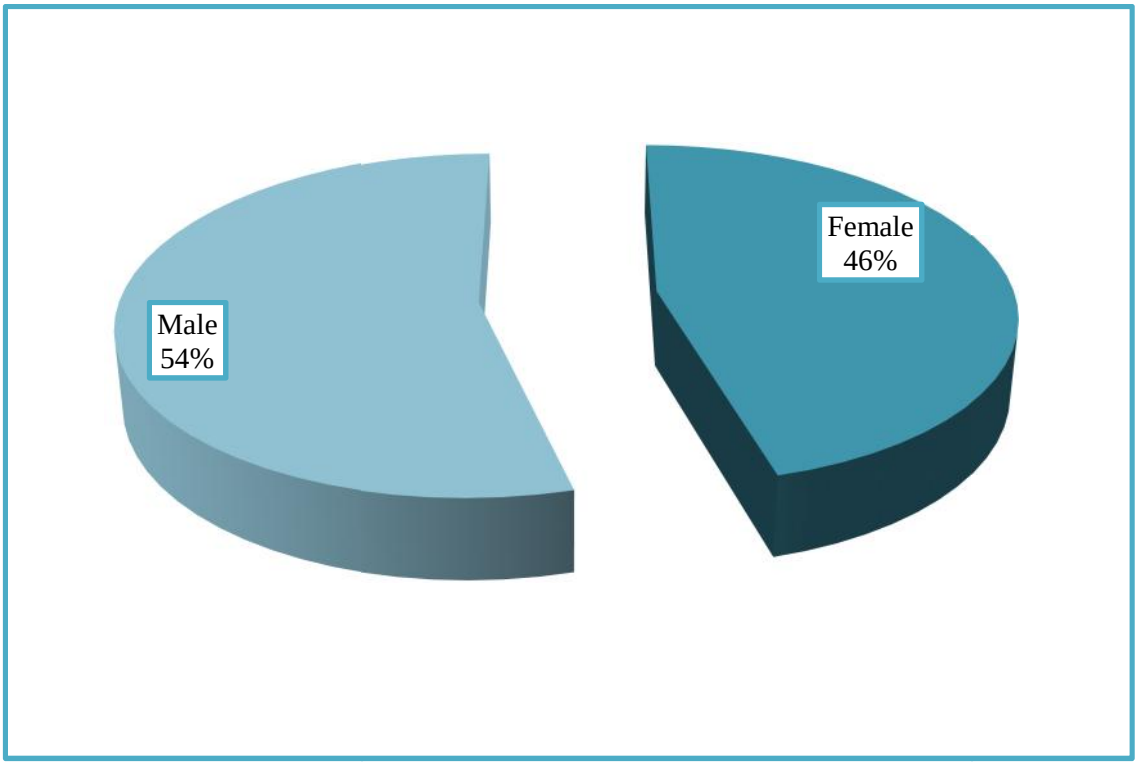

Figure 4.1: Distribution of the study sample according to (Gender)

Table 4.2: Distribution of the study sample according to (Age group)

Age	Frequency	Percent
(15 - 40) Yrs	87	43 %
(41 - 65) Yrs	93	46 %
> 65 Yrs	21	10 %
Total	201	100

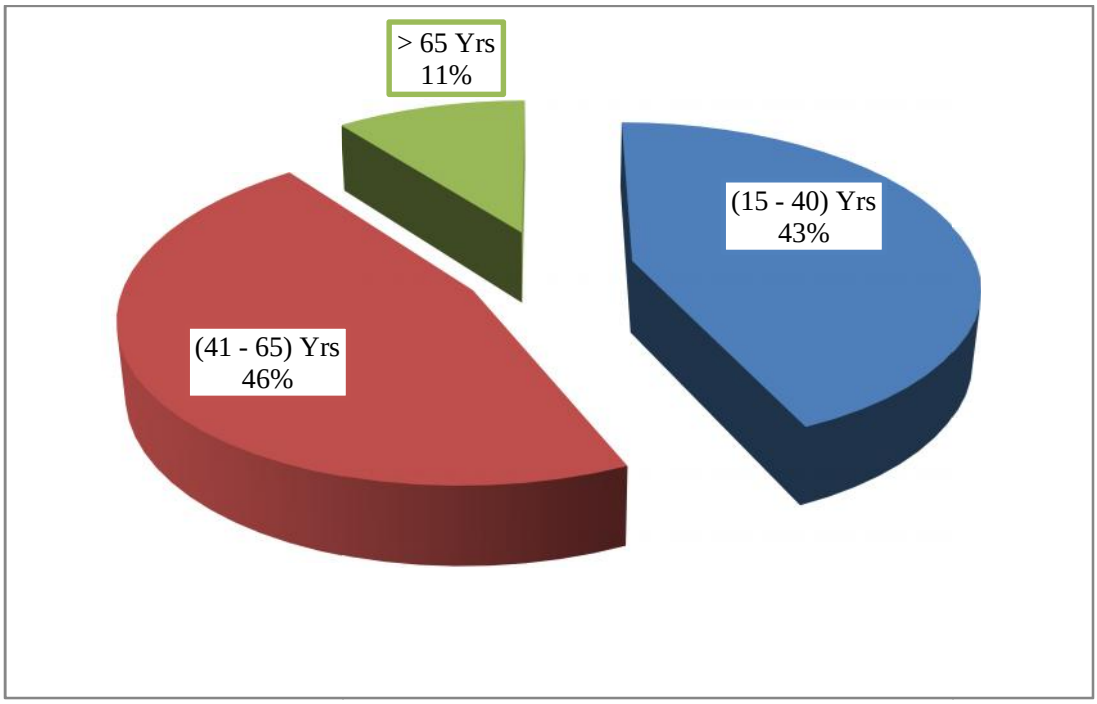

Figure 4.2: Distribution of the study sample according to (Age group)

Table 4.3: Distribution of the study sample according to (Pneumatization, Protrusion and Dehiscence)

Pneumatization		**Bilateral**	**Right side**	**Left side**	**Total**
ACP	**Count**	9	9	10	28
	% of Total	4.5%	4.5%	5.0%	13.9%
GWS	**Count**	31	13	26	70
	% of Total	15.4%	6.5%	12.9%	34.8%
PP	**Count**	47	10	24	81
	% of Total	23.4%	5.0%	11.9%	40.3%
Protrusion		**Bilateral**	**Right side**	**Left side**	**Total**
ICA	**Count**	21	11	19	51
	% of Total	10.4%	5.5%	9.5%	25.4%
ON	**Count**	1	0	5	6
	% of Total	0.5%	0.0%	2.5%	3.0%
MxN	**Count**	21	18	17	56
	% of Total	10.4%	9.0%	8.5%	27.9%
VN	**Count**	52	10	23	85
	% of Total	25.9%	5.0%	11.4%	42.3%
Dehiscence		**Bilateral**	**Right side**	**Left side**	**Total**
ICA	**Count**	13	6	6	25
	% of Total	6.5%	3.0%	3.0%	12.4%
ON	**Count**	19	7	6	32
	% of Total	9.5%	3.5%	3.0%	15.9%
MxN	**Count**	49	23	19	91
	% of Total	24.4%	11.4%	9.5%	45.3%
VN	**Count**	74	18	19	111
	% of Total	36.8%	9.0%	9.5%	55.2%

Table 4.4: Association Relationship between (Pneumatization of ACP, GWS and PP) and (Protrusion & Dehiscence of ICA, ON, MxN and VN respectively):

	Frequency	**P-value**
Pneumatization ACP	28	0.003
Protrusion ICA	51	
Dehiscence ICA	25	
Pneumatization ACP	28	0.003
Protrusion ON	6	
Dehiscence ON	32	
Pneumatization GWS	70	0.003
Protrusion MxN	56	
Dehiscence MxN	91	
Pneumatization PP	81	0.004
Protrusion VN	85	
Dehiscence VN	111	

S.S Classification	Yes	No	% Yes	Figuration
Sellar	158	43	78.6%	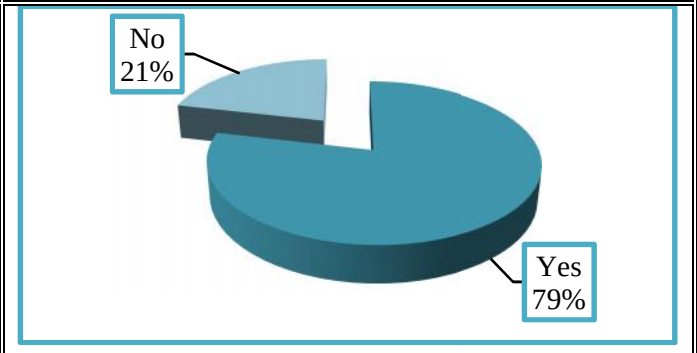
Conchal	0	201	0.0%	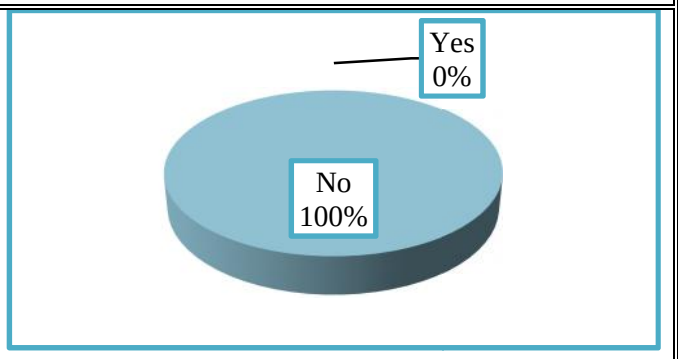
Pre Sellar	43	158	21.4%	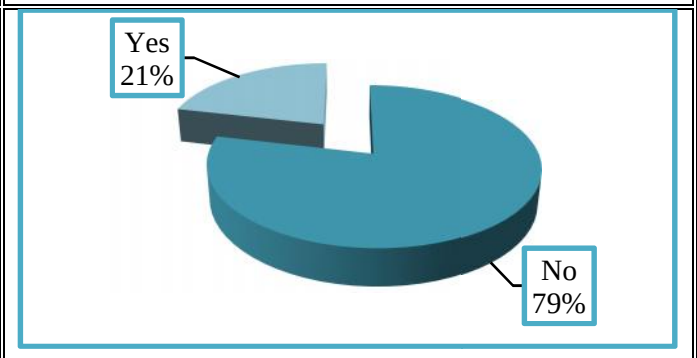

Figure 4.3: Distribution of the study sample according to (S.S Classification)

Table 4.5: Relationship between (Pneumatization) and (Gender) (P-value=0.833)

Pneumatization		Gender		Total
		Female	Male	
ACP	Count	12	16	28
	% of Gender	16.2%	15.2%	31.5%
GWS	Count	27	43	70
	% of Gender	36.5%	41.0%	77%
PP	Count	35	46	81
	% of Gender	47.3%	43.8%	91.1%
Total	Count	74	105	179
	% of Gender	100%	100%	100%

Table 4.6: Relationship between (Pneumatization) and (Age) (P-value=0.909)

Pneumatization		Age		
		(15 - 40) Yrs	(41 - 65) Yrs	> 65 Yrs
ACP	Count	11	14	3
	% of Age	14.9%	17.1%	13.0%
GWS	Count	28	31	11
	% of Age	37.8%	37.8%	47.8%
PP	Count	35	37	9
	% of Age	47.3%	45.1%	39.1%
Total	Count	74	82	23
	% of Age	100.0%	100.0%	100.0%

Table 4.7: Relationship between (Protrusion) and (Gender) (P-value=0.431)

Protrusion		Gender		Total
		Female	Male	
ICA	Count	24	27	51
	% of Gender	32.4%	21.8%	25.8%
ON	Count	2	4	6
	% of Gender	2.7%	3.2%	3.0%
MxN	Count	19	37	56
	% of Gender	25.7%	29.8%	28.3%
VN	Count	29	56	85
	% of Gender	39.2%	45.2%	42.9%
Total	Count	74	124	198
	% of Gender	100%	100%	100%

Table 4.8: Relationship between (Protrusion) and (Age) (P-value=0.645)

Protrusion		Age		
		(15 - 40) Yrs	(41 - 65) Yrs	> 65 Yrs
ICA	Count	21	25	5
	% of Age	23.9%	30.1%	18.5%
ON	Count	2	2	2
	% of Age	2.3%	2.4%	7.4%
MxN	Count	27	20	9
	% of Age	30.7%	24.1%	33.3%
VN	Count	38	36	11
	% of Age	43.2%	43.4%	40.7%
Total	Count	88	83	27
	% of Age	100.0%	100.0%	100.0%

Table 4.9: Relationship between (Dehiscence) and (Gender) (P-value=0.677)

Dehiscence		Gender		Total
		Female	Male	
ICA	Count	10	15	25
	% of Gender	8.8%	10.3%	9.7%
ON	Count	12	20	32
	% of Gender	10.6%	13.7%	12.4%
MxN	Count	44	47	91
	% of Gender	38.9%	32.2%	35.1%
VN	Count	47	64	111
	% of Gender	41.6%	43.8%	42.9%
Total	Count	113	146	259
	% of Gender	100%	100%	100%

Table 4.10: Relationship between (Dehiscence) and (Age) (P-value=0.859)

Dehiscence		Age		
		(15 - 40) Yrs	(41 - 65) Yrs	> 65 Yrs
ICA	Count	7	15	3
	% of Age	6.5%	12.3%	10.0%
ON	Count	14	15	3
	% of Age	13.1%	12.3%	10.0%
MxN	Count	38	43	10
	% of Age	35.5%	35.2%	33.3%
VN	Count	48	49	14
	% of Age	44.9%	40.2%	46.7%
Total	Count	107	122	30
	% of Age	100.0%	100.0%	100.0%

Table 4.11: Descriptive statistics of line

Line		Mean ± SD	Min	Max	P-value
Line1	**Right**	10.0 ± 3.3	2.5	23.1	0.757
	Left	9.9 ± 3.3	2.6	19.2	
Line2	**Right**	10.7 ± 3.2	2.8	24.6	0.962
	Left	10.7 ± 3.5	2.8	24.6	
Line 3	**Right**	22.0 ± 7.0	5.6	36.5	0.991
	Left	22.0 ± 7.1	6.6	36.8	
Line4	**Right**	16.3 ± 3.7	5.6	25.2	0.588
	Left	16.5 ± 3.7	6.9	26.5	
Line5	**Right**	10.6 ± 3.2	3.3	19.3	0.994
	Left	10.6 ± 3.5	4.5	21.5	
Line6	**Right**	24.2 ± 6.8	7.3	36.5	0.406
	Left	24.7 ± 6.6	6.9	37.5	
Line7	**Right**	16.8 ± 5.1	6.6	32.7	0.086
	Left	17.7 ± 6.1	7.3	46.8	

Table 4.12: Over all mean for any line:

Line	Mean ± SD
Line 1	9.9 ± 3.3
Line 2	10.7 ± 3.4
Line 3	22.0 ± 7.1
Line 4	16.4 ± 3.7
Line 5	10.6 ± 3.4
Line 6	24.5 ± 6.7
Line 7	17.3 ± 5.7

Table 4.13: Descriptive statistics of age

	Mean ± SD	Min	Max
Age	44.8 ± 16.8	18	90

Table 4.14: Cross tabulation between line & gender:

	Gender	Right side	Left side
Line 1	**Female**	9.7 ± 3.1	9.8 ± 3.0
	Male	10.2 ± 3.5	9.9 ± 3.4
	Total	10.0 ± 3.3	9.9 ± 3.3
	P-value	0.244	0.949
Line 2	**Female**	10.3 ± 3.3	9.8 ± 3.3
	Male	11.1 ± 3.2	11.5 ± 3.5
	Total	10.7 ± 3.2	10.7 ± 3.5
	P-value	0.078	0.001*
Line 3	**Female**	20.5 ± 6.5	20.6 ± 6.1
	Male	23.2 ± 7.2	23.1 ± 7.7
	Total	22.0 ± 7.0	22.0 ± 7.1
	P-value	0.007*	0.011*
Line 4	**Female**	15.6 ± 3.8	15.9 ± 3.7
	Male	16.8 ± 3.6	16.9 ± 3.8
	Total	16.3 ± 3.7	16.5 ± 3.7
	P-value	0.031*	0.070
Line 5	**Female**	10.4 ± 3.6	10.4 ± 3.6
	Male	10.9 ± 2.9	10.9 ± 3.3
	Total	10.6 ± 3.2	10.6 ± 3.5
	P-value	0.287	0.315
Line 6	**Female**	22.8 ± 7.0	23.1 ± 6.3
	Male	25.4 ± 6.4	26.1 ± 6.6
	Total	24.2 ± 6.8	24.7 ± 6.6
	P-value	0.006*	0.001*
Line 7	**Female**	16.5 ± 5.1	15.9 ± 5.6
	Male	17.0 ± 5.1	19.3 ± 6.1
	Total	16.8 ± 5.1	17.7 ± 6.1
	P-value	0.476	0.000*

Value are expressed as Mean ± SD; * Significant at P<0.05

Table 4.15: Cross tabulation between line, Onodi cell & gender:

	Onodi cell	Gender	Right side	Left side	P-value
Line 1	Non Onodi Cell	Female	10.0 ± 2.9	10.2 ± 3.1	0.011*
		Male	10.6 ± 3.3	10.1 ± 3.5	
		Total	10.3 ± 3.1	10.1 ± 3.3s	
	Onodi Cell	Female	7.9 ± 3.7	8.3 ± 2.5	0.001*
		Male	8.7 ± 3.8	8.9 ± 3.2	
		Total	8.4 ± 3.7	8.6 ± 2.9	
Line 2	Non Onodi Cell	Female	10.5 ± 2.5	10.1 ± 3.3	0.327
		Male	10.1 ± 2.2	10.3 ± 1.9	
		Total	10.3 ± 2.3	10.2 ± 2.5	
	Onodi Cell	Female	10.3 ± 3.4	9.8 ± 3.3	0.322
		Male	11.4 ± 3.3	11.8 ± 3.7	
		Total	10.8 ± 3.4	10.8 ± 3.7	
Line 4	Non Onodi Cell	Female	14.2 ± 4.3	14.6 ± 3.2	0.001*
		Male	14.6 ± 4.4	15.3 ± 4.3	
		Total	14.5 ± 4.3	15.0 ± 3.8	
	Onodi Cell	Female	15.9 ± 3.7	16.2 ± 3.7	0.011*
		Male	17.3 ± 3.2	17.3 ± 3.6	
		Total	16.7 ± 3.5	16.8 ± 3.7	
Line 5	Non Onodi Cell	Female	9.3 ± 3.1	8.7 ± 2.4	0.180
		Male	10.2 ± 3.0	10.1 ± 3.4	
		Total	10.0 ± 3.0	9.5 ± 3.0	

	Onodi Cell	**Female**	10.5 ± 3.7	10.7 ± 3.8	0.032*
		Male	11.0 ± 2.8	11.1 ± 3.3	
		Total	10.8 ± 3.3	10.9 ± 3.5	
Line 6	**Non Onodi Cell**	**Female**	21.8 ± 6.9	22.5 ± 4.2	0.074
		Male	22.8 ± 5.7	23.2 ± 6.7	
		Total	22.4 ± 6.1	22.9 ± 5.7	
	Onodi Cell	**Female**	23.0 ± 7.0	23.2 ± 6.6	0.065
		Male	26.1 ± 6.5	26.8 ± 6.4	
		Total	24.6 ± 6.9	25.1 ± 6.7	
Line 7	**Non Onodi Cell**	**Female**	17.8 ± 5.0	16.0 ± 5.3	0.418
		Male	17.2 ± 5.3	17.6 ± 6.4	
		Total	17.4 ± 5.1	17.0 ± 5.9	
	Onodi Cell	**Female**	16.3 ± 5.1	15.9 ± 5.7	0.406
		Male	17.0 ± 5.1	19.6 ± 6.0	
		Total	16.7 ± 5.1	17.9 ± 6.2	

Value are expressed as Mean ± SD; * Significant at P<0.05

Table 4.16: Cross tabulation between superior & Inferior with gender in line 3:

	Gender	Right side	Left side
Inferior	**Female**	23.3 ± 6.0	22.7 ± 6.5
	Male	18.1 ± 5.1	20.7 ± 6.0
	Total	17.7 ± 5.3	19.1 ± 6.5
	P-value	0.369	0.007
Superior	**Female**	15.1 ± 5.1	16.1 ± 5.1
	Male	16.7 ± 4.6	17.5 ± 5.7
	Total	16.0 ± 4.8	16.8 ± 4.5
	P-value	0.428	0.533

Table 4.17: Cross tabulation between Onodi cell & lines:

Lines	Onodi Cell (Yes)	Non Onodi Cell (No)	P-value
Line 1	8.5 ± 3.3	10.2 ± 3.2	0.000*
Line 2	10.2± 2.4	10.8 ± 3.5	0.162
Line 3	20.8 ± 6.3	22.2 ± 7.2	0.117
Line 4	14.7 ± 4.0	16.7 ± 3.6	0.000*
Line 5	9.8 ± 3.0	10.8 ± 3.4	0.013*
Line 6	22.6 ± 5.9	24.9 ± 6.8	0.010*
Line 7	17.2 ± 5.5	17.3 ± 5.7	0.903

Value are expressed as Mean ± SD; * Significant at P<0.05

Table 4.18: Cross tabulation between Onodi cell & gender:

Onodi cell		Gender		Total
		Female	Male	
Onodi Cell	Count	15.0	21.0	36.0
	% within Gender	16.3%	19.3%	17.9%
Non Onodi Cell	Count	77.0	88.0	165.0
	% within Gender	83.7%	80.7%	82.1%
Total	Count	92.0	109.0	201.0
	% within Gender	100.0%	100.0%	100.0%

Figure 4.4: Cross tabulation between Onodi cell & gender:

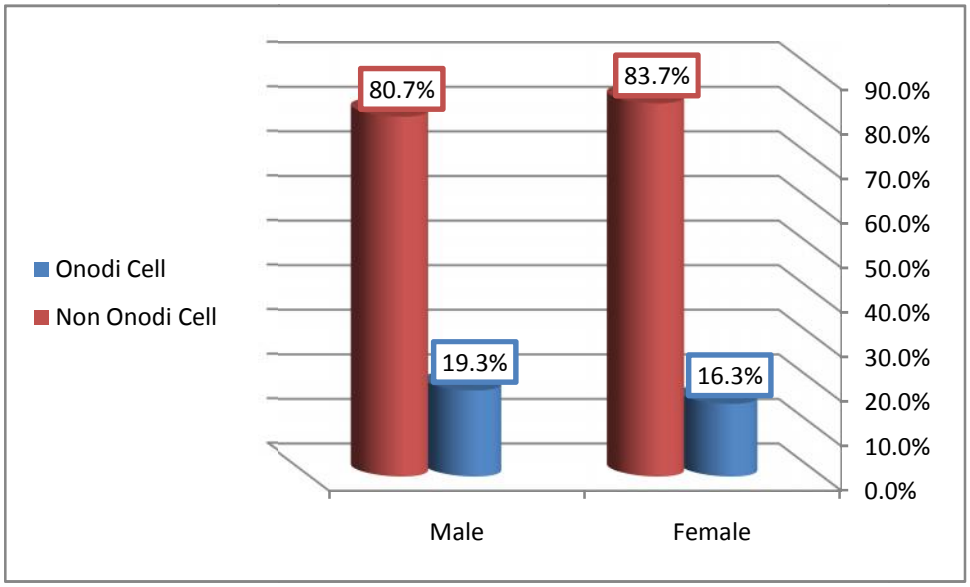

Table 4.19: Cross tabulation between Sellar, presellar and conchal with gender

SS Classification			Gender		Total
			Female	Male	
sphenoid sinuses Classification	Sellar	Count	68	90	158
		% within Gender	73.9%	82.6%	78.6%
	Pre-sellar	Count	24	19	43
		% within Gender	26.1%	17.4%	21.4%
	Conchal	Count	0	0	0
		% within Gender	0.0%	0.0%	0.0%
	Total	Count	92.0	109.0	201.0
		% within Gender	100.0%	100.0%	100.0%

CHAPTER FIVE

DISCUSSION, CONCLUSION & RECOMMENDATION

5.1 Discussion:

5.1.1 Anterior clinoid process

The incidence of anterior clinoid process pneumatization has been well reported in the literature. Bolger et al. found anterior clinoid process pneumatization in 13% of 202 paranasal sinus CT scans (Bolger et al., 1999). In a review of 150 paranasal sinus CT scans, De Lano et al. found anterior clinoid process pneumatization in only 13 of 300 sides (4%) (Delano et al., 1996). Sirikci et al. found anterior clinoid process pneumatization in 29.3% of 92 paranasal sinus coronal CT scans studied at 2.5 mm slice thickness (Sirikci et al., 2000). Birsen et al. encountered pneumatization of anterior clinoid process in 24.1% of 260 patients, for whom coronal sinonasal CT cuts were obtained at 3 mm slice thickness (Birsen et al., 2006). Another study reports anterior clinoid process pneumatization in 15.3%. (Hewaidi and Omami, 2008). Rudresh et al. found pneumatization of the anterior clinoid process in 15 % of 400 patients (Rudresh et al. 2012).

In this study, Pneumatization of the anterior clinoid process (ACP): for Sudanese was encountered in 28 patients (13.9%). It was bilateral in 9 (4.5%), on the right in 9 (4.5%) and on the left in 10 (5.0%) (Table 4.3), which was similar to the findings of the studies which were conducted by Hewaidi and Omami, (2008), Rudresh et al. (2012) and Bolger et al. (1999). Furthermore, the study found that there was no significant difference in the

side of the pneumatized ACP. Moreover, there was no gender difference in the patients with pneumatized ACP.

Obviously, the result of this study was different to the findings of the studies which were conducted by Delano et al. (1996), Sirikci et al. (2000) and Birsen et al. (2006). This may reflect differences between the studied populations; however, it is more likely that thin CT scan sections are considerably more precise. Thus, the previous reports of prevalence of anterior clinoid process pneumatization based on thick-cut CT scan review may underestimate the prevalence of this anatomic variant. Pneumatization of anterior clinoid process forms the opticocarotid recess, i.e. the small space on the lateral wall of the sphenoid sinus, between the optic canals, superiorly, and the carotid prominence, inferiorly. The opticocarotid recess is supposed to concur with ipsilateral optic nerve and/or internal carotid artery protrusion into the sphenoid sinus. That was what we observed in our series as well. Two previous studies suggested that there is a statistically significant relationship between the pneumatization of anterior clinoid process and the protrusion of optic nerve (Sirikci et al., 2000); (Birsen et al., 2006). This study found high association between the pneumatization of anterior clinoid process and the dehiscence of optic nerve.

5.1.2 Greater wing of sphenoid

This study defined pneumatization of greater wing of sphenoid as extension beyond a vertical line crossing foramen rotundum. Pneumatization of the greater wing of sphenoid bone (GWS): for Sudanese was encountered in 70 patients (34.8%), of whom 31 (15.4%) were bilateral, 13 (6.5%) were on the right side, and 26 (12.9%) were on the left side. There was no significant difference in the side of the pneumatized GWS. These results shown in

(Table 4.3). Furthermore, there was no gender difference in the patients with pneumatized GWS (Table 4.7). This was considered larger than what was mentioned by John Earwaker who revealed pneumatization of greater wing of sphenoid in 10.7% of patients (Earwaker, 1993). Furthermore Hewaidi and Omami identified it in 20.0% patients (Hewaidi and Omami, 2008). Rudresh et al. found pneumatization of the greater wing of the sphenoid in 12.75 % of 400 patients (Rudresh et al. 2012).

The pneumatization of the floor of the middle cranial fossa, in the presence of arachnoid granulations, forms 'pit holes'. The enlargement of these pits has been casually implicated in the development of non traumatic cerebrospinal leaks (Hewaidi GH et al., 2008).

5.1.3 Pneumatization of the pterygoid process

Pterygoid process pneumatization is recognized if it extends beyond a horizontal plane crossing the vidian canal. We found a pneumatized pterygoid process in 81 patients (40.3%) of whom 47 (23.4%), 10 (5%), and 24 (11.9%) were bilateral, right sided, and left sided, respectively. There was no significant difference in the side of the pneumatized PP. These results shown in (Table 4.3). Furthermore, there was no gender difference in the patients with pneumatized PP (Table 4.7). In Libyan population a pneumatized pterygoid process was found in 29% of the patients (Hewaidi and Omami, 2008). Sirikci et al., reported pneumatization of the pterygoid process in 29.3% (Sirikci et al., 2000). Rudresh et al. found pneumatization of the pterygoid process in 31 % of 400 patients (Rudresh et al. 2012). This wide range of prevalence may be attributed to the use of different criteria (Hewaidi and Omami, 2012).

Pneumatization of the pterygoid process, when it was present, was an important pathway for access to the central skull base, as for the extended transnasal endoscopic approaches which may reach the pterygoid process through the medial part of the posterior maxillary wall (Hewaidi and Omami, 2012); (Lane and Bolger, 2002). These techniques may provide a route for endoscopic repair of cerebrospinal fluid leaks and endoscopic biopsy of skull base lesions. Such information may be important in preoperative planning for skull base surgery. Pneumatization of pterygoid process thins the bony floor of the scaphoid fossa to as little as 0.2 mm, producing an intimate relation between the sinus and the auditory tube (Vidic, 1986). Bolger et al. identified pterygoid process pneumatization in 43.6% of patients (Bolgeret et al., 1991). They recognized pterygoid process pneumatization if it extended beyond a plane tangential to the most inferolateral aspect of the maxillary division of the trigeminal and vidian nerves. Despite the different criterion used to define pneumatization of the pterygoid process, the results reported by Bolgeret et al. and those reported here are almost the same. The statistical analysis in this study revealed a high significant relationship between the pterygoid process pneumatization, Vidin nerve protrusion and Vidin nerve dehiscence.

5.1.4 Internal carotid artery

In this study, the protrusion of (ICA) was found in 51 patients (25.4%), of whom 21 (10.4%) were bilateral, 11 (5.5%) were right sided, and 19 (9.5%) were left sided. Dehiscence of (ICA) was seen in 25 patients (12.4%) of whom 13 (6.5%) were bilateral, 6 (3%) were on the right, and 6 (3%) were on the left. The statistical analysis show not significant difference of Protrusion and dehiscence of the internal carotid artery between male and

female groups (P-value = 0.431), (P-value=0.677) respectivly. These results were illustrated in (Table 4.7). Furthermore, there was no significant difference of Protrusion and dehiscence between groups of age, (P-value = 0.859), (P-value=0.859) respectivly .

Fuji et al. studied 25 cadaver sphenoid bones and found 8% of carotid arteries dehiscent of bone in the lateral sphenoid (Fuji et al., 1979). Kennedy et al. found dehiscence on the bony wall of the internal carotid artery in 25% of patients (Kennedy et al., 1990). Sirikci et al. reported protrusion of internal carotid artery in 26.1% of patients and dehiscence of the artery in 23% (Sirikci et al., 2000). Sareen et al. studied sagittal sections of 20 dried skulls and found dehiscence of the carotid artery in 5% (Sareen et al., 2005). Birsen et al. encountered protrusion of internal carotid artery in 30.3% and dehiscence in 5.3% of patients (Birsen et al., 2006). Both Sirikci and Birsen recognized protrusion of internal carotid artery or optic nerve into the sphenoid sinus as the presence of more than half the circumference of the concerned structures into the sinus cavity. In this study, presence of the circumference into the sinus cavity, at any degree, was enough to define protrusion. Dehiscence is defined as the absence of the visible bone density which separates the sinus from the course of the concerned structures. Whereas Hewaidi and Omami, (2008) found protrusion of internal carotid artery into the sphenoid in 41% of patients, and dehiscence of the artery in 30% (Hewaidi and Omami, 2008). Rudresh et al. found protrusion of the internal carotid artery into the sphenoid was noted in 7% patients and dehiscence of the artery was found in 3% patients (Rudresh et al., 2012). Vimal et al. reported that the internal carotid artery was protruded into the sinus cavity in 25% of patients, and dehiscence of the artery in 16.5% (Vimal et al., 2012). Without explaining their criteria, Elwany et al.

observed protrusion of carotid artery in 29% and dehiscence in 4.8% of patients (Elwany et al., 1999) and Sethi et al. identified carotid protrusion in 93% (Sethi et al., 1995). These findings were different from what was found this study that and the incongruity between these prevalence rates may be due to different techniques or ethnic differences between the populations (Hewaidi and Omami, 2012; Davoodi et al., 2008). If the surgeon is unaware of dehiscence or protrusion of the artery, even fatal hemorrhage may happen, because is hardly possible to control bleeding from an injured internal carotid artery within the sphenoid sinus (Sirikci et al., 2000). The results in this study found high significant association between the pneumatization of anterior clinoid process and protrusion of internal carotid artery into the sphenoid sinuses (P-value = 0.003).

5.1.5 Optic nerve

In this study, Protrusion of the optic nerve was defined as a bulging of the the optic canal into the sphenoid sinus cavity at any degree, was enough to define protrusion. Dehiscence is defined as the absence of the visible bone density which separates the sinus from the course of the concerned structures.

In this study, the protrusion of the optic nerve was found in 6 patients (3%). Protrusions were bilateral, right sided, and left sided in 1 (0.5%), 0 (0%), and 5 (2.5%) of patients, respectively. Dehiscence of ON was observed in 32 (15.9%) patients, of whom 19 (9.5%) were bilateral, 7 (3.5%) were right sided, and 6 (3%) were left sided; this was seen in (Table 4.3). The statistical analysis show not significant difference of Protrusion and dehiscence between male and female groups. These results were illustrated in (Table

4.7). Additionally, there was no significant difference of Protrusion and dehiscence between groups of age.

However, previous studies reported a wide range of protrusion rates of 8 to 70% (Dessi et al., 1994; Teatini et al., 1987). Another study found only 4% of optic nerves was dehiscent in the lateral sphenoid (Fuji et al., 1979). Rudresh et al. found protrusion of the optic nerver into the sphenoid was noted in 10% patients and dehiscence of the nerve was found in 5 % patients (Rudresh et al., 2012). Hewaidi and Omami, (2008) encountered the protrusion of the optic nerve in 35.6% patients and dehiscence of the nerve in 30.6% patients (Hewaidi and Omami, 2008). Siricki et al., and Unal et al. reported optic nerve protrusion into the sphenoid sinus in Turkish patients at the rate of 31 % each, which is equivalent to one in three patients having optic nerve protrusion (Siricki et al., 2000); (Unal et al., 2006). Whereas, Tan et al. reported a remarkably high rate of 69 % optic nerve protrusion in the Asian counterparts (Tan et al., 2007). Vimal et al. reported that the optic nerve was protruded into the sinus cavity in 63.7% of patients, and dehiscence of nerve in 22.5% (Vimal et al., 2012). Sudanese were found to score fewer percentages of protrusion and dehiscence. What was mentioned in the study done on Asin and Indian population (Vimal et al., 2012); (Tan et al., 2007) were obviously very high and most likely explained by their criteria for defining protrusion and dehiscence and may reflect differences between the studied populations.

Optic nerve injury resulting in blindness is a potential undesirable complication of endoscopic sinus surgery, especially when operating on the sphenoid sinus (Metson et al., 1996). Axial view CT scans are essential in the assessment of the posterior ethmoidal cells in relation to the optic nerve

(Bayram et al., 2001). The optic nerve is at greater risk of injury with the presence of Onodi cells (Driben et al., 1998).

5.1.6 Maxillary nerve

A study which was conducted by Hewaidi GH et al. showed that maxillary nerve protrusion was noted in 24.3% patients and that dehiscence of the nerve was noted in 13% patients (Hewaidi and Omami, 2008). Birsen et al. encountered the maxillary nerve protrusion in 30.3% patients and dehiscence in 3.5% patients (Birsen et al., 2006). Rudresh et al. found protrusion of the maxillary nerve into the sphenoid was noted in 12.25% patients and dehiscence of the nerve was found in 2.75 % patients (Rudresh et al., 2012). On the other hand, another study found that the sinuses were neither with protrusion nor dehiscence of maxillary nerve (Sareen et al., 2005).

In this study, the protrusion of MxN was encountered in 56 (27.9%) patients, of whom 21 (10.4%) were bilateral, 18 (9%) were on the right side, and 17 (8.5%) were on the left side. Sudanese were found to score higher dehiscence rate than what was mentioned in the previous studies. Dehiscence of MxN was seen in 91 (45.3%) patients, of whom 49 (24.4%) were bilateral, 23 (11.4%) were right sided, and 19 (9.5%) were left sided; this was seen in (Table 4.3). This difference may be due to ethnicity divergence. The statistical analysis also shows not significant difference of Protrusion and dehiscence between male and female groups. These results were shown in (Table 4.7). Additionally, there was no significant difference of Protrusion and dehiscence between groups of age. The importance of the knowledge about this anatomical difference; is that in the endoscopic sphenoid surgery, a protruded or dehiscent maxillary nerve is accountable to injury.

5.1.7 Vidian nerve

The protrusion of (VN) was present in 85 (42.3%) patients of whom 52 (25.9%) were bilateral, 10 (5%) were on the right side, and 23 (11.4%) were on the left side. Dehiscence of (VN) was identified in 111 (55.2%) patients, of whom 74 (36.8%), 18 (9%), and 19 (9.5%) were bilateral, right sided, and left sided, respectively; this was seen in table (4.3). The importance of Vidian nerve is that when it was affected, it can cause pain and Vidian neuralgia. Different studies were obtained and revealed that Vidian canal was protruded into the sinus cavity in 18% (Lang and Keller, 1978) and 27% (Hewaidi and Omami, 2008). Rudresh et al. found protrusion of the Vidian nerve into the sphenoid was noted in 30% patients and dehiscence of the nerve was found in 7.75 % patients (Rudresh et al., 2012).

Sudanese were found to have greater percentages for protrusion and dehiscence. Our study may serve the surgeons to be as a reference for the description of anatomic relationship of the Vidian canal to the sphenoid sinus cavity for Sudanese population, as well as decreasing the complication of the endoscopic trans-sphenoidal and Vidian neurectomy surgery.

5.1.8 PosteriorEthmoid Cell

Posterior ethmoid cell may expand beyond the confines of the ethmoid bone and grow into the body of sphenoid bone (Ritter, 1978). The migration tends to go supero-laterlly. Cell may surround the optic canal or may completely overgrow the sphenoid sinus and extend slightly posterior to it. In this study, over ridding ethmoid cell were present in 36 (17.9 %) of the subjects, males were 21 (19.3%), females were 15 (16.3%) where the non- onodi type was found in 165 (82.1 %) of the sample 77 (83.7%), 88 (80.7%) for females and males respectively (Table 3). As we mention before in this study, the optic

nerve is at greater danger of injury with the incidence of Onodi cells (Driben et al., 1998).

5.1.9 Classification of the Sphenoid Sinus

There are various ways to classify the types of sphenoid sinus. However, the conventional and widely accepted Hammer and Radberg classication is used in most practices till today. It describes sphenoid sinus pneumatization as conchal, presellar and sellar types, based on pneumatization around the sella turcica (Hammer and Radberg, 1961). In the conchal type, pneumatization is absent, the sphenoid sinus is filled by cancellous bone, and there is no association with the sella turcica. In the presellar type, the sinus cavity remains anterior to a vertical line drawn through the tuberculum sellae. Whereas in the sellar type, sinus pneumatization extends beyond a vertical line drawn through the tuberculum sellae, and this type is related to the floor and anterior wall of the sella turcica. The various patterns of pneumatization are illustrated in Fig. (2.5).

Madiha et al. in 2007 reported 76 % of presellar type and the rest sellar pneumatization, in 25 Egyptian sinuses consisting of patients and cadavers. Conchal type was not encountered in this study. In contrast, in Tan et al.'s Asian cadaveric study, the sellar type was the commonest at 55 %, and the least commonest was pre-sellar at 17 %. The sellar type was the predominant type with 90 %, followed by presellar type at 9 % and conchal at 1 % in 100 Korean cadaveric heads examined by Cho et al. There appears to be a difference in the main type of pneumatization with regard to ethnicity, i.e., the sellar type of pneumatization seems to be commoner in Asians. This highlights the importance of studying the patterns of pneumatization in a local population as the type of pneumatization in turn could affect the outcome of surgical access (Anusha et al., 2014).

The present study, found out that the sphenoid sinuses was of the sellar pneumatization type in 158 (78.6%), males were 90 (82.6%) and females were 68 (73.9%). Presellar pneumatization was seen in the remaining 43 (21.4%), males were 19(17.4%) and females were 24 (26.1%) and no subject was choncal in Sudanese population. We noticed that female has high presence in pre seller type.

5.1.10 Measurement of the Sphenoid Sinus

The anatomy of the sinuses plays a key role in surgery. Sphenoid sinus surgeries are quite complicated due to the location and structural variations of this sinus. In this study, the sphenoid sinus was evaluated with multiplanar CT, and different lines were designed to obtain surgical data for the Sudanese population.

The natural ostium of the sphenoid sinus can be visualized easily with CT and endoscopy. In addition, endoscopic sphenoid sinus surgery can be performed more safely through the natural ostium (Wu et al., 2011). Therefore, the distance from the ostium to the vital anatomic structures surrounding the sphenoid sinus is important.

In this study, we designed 7 lines to measure the distance of sphenoid sinus, 6 lines in sagittal plane and one line in coronal plane. Consequently, to measure the distances from the center of the sphenoid sinus ostium to the sphenoid sinus roof, base and posterior wall, lines 1, 2, and 3 were designated. Lines 4 and 5 were used to evaluate the relationships and show the distances at different levels between the sella and the anterior wall of the sphenoid sinus. Line 6 was used to show the horizontal range of the sphenoid sinus. Line 7 was used to measure the maximum width at the middle of the sphenoid sinus from the lateral wall to the medial wall of

sphenoid sinus. Obtaining noninvasive measurements of the sphenoid sinus was possible using the thin slice multiplanar reconstruction technique. With this technique, the systemic errors that occur in cadaver research due to the shrinking of tissues in formaldehyde can be prevented. The transverse and coronal planes are important in the visualization of the sphenoid ostium and onodi cells. To obtain more surgical anatomic information, sagittal plane measurements of the surgical path should be performed.

In this study, the mean length of Line 1 was 9.9 ± 3.3mm so if the surgeon proceeds to more than the defined height, the skull base might be perforated. There are a similar studies performed by Wu et al. (2011) on a Chinese population, Hatice et al. (2013) on Turkish population and Jae et al. (2012) on Korean population found that the average length of Line 1 was found to be 10.6± 1.5 mm, 7.3±2.4 mm and 9, 97± 3.06 mm consequently, demonstrating that line 1 in Sudanese population has the similar value with Korean population and difference value with Chinese and Turkish population values. The mean length of (Line 2) was 10.7 ± 3.4mm. In the study by Wu et al. (2011), the average length of Line 2 was 12 ± 3.7 mm. Hatice et al. (2013) on Turkish population found that line 2 was 12.9 ± 3.8 mm and Jae et al. (2012) on Korean population found that the value of line 2 was 10.44 ± 2.6 mm. All these values were not similar to that obtained in this study, demonstrating that the surgeon should be very aware when he wants to dilate the sphenoid ostium downward , and these differences may be due to Sudanese subjects vary from other populations .

Line 3 according to the localization of the ostium, was 16.4 ± 4.7 mm or 18.4 ± 4.7 mm. According to the distances defined, to avoid the injuries to the sella, sphenoid sinus procedures should not exceed a depth of 16.4 mm. In the study by Wu et al. (2011), the average length of Line 3, according to

the localization of the ostium, was 18 ± 1.5 mm or 28± 2.5 mm. Hatice et al. (2013) on Turkish population found that line 3 was 14.4±3.8 mm or 24.2±5.4 mm and Jae et al (2012) on Korean population found that the value of line 3 was 13.44 ± 3.27 mm or 20.30± 7.63. The risk of injury to the sella was found to be greater in the Sudanese, Korean and Turkish populations than in the Chinese populations. If the sphenoid ostium is localized superior to the lowest point of the sella, the surgeon should be very careful during the procedure (Kim et al., 2001; Kieff & Busaba, 2002). When entering the sphenoid sinus, the unique borderline for guiding the surgeon into the depths of the sinus and finding the targeted point is the posterior wall of the sphenoid sinus, although the risk of injury to the pituitary gland is quite high (Li et al., 2008). If the sinus ostium is localized inferior to the lowest point of the sella, then when entering the sphenoid sinus, the surgeon will immediately come across the posterior wall of the sinus.

Line 4 was 16.4 ± 3.7mm. In the study by Wu et al. (2011), the average length of Line 4 was found to be 17.5±1.3 mm. Hatice et al. (2013) on Turkish population found that line 4 was 19.09± 3.5 mm and Jae et al. (2012) on Korean population found that the value of line 4 was 10.44 ± 2.6 mm, which the shortest value was comparing with other population. Line 5 was 10.6 ± 3.4 mm, Wu et al. (2011) in their study found that the average length of Line 5 was 10.1 ±1.0 mm. Hatice et al. (2013) on Turkish population found that line 5 was 10.8 ± 5.03 mm and Jae et al. (2012) on Korean population found that the value of line 5 was 9.46 ± 4.28 mm. All these values of line 5 are not much different than the length obtained in the present study. Due to the obliquity of Lines 4 and 5 related to the pituitary fossa, we should be attentive not to wrongly estimate the distance, in order to avoid complications of sella while performing the surgery.

The maximum depth (Line 6) was 24.5 ± 6.7mm in length. The results in this study showed that this depth is 2.5 times longer than line 5 and that means the entrance of sphenoid sinus in Sudanese population to drainage of inflammatory processes involving the sphenoid sinus (mucoceles, mucopyoceles, fungal sinusitis, etc.) as well as surgery is safer from below. In the study by Wu et al. (2011), the average length of Line 6 was 22.0 ±7.7 mm. Hatice et al. (2013) on Turkish population found that line 6 was 24.2 ± 6.8 mm and (Jae et al,2012) on Korean population found that the value of line 6 was 25.5 ± 7.55 mm. The maximum width (Line 7) was 18.4 ± 5.9 mm. To our knowledge there was no research done for measuring the width of sphenoid sinus using CT in coronal plane in adult patients. In the study by Barghouth et al. (2002), the average width of sphenoid sinus in children under 17 years old was 12.8± 3.1, using MRI machine.

Studies by Wu et al. (2011), and Jae et al. (2012), revealed that no differences between the left and the right sides and males and females were found concerning the defined distances. On the other hand, in the study by Hatice et al. (2013) found that lines 4 and 6 were longer on the left side than on the right side. Additionally, Lines 2, 3, 4 and 6 were found to be longer in males than in females. However, in the present study, no differences between the left and the right sides were noted but the Lines 3 and 6 found to be longer in males than in females in both sides , the lines 2 and 7 were longer in males than in females only on the left side than on the right side and line 4 wae longer in male than in female only in the right side. Signifying that gender differences should be considered in sphenoid sinus procedures in Sudanese population.

Kainz and Stammberger defined an onodi cell and its relation to the optic nerve and optic canal (Kainz & Stammbergcr, 1991). Its prevalence in

Sudanese population is unknown before this study, which showed that there is a significant presence of posterior ethmoid cells in Sudanese population and the surgeons should be aware during surgery because the cerebrospinal fluid leakage is the most common complication (Von Aken et al., 2004; Marc et al., 2006) during transsphenoidal surgery, and the sagittal CT image is necessary before dilatation the sphenoid ostium. In all 201 patients in this study, onodi cells were present in 36 (17.9 %), patients 21 (19.3%) males, 15 (16.3% females).

Onodi cells were absent in (82.1%) of the patients (Table 4.18). The presence of onodi cells should be routinely looked for by Functional endoscopic sinus surgery surgeons to prevent damaging the optic nerve. There was a significant difference between non- onodi cell and onodi cell in line (1, 4, 5, 6) (P-value < 0.05), but in line 2, 3, 7 there was no significant difference between non- onodi cell and onodi cell (P-value > 0.05) (Table 4.17). In onodi cell-positive subjects, the superior wall of the sphenoid sinus did not form the skull bottom; rather, it formed the bottom of the Onodi cells. Line 1 was found to be shorter in Onodi cell-positive patients compared to the Onodi cell-negative patients. In spite of being shorter, the distance in Onodi cell-positive patients is much safer, because during sphenoid surgery, the skull base is not directly bordering to the sphenoid sinus (Wu et al., 2011). In Onodi cell-positive patients, the anterior wall of the sphenoid sinus (Line 5) was located more posteriorly. In such cases, the danger of injury to the sella is not greater compared to the other groups because the sphenoid ostium is located more superior to this level. These results were similar results obtained by Wu et al. (2011), Hatice et al. (2013) and Shin et al. (2012).

5.2 Conclusion

The Study concluded that the Sudanese sphenoid sinus morphology is different from other populations mentioned in the previous studies. Prevalence of Protrusion of the internal carotid artery, maxillary nerve and vidian nerve were high. Prevalence of dehiscence of the maxillary nerve and vidian nerve were high. Furthermore, the bony wall over these structures is very thin. During surgery, careful attention must be paid so as not to damage these structures during manipulation of the sinus. The prevalence of Protrusion in the optic nerve, the ICA, and the maxillary and vidian nerves depends on the degree of sphenoid sinus pneumatization. Protrusion in the surrounding structures increases in proportion to the degree of pneumatization.

Protrusion of the internal carotid artery and dehiscence optic nerve was strongly associated with ipsilateral pneumatization of the anterior clinoid process. Protrusion and dehiscence of the maxillary nerve and vidian canal into the sinus cavity was strongly associated with pneumatization of the pterygoid process, on the same side.

CT is a more valuable tool in the imaging of sphenoid sinus. CT scans also detect the anatomic variations that may place the patient at an increased risk for intraoperative complications. Coronal CT may prove beneficial for demonstration of sphenoid sinus anatomy .A detailed knowledge about anatomic variations will avoid morbid consequences during surgery. The clearest understanding of the sinus morphology enhances identification of the limits of dissection and hence may help to reduce the possibility of complications.

The present data regarding the vertical and horizontal dimensions of sphenoid sinus indicate that the dimensions of sphenoid sinus may anatomically vary. Sudanese population sphenoid sinuses character differs from other studied populations and also the differences in the size of sphenoid sinus take place between males and females. These Anatomic differences of the sphenoid sinus between genders should be taken into consideration during surgery.

In the study performed, it was shown that the presence of Onodi cells was greater in Sudanese population. Therefore, during surgery, surgeons should be aware of the significantly greater presence of Onodi cells in Sudanese population because the most common complication during transsphenoidal surgery is cerebrospinal fluid leak (CSF) leakage. In Onodi cell-positive patients, the sphenoid sinus roof did not form the skull base; rather, it formed the base of the Onodi cells. Line 1 was found to be shorter in Onodi cell-positive patients compared to the Onodi cell-negative patients. Despite being shorter, the distance in Onodi cell-positive patients is much safer because during sphenoid surgery, the skull base is not directly adjacent to the sphenoid sinus. In Onodi cell-positive patients, the anterior wall of the sphenoid sinus (Line 5) was located more posteriorly. In such cases, the risk of injury to the sella is not greater compared to the other group because the sphenoid ostium is located more superior to this level.

The present study results show that the pneumatization of the sphenoid sinuses in Sudanese population was sellar and presellar types and no presence of choncal type was found .Using sagittal and coronal CT images is of significant value in characterization of sphenoid sinuses.

5.3 Recommendation

- The clearest understanding of the sphenoid sinus morphology enhances identification of the limits of dissection and hence may help to reduce the possibility of complications.
- Sudanese population sphenoid sinuses character differs from other studied populations and also the differences in the size of sphenoid sinus take place between males and females. These Anatomic differences of the sphenoid sinus between genders should be taken into consideration during surgery.
- During surgery, surgeons should be aware of the significantly greater presence of Onodi cells in Sudanese population because the most common complication during transsphenoidal surgery is cerebrospinal fluid leak (CSF) leakage.
- CT is a more valuable tool in the imaging of sphenoid sinus. CT scans also detect the anatomic variations that may place the patient at an increased risk for intraoperative complications.
- Using sagittal and coronal CT images is of significant value in characterization of sphenoid sinuses.
- Further study about the use of CT compare to MRI in assessment of sphenoid sinus measurements is recommended.
- Further studies of the sphenoid sinuses measurement in different tribe in Sudan using CT.

References:

Aibara R, Kawakita S, Yumoto E, Yanagihara N (1997). Relationship of Onodi cell to optic neuritis–radiological natomy on coronal CT scanning. Nippon Iibiinkoka Gakkai Kaiho;100:663-70.

Alexandra Mavrodi, George Paraskevas (2013). Evolution of the paranasal sinuses' anatomy through the ages. pISSN 2093-3665 eISSN 2093-3673.

Allan Keast, Sofie Yelavich, Patrick Dawes, Brett Lyons (2008). Anatomical variations of the paranasal sinuses in Polynesian and New Zealand European computerized tomography scans. Otolaryngology–Head and Neck Surgery 139, 216-221.

A. John Vartanian, MD (2014). CT Scan of the Paranasal Sinuses.

Anderhuber W, Weiglein A, Wolf G (1992). Nasal cavities and paranasal sinuses in newborn and children. Acta Anat 144:120–126.

Anik I, Anik Y, Koc K, Ceylan S (2005). Agenesis of sphenoid sinuses. Clin Anat 18(3):217–219.

Anon JB, Rontal M, Zinreich SJ (1996). Anatomy of the paranasalsinuses, Thieme, New York.

Antoniades K, Vahtsevanos K, Psimopoulou M, Karakasis D (1996). Agenesis of sphenoid sinus: case report. ORL J Otorhinolaryngol Relat Spec 58(6):347–349.

Arslan H, Aydinlioglu A, Bozkurt M, Egeli E (1999). Anatomic variations of the paranasal sinuses: CT examination for endoscopic sinus surgery. Auris Nasus Larynx;26:39-48.

A. UNLU, et al (2008). Endoscopic Anatomy of Sphenoid Sinus for Pituitary Surgery.

Aydinlioglu A, Erdem S (2004). Maxillary and sphenoid sinus aplasia in Turkish individuals: a retrospective review using computed tomography. Clin Anat 17(8):618–622.

Balasubramanian Thiagarajan (2012). Anatomy of Paranasal sinuses. Drtbalu's otolaryngology online.

B. Anusha · A. Baharudin · R. Philip ·S. Harvinder · B. Mohd Shaffie. Anatomical variations of the sphenoid sinus and its adjacent structures: a review of existing literature. Surg Radiol Anat. DOI 10.1007/s00276-013-1214-1.

Bannister LH, Berry MM, Collins Petal (1995). Grays Anatomy, 38th edn. Edinburgh: Churchill Livingstone: 585-589.

Banna M, Olutola PS (1983). Patterns of pneumatization and septation of the sphenoidal sinus. J Can Assoc Radiol.; 34(4):291-3.

Bayram M, Sirikci A, Bayazit YA (2001). Important anatomic variations of the sinonasal anatomy in light of endoscopic sinus surgery: a pictorial review. eur Radiol 11:1991–1997.

Basˇic´ N, Basˇic´ V, Jukic´ T, *et al. (*1999). Computed tomographic imaging to determine the frequency of anatomical variations in pneumatization of the ethmoid bone. Eur Arch Otorhinolaryngol;256:69-71.

Bouthillier A, van Loveren HR, Keller JT (1996). Segments of the internal carotid artery: a new classification. Neurosurgery 38(3):4254–4332.

Blitzer A, Carmel PW, and Post KD. Sphenoid Sinus. In Surgery of the Paranasal Sinuses. 2nd edition. Pages 251 – 276.

Bolger WE, Butzin CA, Parsons DS (1991). Paranasal sinus bony anatomic variations and mucosal abnormalities: CT analysis for endoscopic sinus surgery. Laryngoscope 101:56–64.

Bosma J, Introduction to the symposium on development of the basicranium. In: Bosma JF (ed), Symposium on development of the basicranium, Publication No. (NIH) 76- 989, U.S. Department of Health, Education and Welfare (DHEW), Bethesda, MD, 3–43.

Cakmok O, Shohet MR, Kern EB (2000). Isolated sphenoid sinus lesions. Am J Rhinol 14:13–19.

Cappabianca P, Cavallo LM, Coloa A, et al. (2002). An endoscopic endonasal transsphenoidal approach: an outcome analysis of 100 consecutive procedures. Minim Invas Neurosurg; 45:193-200.

Castelnuovo P, Pistochini A, Locatelli D (2006). Different surgical approaches to the sellar region: focus on the "two nostrils four hands technique". Rhinology 44:2–7.

Chapman PR, Shah R, Cure JK et al (2011). Petrous apex lesions: pictorial review. AJR Am J Roentgenol 196(3 suppl).

Ciric I, Ragin A, Baumgartner C, Pierce D (1997). Complications of transsphenoidal surgery: results of a national survey, review of the literature, and personal experience. Neurosurgery 40:225–236.

Citardi MJ, Gallivan RP, Batra PS, Maurer CR, Rohlfing T, Roh HJ et al. Quantitative Computer-Aided Computed Tomography Analysis of Sphenoid Sinus Anatomical Relationships. Am J Rhinol 2004;18(3):173-8.

Cope VZ (1917). The internal structure of the sphenoidal sinus. J Anat.;51(Pt 2):127- 136.

Cumberworth VL, Sudderick RM, Mackay IS (1994). Major complications of functional endoscopic sinus surgery. Clin Otolaryngol;19:248-53.

Curtin HD, Som PM, Braun IF, Nadel L(1996). Skull base. In: Som PM, Curtin HD (eds) Head and neck imaging, Mosby– Year Book, St. Louis, 2:1233–1299.

Degirmenci B, Haktanir A, Acar M, Albayrak R, Yucel A (2005). Agenesis of sphenoid sinus: three cases. Surg Radiol Anat 27(4):351–353

Dessi P, Moulin G, Castro F, Chagnaud C, Cannoni M (1994). Protrusion of the optic nerve into the ethmoid and sphenoid sinus: prospective study of 150 CT studies. Neuroradiology 36:515–516.

Digre KB, Maxner CE, Crawford S, Yuh WT (1989). SigniWcance of CT and MR Wndings in sphenoid sinus disease. Am J Neuroradiol 10:603–606.

Doglietto F, Prevedello DM, Jane JA Jr, Han JA, Laws ER Jr (2005). A brief history of endoscopic transsphenoidal surgery – from Philipp Bozzini to the First World Congress of Endoscopic Skull Base Surgery. Neurosurg Focus 19:E3.

Driben JS, Bolger WE, Robles HA *et al.(* 1998). The reliability of computerized tomographic detection of the Onodi (sphenoethmoid) cell. AmJ Rhinot;12:105-111.

D Szolar, K Preidler, G Ranner, H Braun, C Kugler, G Wolf, H Stammberger and F Ebner, The sphenoid sinus during childhood: establishment of normal developmental standards by MRI. Surgical and Radiologic Anatomy,16(2):193-198.

Elwany S, Elsaeid I, Thabert H (1999). Endoscopic anatomy of sphenoid sinus. J Laryngol Otol 113:122–126.

Embryology of the paranasal sinuses (Feb 4,5 2013) available at: URL: https://www.uvm.edu/medicine/surgery/documents/SinusSurgery3.pdf

Estudio Anatómico del Seno Esfenoidal en Relación con la Cirugía Endoscópica Study of Sphenoid Sinus Anatomy in Relation to Endoscopic Surgery.

Feldmann H. (1998). The maxillary sinus and its illness in the history of rhinology. Images from the history of otorhinolaryngology, highlighted by instruments from the collection of the German Medical History Museum in Ingolstadt. Laryngorhinootologie;77:587-95.

Formby ML. The maxillary sinus. Proc R Soc Med (1960).;53:163-8.

Francis B. Quinn, Jr., MD and Matthew W. Ryan, MD. (2002). Paranasal Sinus Anatomy and Function.

Fujii K, Chambers SM, Rhoton AL Jr (1979). Neurovascular relationships of the sphenoid sinus: A microsurgical study. J Neurosurg 50:31-39.

Gady Har-El, Surgical Approaches to the Sphenoid Sinus, Rhinologic and Sleep Apnea Surgical Techniques, chapter seven ,Springer, 2007, pp 73-81, ISBN: 978-3-540-34019-5, Berlin.

Garrison D, Hast M. On the fabric of the human body: an annotated translation of the 1543 and 1555 editions of Andreas Vesalius' De Humani Corporis Fabrica [Internet]. Illinois: Northwestern University; 2003 [cited 2013 Apr 28]. Available from: http://vesalius.northwestern.edu/flash.html.

Garrison DH, Hast MH. Andreas Vesalius on the larynx and hyoid bone: an annotated translation from the 1543 and 1555 editions of De humani corporis fabrica. Med Hist 1993;37:3-36.

Goldsmith AJ (1999). The traspalatal approach for juvenile angiofi broma. Oper Tech Otolaryngol Head Neck Surg 10:98–100.

Gray H. (37th edn.) (1989): Gray's anatomy. Edinburgh: Churchill Livingstone, pp376-377.

Greenfield JP, Anand VK, Kacker A et al (2010). Endoscopic endonasal transethmoidal transcribriform transfovea ethmoidalis approach to the anterior cranial fossa and skull base. Neurosurgery 66(5):883–892.

Gupta T, Aggarwal A, Sahni D (2013). Anatomical landmarks for locating the sphenoid ostium during endoscopic endonasal approach: a cadaveric study. Surg Radiol Anat 35(2):137–142.

Hai-bo Wu · Li Zhu · Hui-shu Yuan (2011). Chao Hou –Surgical measurement to sphenoid sinus for the Chinese in Asia based on CT using sagittal reconstruction images - Eur Arch Otorhinolaryngol - DOI 10.1007/s00405-010-1373-1.

Hajek M (1926). Pathologie und Therapie der entzündlichen Erkranungen der Nebenhöhlen der Nase, 5th edn. Leipzig, p 76.

Hamberger CA, Hammer G, Norlen G, et al (1961). Transphenoidal hypophysectomy. Arch Otol 74%8,

Hammer G, Radberg C (1961). Sphenoidal sinus: Anatomical and roentgenological study with reference to transphenoidal hypophysectomy. Acta Radio1 56:401-422

Hardy J (1969). Transphenoidal microsurgery of the normal and pathological pituitary. Clin Neurosur 16:185–217.

Har-El G (1994). The anterior wall of the sphenoid sinus. Ear Nose Th roat J 73:446–448.

Har-El G (2002). Approaches to the sphenoid sinus. In: Bluestone CD, Rosenfeld RM (eds) Surgical atlas of pediataric otolaryngology, 2nd edn. BC Decker, Hamilton, pp 353–365.

Har-El G, Todor R (2003). Endoscopic pituitary surgery. In: Har-El G, Weber PC (eds) Rhinologic and otologic aspects of skull base medicine and surgery. American Academy of Otolaryngology-Head and Neck Surgery, Alexandria, pp 114–130.

Har-El G, Todor R (2003). Endoscopic transnasal approach to the pituitary gland. Oper Tech Otolaryngol Head Neck Surg 14:205–206.

Har-El G (2003). Endoscpic direct transnasal sphenoidotomy. Oper Tech Otolaryngol Head Neck Surg 14:185–187.

Har-El G (2003). Extracraial approaches to the sphenoid sinus. In: Har-El G, Weber PC (eds) Rhinologic and otologic aspects of skull base medicine and surgery. American Academy of Otolaryngology-Head and Neck Surgery, Alexandria, pp 53–64.

Har-El G (2005). Combined endoscopic transmaxillary – transnasal approach to the pterygoids, lateral sphenoid and retrobulbar orbit. Ann Otol Rhinol Laryngol 114:439– 442.

Hidir Y, Battal B, Durmaz A et al (2011). Optimum height from the roof of the choana for seeking the sphenoid ostium. J Craniofac Surg 22(3):1077–1079.

H.K.K. Tan* and Y.K. Ong (2007). Sphenoid Sinus: An Anatomic And Endoscopic Study in Asian Cadavers - Clinical Anatomy 20:745–750.

H. Mamatha, G. Saraswathi, L.C. Prasanna (2010). Variations of sphenoid sinus and their impact on related neurovascular structures. Current Neurobiology; 1 (2): 121-124.

Hudgins PA (1993). Complications of endoscopic sinus surgery. Radiol Clin North Am 31:21–32.

Jian Wang, Bidari Sharatchandra, Inoue Kohei, et al. (2010). Extensions of the sphenoid sinus: a new classification. Neurosurgery; 66:797–816.

Idowu.O.E., Balogun.B.O., Okoli .C.A. 2009. "Dimensions, Septation and pattern of pneumatization of the sphenoidal sinus". Folia Morphol .68(4): 228-32

Jonathan Z. Baskin, Md, M.Abraham Kuriakose, Md,Dds, Richard A. Lebowitz, Md (2003).The Anatomy And Physiology Of The Sphenoid Sinus. Operative Techniques In Otolaryngology-Head And Neck Surgery, Vol 14, No 3 (Sept),: Pp 168-172.

Jones NS, Strobl A, Holland I (1997). A study of the CT findings in 100 patients with rhinosinusitis and 100 controls. Clin Otolaryngol; 22:47-51.

Joe JK, Ho SY, Yanagisawa E (2000). Documentation of variations in sinonasal anatomy by intraoperative nasal endoscopy. Laryngoscope 110(2):229–35.

Kainz J, Klimek L, Anderhuber W (1993). Prevention of vascular complications in endonasal paranasal sinus surgery. I Anatomic principles and surgical significance. HNO 41:146– 152.

Kaluskar SK. (2008). Evolution of rhinology. Indian J Otolaryngol Head Neck Surg;60:101-5.

Kantarci M, Karasen RM, Alper F et al. (2004). Remarkable anatomic variations in paranasal sinus region and their clinical importance. Eur J Radiol 50(3):296–302.

36. Kennedy DW (1985). Functional endoscopic sinus surgery technique. Arch Otolaryngol 111:643–649.

Kennedy DW, Zinreich SJ, Rosenbaum AE, Johns ME (1985). Functional endoscopic sinus surgery. Theory and diagnostic evaluation. Arch Otolaryngol;111:576-82.

Kennedy DW (1992). Prognostic factors, outcomes and staging in ethmoid sinus surgery. Laryngoscope;102:1-18.

Kennedy DW, Shaman P, Han W, Selman H, Deems DA, Lanza DC (1994). Complications of ethmoidectomy: a survey of fellows of the American Academy of Otolaryngology-Head and Neck Surgery. Otolaryngol Head Neck Surg;111:589-99.

Kevin Katzenmeyer, Byron J Bailey, Francis B. (2000). Quinn and Melinda Stoner Quinn. Approaches to the Sphenoid.

Kieff, D.A. and N. Busaba (2002). Treatment of isolated sphenoid sinus inflammatory disease by endoscopic sphenoidotomy without ethmoidectomy. Laryngoscope. 112(12): p. 2186-8.

Kitthaweesin K, Theerakul T. (2012). Neuro-ophthalmic manifestations in sinusitis patients who underwent endoscopic sinus surgery. J Med Assoc Thai. Dec;95(12):1543-7.

Koay B, Bates G, Elston J. (1997). Endoscopic orbital decompression for dysthyroid eye disease. J Laryngol Otol;111:946-9.

Kodama G (1976). Developmental studies on the orbitosphenoid of the human sphenoid bone. In: Bosma JF (ed), Symposium on development of the basicranium, Publication No. (NIH) 76-989, U.S. Department of Health, Education and Welfare (DHEW), Bethesda, MD, , 3–43.

Lang J. (1985) Hypophyseal region. Anatomy of the operative approaches. Neurosurg Rev;8:93–124.

Lang J, Keller H (1978). The posterior opening of the pterygopalatine fossa and the position of the pterigopalatine ganglion. (Abstract). Gegenbaurs Morphol Jahrb 124:207–214.

Lang J (1989). Clinical Anatomy of The Nose, Nasal Cavity, and Paranasal Sinuses. New York, NY, Thieme.

86. Laws ER Jr (1999) Vascular complications of transsphenoidal surgery. Pituitary 2:163–170.

Lee, T.J., S.F. Huang, and P.H. (2009). Chang, Characteristics of isolated sphenoid sinus aspergilloma: report of twelve cases and literature review. Ann Otol Rhinol Laryngol. 118(3): p. 211-7.

Leopold D. A history of rhinology in North America. Otolaryngol Head Neck Surg 1996;115:283-97.

Levine HL, May M, Rontal M, Rontal E (1993). Complex anatomy of the lateral nasal wall: simplifi ed for the endoscopic sinus surgeon. In: Levine HL, May M (eds) Endoscopic sinus surgery. Th ieme, New York, pp 1–28.

Levine HL, Clemente MP. (2005). Sinus surgery: endoscopic and microscopic approaches, Thieme, New York, 6–12.

Lioyd S, Lund VJ, Scadding GK (1994). CT of the paranasal sinuses and functional endoscopic surgery: a critical analysis of 100 symptomatic patients. J Laryngol Otol 105:181–185

Liu S, Wang Z, Zhou B, Yang B, Fan E, Li Y. (2002). Related structures of the lateral sphenoid wall anatomy studies in CT and MRI. Lin Chuang Er Bi Yan Hou Ke Za Zhi;16(8):407-9.

Lu Y, Pan J, Qi S, Shi J, Zhang X, Wu K. Pneumatization of the sphenoid sinus in Chinese: the differences from Caucasian and its application in the extended transsphenoidal approach. J Anat 2011;219:132–42. doi:10.1111/j.1469-7580.2011.01380.x.

Lund VJ, Scadding GK. (1994). Objective assessment of endoscopic sinus surgery in the management of chronic rhinosinusitis: an update. J Laryngol Otol;108:749-53.

Madeline LA, Elster AD (1995). Suture closure in the human chondrocranium: CT assessment, Radiology, 196(3): 747–75.

Madiha AES, Raouf AA (2007). Endoscopic anatomy of the sphenoidal air sinus. Bull Alex Fac Med 43:1021–1026.

Maniglia AJ (1987). Complication of endoscopic nasal surgery. Occurrence and treatment. Am J Rhinol 1:45–49.

Martin J. Citardi, Md. (2003). Computer-Aided Sphenoid Sinus Surgery. Operative Techniques In Otolaryngology-Head And Neck Surgery, Vol 14, No 3 (Sept),: Pp 188-194

Maxillary Sinus (Antrum of Higmore) available at: URL:http://dentfac.mans.edu.eg/files/english/pdf/handouts/Maxillary_Sinus.pdf.

Meloni F, Mini R, Rovasio S, Stomeo F, Teatini GP (1992). Anatomic variations of surgical importance in ethmoid labyrinth and sphenoid sinus. A study of radiological anatomy. Surg Radiol Anat 14:65–70

Metson R, Woog JJ, Puliafito CA. (1994). Endoscopic laser dacryocystorhinostomy. Laryngoscope;104: 269-74.

Metson R, Gliklich RE. (1996). Endoscopic treatment of sphenoid sinusitis. Otolaryngol Head Neck Surg. Jun;114(6):736-44.

M.Davoodi, N.Saki, G. Saki and F. Rahim (2009). Anatomical Variation of Neurovascular Structures Adjacent Sphenoid Sinus by Using CT.

Mosher HP. (1903). The anatomy of the sphenoidal sinus and the method of approaching it from the antrum. Laryngoscope;13:177-214.

Mustafa Kazkayasi, Yasemin Karadeniz, Osman K. Arikan (2012). Anatomic variations of the sphenoid sinus on computed tomography*.

Mustafa Orhan · Figen Govsa · Canan Saylam (2010). A quite rare condition: absence of sphenoidal sinuses. Surg Radiol Anat (2010) 32:551–553

Nogueira JF Jr, Hermann DR, Américo Rdos R, Barauna Filho IS, Stamm AE, Pignatari SS. (2007). A brief history of otorhinolaryngolgy: otology, laryngology and rhinology. Braz J Otorhinolaryngol;73:693-703.

O. E. Van Alyea, M.D. (1941). Sphenoid Sinusanatomic Study, With Consideration Of The Clinical Significance Of The Structural Characteristics Of The Sphenoid Sinus. Arch Otolaryngol.;34(2):225-253. Doi:10.1001/Archotol..00660040251002.

Ossama Hamid, M.D.,1 Lobna El Fiky, M.D.,1 Ossama Hassan, Ali Kotb and Sahar El Fiky(2008). Anatomic Variations of the Sphenoid Sinus and Their Impact on Trans-sphenoid Pituitary Surgery. Skull Base.;18 (1): 9-15.

Polavaram R, Devaiah AK, Sakai O et al (2004). Anatomic variants and pearls-functional endoscopic sinus surgery. Otolaryngol Clin North Am 37(2):221–42.

Paolo Castelnuovo, Francesca De Bernardi (2009). The sphenoid Sinus, Rhinology and Facial Plastic Surgery, Springer, , pp 575-586, ISBN: 978-3-540-74379-8 (Print) 978-3-540-74380-4 (Online).

Penttila MA, Rautiainen ME, Pukander JS, Karma PH. (1994). Endoscopic versus Caldwell-Luc approach in chronic maxillary sinusitis: comparison of symptoms at one-year follow-up. Rhinology;32:161-5.

Peres-Pinas I, Sabate J, Carmona A, Catalina-Herrera CJ, Jimenez-Castellanos J (2000). Anatomical variations in the human paranasal sinus region studied by CT. J Anat 197:221–227.

P.Johnson1, M. Jannert1, A. Strömbeck and K. Abul-Kasim2 (2011). Computed tomography measurements of different dimensions of maxillary and frontal sinuses.

Proetz AW (1949). Operation on the sphenoid. Trans Am Acad Ophthalmol Otolaryngol 53:538 –541.

Rice DH (1995). Embryology. In: Donald PJ, Gluckman JL, Rice DH (eds) Th e sinuses. Raven Press, New York, pp 15–23.

Renn WH, Rhoton AL Jr (1975). Microsurgical anatomy of the sellar region. J Neurosurg 43:288-298.

ROBERT S, GRANT B (1998). Functional Endoscopic Sinus Surgery. American Academy of Family Physicians

Sareen D, Agarwal AK, Kaul JM et al (2005) Study of sphenoid sinus anatomy in relation to endoscopic surgery. Int J Morphol 23(3):261–266.

Schaeffer JP (1920). The Nose, Paranasal Sinuses, Naso-Lacrimal Passageways, and Olfactory Organ in Man; A Genetic, Developmental, and Anatomico-Physiological Consideration. Philadelphia, PA, Blakiston.

Schwartz JS, Har-El G (2003) Posterior septal perforation after nontransseptal sphenoid sinus surgery. Oper Tech Otolaryngol Head Neck Surg 14:221–222.

S. Elwany, Y.M. Yacourt, M. Talaat, et al. (1983). Surgical anatomy of the sphenoid sinus J Laryngol Otol, 97 pp. 227–241.

Setliff RC. (1995). New concepts and the use of powered instrumentation (the Hummer) for functional endoscopic sinus surgery. In: Stankiewicz JA, ed. Advanced endoscopic sinus surgery. St. Louis: Mosby,:161-70.

Sethi D, Stanley RE, Pillay PK (1995). Endoscopic anatomy of the sphenoid sinus and sella turcica. J Laryangol Otol 109:951–955.

Sethi, D.S., D.P. Lau, and C. Chan (1997). Sphenoid sinus mucocoele presenting with isolated oculomotor nerve palsy. J Laryngol Otol,. 111(5): p. 471-3.

Sethi, D.S. (1999). Isolated sphenoid lesions: diagnosis and management. Otolaryngol Head Neck Surg,. 120(5): p. 730-6.

Shah S, Har-El G (2001). Diabetes insipidus aft er pituitary surgery: incidence after traditional versus endoscopic transsphenoidal approaches. Am J Rhinol 15:377–379.

Sinnathamby CS (2006). Last's anatomy, regional and applied, 11th edn. Churchill Livingstone Elsevier, UK.

Sirikci A, Bayazit YA, Bayram M, Mumbuc S, Gungor K, Kanlikama M (2000). Variations of sphenoid and related structures. Eur Radiol 10:844–848.

S. James Zinreich, Sait Albayram, Mark L. Benson, and Patrick J. Oliverio (2003). The Ostiomeatal Complex and Functional Endoscopic Surgery.

Sphenoid Sinus and Its Related Structures in a North Karnataka Population. ID: JCDR/2012/4173:2428.

Stammberger H. (1989). History of rhinology: anatomy of the paranasal sinuses. Rhinology. Sep;27(3):197-210.

Stammberger H, Posawetz W. (1990). Functional endoscopic sinus surgery. Concept, indications and results of the Messerklinger technique. Eur Arch Otorhinolaryngol;247:63-76.

Stammberger H. (1991). Functional endoscopic sinus surgery: the Messerklinger technique. Philadelphia: Decker,:283.

Stammberger H, Hawke M (1993). Essentials of functional endoscopic sinus surgery. Mosby-Year.

Stankiewicz JA (1987). Complications of endoscopic nasal surgery. Occurence and treatment. Am J Rhinol 1:45–49.

Starke RM, Raper DM, Payne SC, Vance ML, Oldfield EH, Jane JA Jr. (2013). Endoscopic vs microsurgical transsphenoidal surgery for

acromegaly: outcomes in a concurrent series of patients using modern criteria for remission. J Clin Endocrinol Metab. Aug;98(8):3190-8.

Sonkens JW, Harnsberger HR, Blanch MG, Babbel RW, Hunt S (1991). The impact of screening sinus CT on the planning of functional endoscopic sinus surgery. Otolaryngol Head Neck Surg 105:802–813.

Sondheimer FK. (1971). Basal foramina and canals. In: Newton TH, Potts DG, eds. Radiology of the Skull Base and Brain. New York: Mosby, , 287-347.

Soon, S.R., et al. (2010). Sphenoid sinus mucocele: 10 cases and literature review. J Laryngol Otol,. 124(1): p. 44-7.

Ssiiooww Jjiinn Kkeeaatt (1998). A Study Of Asian Paranasal Sinus Anatomy Using Triplanar Computed Tomography Scans.

Stool S, Post J. (1996). Cranial growth, development and malformations:phylogenetic aspects and embryology. In: Bluestone CD, Stool SE, Kenna MA (eds), Pediatric otolaryngology, 3rd edition, W.B. Saunders Co., Philadelphia, , 1:1–18.

Sung E. LoGerfo, Michael L. Richardson, Robert W. Dalley, Yoshimi Anzai, Interactive CT Sinus Anatomy. Aviaalble at URL: http://uwmsk.org/sinusanatomy2/Frontal-Normal.html

Tasar M, Yetiser S, Saglam M, Tasar A (2003). Congenital common cavity deformity of frontal, ethmoid, and sphenoid sinuses. Cleft Palate Craniofac J 40(6):639–641

The University of Vermont. Embryology of the paranasal sinuses (Feb 4,5 2013). available at: URL: https://www.uvm.edu/medicine/surgery/documents/SinusSurgery3.pdf

T. Hiyama, M. Shiigai, T. Masumoto, M. Minami; Tsukuba/JP, Ibaraki/JP. (2015).The sphenoid sinus: clinical imaging anatomy and pathology. 10.1594/ecr/C-1410. http://dx.doi.org/10.1594/ecr2015/C-1410.

The drawings of Leonardo da Vinci [Internet]. [cited 2013 Dec 23]. Available from: http://www.drawingsofleonardo.org/.

Tsoucalas G, Gentimi F, Kousoulis AA, Karamanou M, Androutsos G. Joseph Gensoul (2013). The earliest illustrated operations for maxillary sinus carcinoma. Eur Arch Otorhinolaryngol;270:359-62.

Valerie J Lund, Anthony Wright and Joannis Yiotakis (1997). Complications and medicolegal aspects of endoscopic sinus surgery.

Van Alyea OE (1949). Discussion of operation on the sphenoid sinus. Trans Am Acad Ophthalmol Otolaryngol 53:542–545.

Van Cauwenberge P, Sys L, De Belder T et al (2004). Anatomy and physiology of the nose and the paranasal sinuses. Immunol Allergy Clin North Am 24(1):1–17.

V. Budu1, Carmen Aurelia Mogoantă, B. Fănuţă, I. BULESCU. (2013). The anatomical relations of the sphenoid sinus and their implications in sphenoid endoscopic surgery. Rom J Morphol Embryol, 54(1):13–16.

Vimal Kumar M, Suresh Sukumar And Dr. Mamatha* H. (2012). Computed Tomograpic Studies On Sphenoid Sinus Variants. Int J Pharm Bio Sci July; 3(3): (B) 482 – 486.

V. F. H. Chong, Y. F. Fan And C. H. Tng (1998). Pictorial Review: Radiology of the Sphenoid Bone. Clinical Radiology (1998) 53, 882-893.

Wang J, Bidari S, Inoue K, Yang H, Rhoton A. (2010). Extensions of the sphenoid sinus: a new classification. Neurosurgery; 66:797 – 816. doi:10.1227/01.NEU.0000367619.24800.B1.

Weinberger DG, Anand VK, Al-Rawi M *et al.* Am I Rhino (1996). Surgical anatomy and variations of the Onodi cell.;10:365-70.

Wong AM, Bilaniuk LT, Zimmerman RA, Simon EM, Pollock AN (2004). Magnetic resonance imaging of carotid artery abnormalities in patients with sphenoid sinusitis. Neuroradiology 46(1):54– 59.

Xiao B, Lang J, Wang H (1998). Application of coronal CT scan and three-dimensional reconstruction in rhinology (abstract). Lin Chuang Er Bi Yan Hou Ke Za Zhi 12:439–441.

Yousem DM. (1993). Imaging of sinonasal inflammatory disease. *Radiology*. Aug;188(2):303-14.

Yonetsu K, Watanabe M, Nakamura T. (2000). Age-related expansion and reduction in aeration of the sphenoid sinus: volume assessment by helical CT scanning. AJNR Am J Neuroradiol.;21(1):179-182.

Zinreich S, Kennedy D, Rosenbaum A, et al. (1987). Paranasal sinuses: CT imaging requirements for endoscopic surgery. Radiology;163: 769–775.

Zinreich S. (1990). Paranasal sinus imaging. Otolaryngol Head Neck Surg;103:863–868.

Zinreich S. (1993). Imaging of inflammatory sinus disease. Otolaryngol Clin North Am;26:535–547.

Appendix:

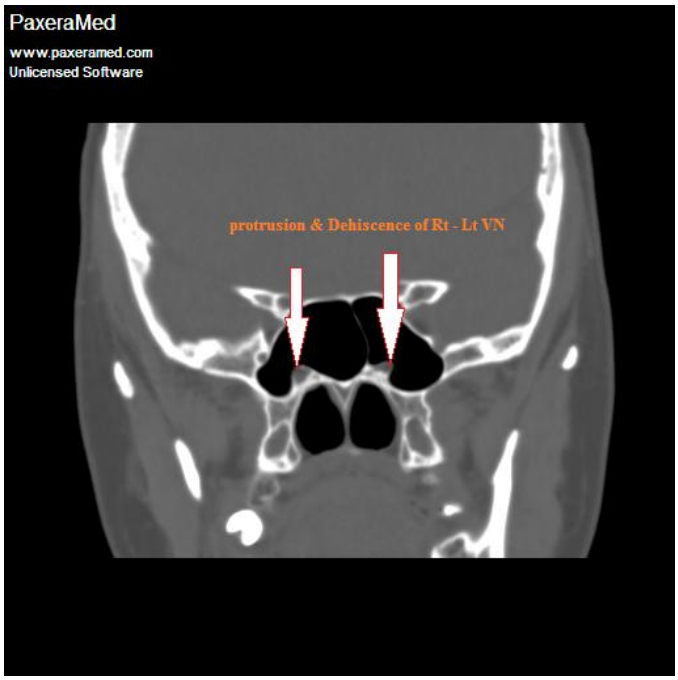

Image 1: Protrusion and Dehiscence of the Right and Left Vidian Nervers, male, 24 yr

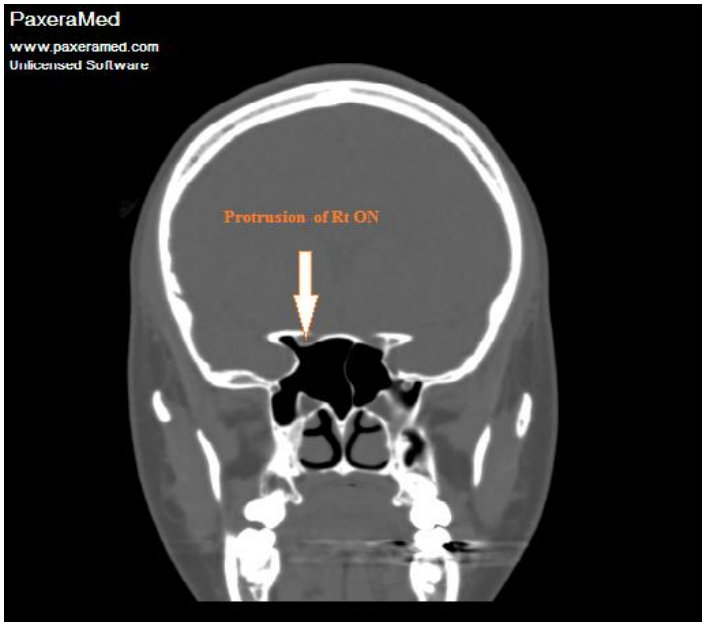

Image 2: Protrusion of the Right Optic Nerve, male, 36 yr

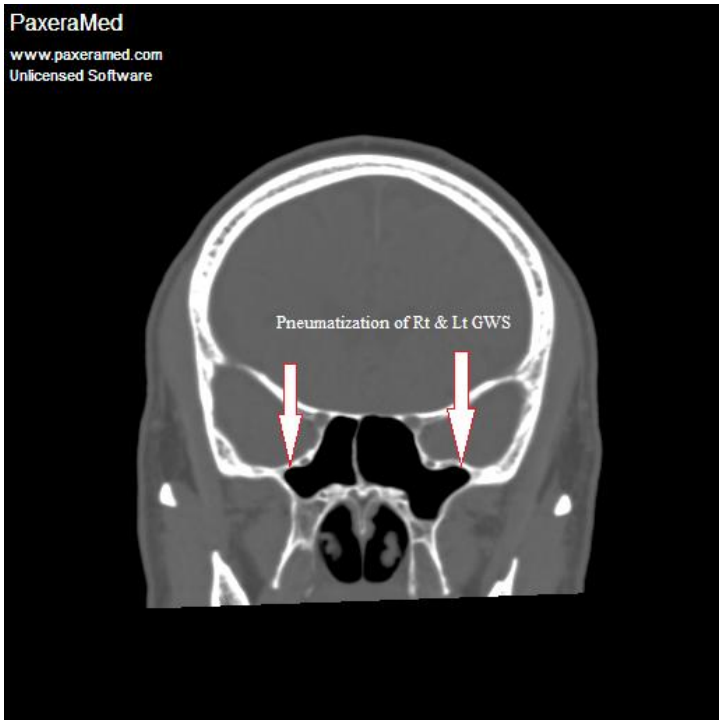

Image 3: Pneumatization of Right and Left Greater Wing of Sphenoid Bone, male, 44 yr

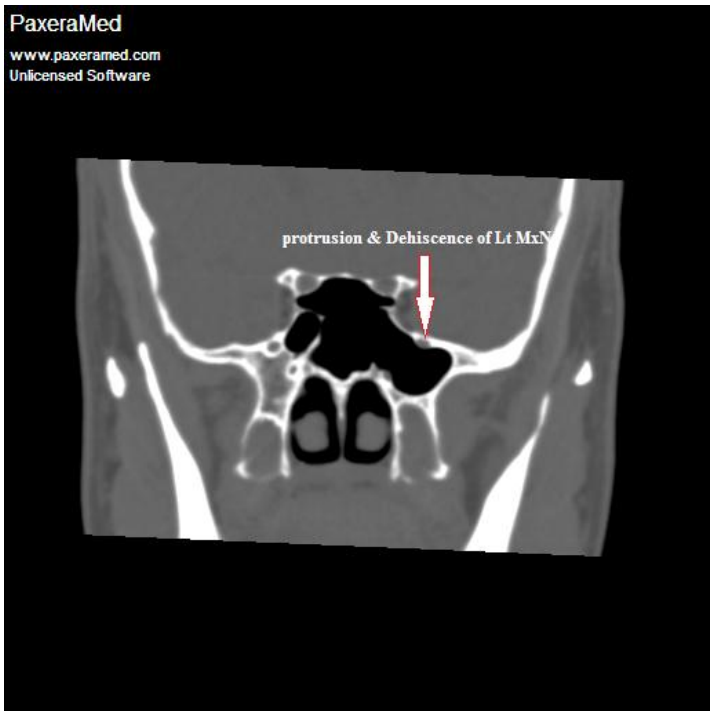

Image 4: Protrusion and Dehiscence of the left maxillary Nerve,fe male, 24 yr

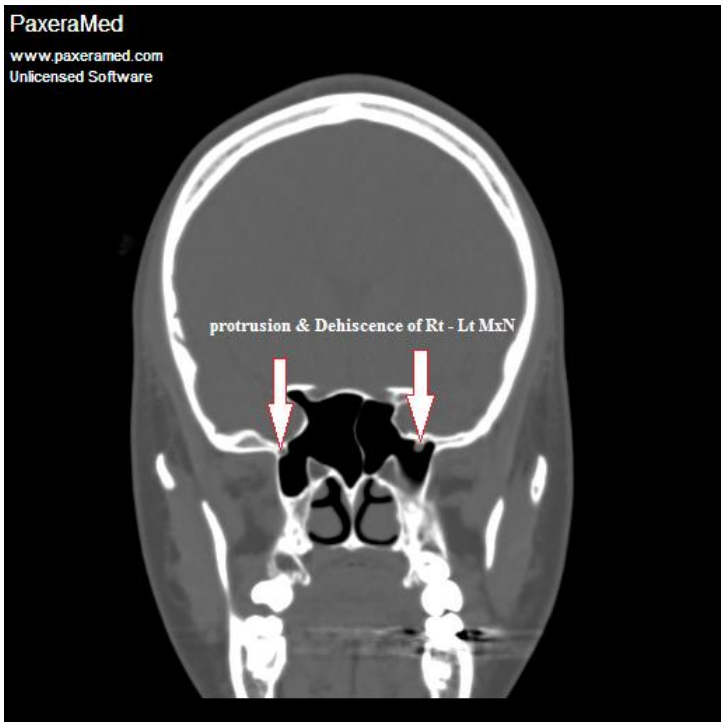

Image 5: Protrusion and Dehiscence of the Right and Left Maxillary Nerves, male, 33 yr

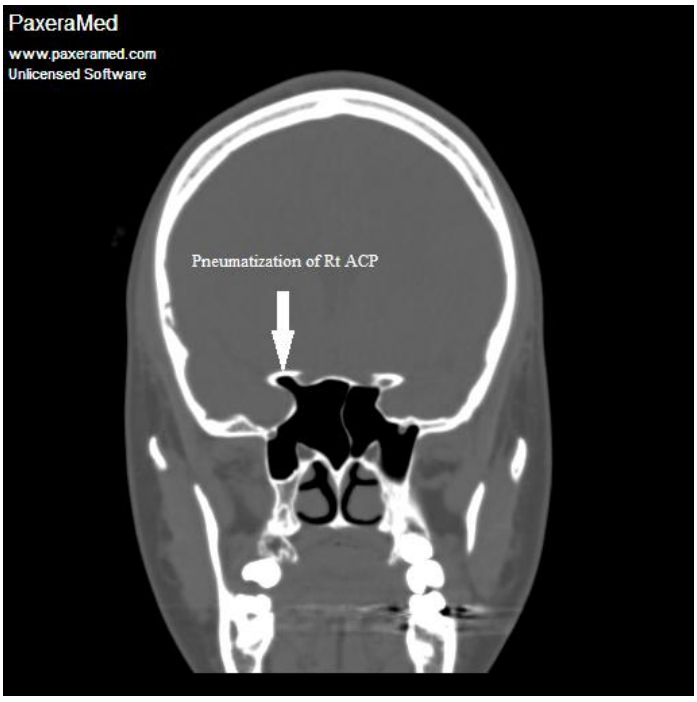

Image 6: Pneumatization of Right anterior clinoid process, male, 20 yr

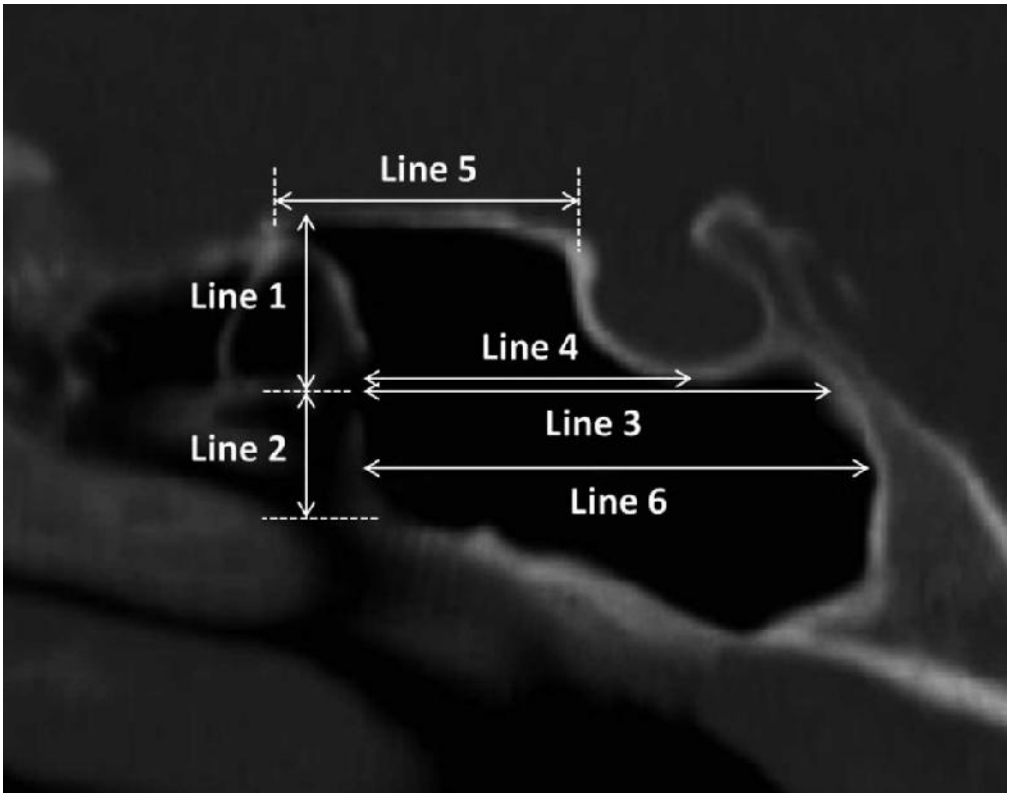

Image 7: Measurements of the sphenoid sinus lengths at the level of sphenoid ostium in sagittal plane. Line 1: the vertical distance from the center of the sphenoid ostium to the roof of the sphenoid sinus, Line 2: the vertical distance from the center of the sphenoid ostium to the floor of the sphenoid sinus, Line 3: the horizontal distance from the center of the sphenoid ostium to the posterior wall of the sphenoid sinus, Line 4: the horizontal distance from the anterior wall of the sphenoid sinus to the lowest point of the sella, Line 5: the length of the sphenoid sinus roof, Line 6: the longest horizontal distance of the sphenoid sinus.

PATIENT DATA SHEET

Patient (1) ……

Patient Data				Variable Data								
Age	**Gender**	**Head circumference**	**Clinical Data**	**Coronal Image**				**Sagittal Image**			**S.S Calssifaction**	
66	**Male** ☐	22.5 mm		**Pneumatization**	**Bi.L**	**Rt. S**	**Lt. S**		**Rt. S**	**Lt. S**	**Sellar** ☐	**Onodi cell** ☐
	Female (√)			ACP	X	X	**(√)**	**Line 1**	10.05	11.03	**Pre-sellar (√)**	**Non Onodi cell (√)**
				GWS	X	X	**(√)**	**Line 2**	17.34	14.27	**Conchal** ☐	
				PP	**(√)**	-	**-**	**Line 3**	20.25	25.56		
				Protrusion				**Line 4**	14.60	16.60		
				ICA	X	X	X	**Line 5**	10.62	9.96		
				ON	X	X	X	**Line 6**	27.22	27.22		
				Mx.N	X	X	**(√)**					
				V.N	**(√)**	-	-					
				Dehiscence								
				ICA	X	X	X					
				ON	X	X	X					
				MxN	X	X	**(√)**					
				VN	**(√)**	-	-					
				Line 7	**Rt. S:** 13.61 mm							
					Lt. S: 7.30 mm							

Accomplishment

Two papers were published:

1- Characterization of Sphenoid Sinuses for Sudanese Population Using Computed Tomography ***(Attached).***

2- Computerized Tomography Morphometric Analysis of the Sphenoid Sinus and Related Structures in Sudanese Population ***(Attached).***